



POLITECNICO
MILANO 1863

School of Industrial and Information Engineering

**Master of Science in
Mechanical Engineering**

**Optimisation of the tyre model in rFactor2
environment for AVEHIL professional simulator**

Supervisor: Prof. Gianpiero MASTINU

Tutor: Ing. Stefano BARLOCCO

Domenico PREITI
905958

Academic Year 2018/2019

Abstract

Nowadays nothing is left to chance in Motorsport for what concerns both the mechanical and the human aspects: the development a good strategy, based on highly accurate forecast models, determines the success in a race. For a driver, as well as the athletes of every discipline, the training plays a crucial role in the approach to the race, but the track tests are limited for both economic reasons and regulation restrictions.

Cristiano Giardina, thanks to his almost thirty-year experience in Motorsport as Team Manager, came to meet these two demands and founded Skydrive in 2015. Skydrive is an innovative start up that realizes professional simulators of the latest generation called AVEHIL (Advance Vehicle Engineering Human In the Loop) and the field office located in the Monza Eni Circuit has become a technological hub in Northern Italy for drivers and racing teams in few months.

In particular, the Formula simulator uses the commercial videogame “rFactor2” as virtual platform. Being “rFactor2” developed for users with no experience with a racing car, the mathematical model of the tyre is simplified and several aspects are neglected.

The aim of this master thesis is an in depth analysis of the physical model of the tyre and the algorithms of rFactor2 that affect the gameplay: the mechanical and thermal behaviour are deeply revised in such way that the force and temperature outputs generated by the virtual tyres are comparable with the ones obtained with the equivalent real tyres.

KEYWORDS: Skydrive, Avehil, rFactor2, tyre model

Sommario

Oggigiorno nel Motorsport ogni aspetto viene curato nei minimi dettagli, sia a livello meccanico che umano: sviluppare una buona strategia, basata su modelli di previsione altamente accurati, determina il buon esito di una gara. L'allenamento per un pilota, così come per qualsiasi atleta di ogni disciplina, svolge un ruolo cruciale nell'approccio a una corsa, ma le prove in pista vengono molto spesso limitate sia per un aspetto economico sia per le restrizioni da regolamento.

Cristiano Giardina, grazie alla sua esperienza quasi trentennale nel Motorsport come Team Manager, è venuto incontro a queste due esigenze e nel 2015 ha fondato Skydrive. Skydrive è un'innovativa start up che realizza simulatori professionali di ultima generazione denominati AVEHIL (Advance Vehicle Engineering Human In the Loop) e in pochi mesi l'ufficio operativo situato al Monza Eni Circuit è diventato un punto di riferimento per piloti e squadre in tutto il Nord Italia.

Più nel dettaglio, il simulatore Formula utilizza come piattaforma virtuale il videogame commerciale "rFactor2". Essendo sviluppato per utenti senza alcuna esperienza con le auto da corsa, il modello matematico degli pneumatici è semplificato e molti aspetti vengono trascurati.

Lo scopo di questa tesi è un'analisi approfondita del modello fisico dello pneumatico e degli algoritmi di rFactor2 che regolano la dinamica di gioco: il comportamento meccanico e termico vengono profondamente rivisitati in modo tale che gli output di forza e temperatura generati dallo pneumatico virtuale siano comparabili a quelli ottenuti dallo pneumatico reale equivalente.

PAROLE CHIAVE: Skydrive, Avehil, rFactor2, modello di pneumatico

Contents

1	Introduction	1
1.1	Problem statement	1
1.2	Thesis outline	2
2	Skydrive S.r.L.	3
2.1	“Driver R&D” training approach	4
2.2	rFactor1 & rFactor2 comparison	5
3	Tyre physics within rFactor2	7
3.1	Brush model	8
3.1.1	Pure lateral slip condition	9
3.1.2	Pure longitudinal slip condition	13
3.1.3	Combined slip condition	17
3.1.4	Carcass flexibility	20
3.2	Rubber friction model	22
3.2.1	Indentation mechanism	23
3.2.2	Molecular adhesion	25
3.3	Thermal model	26
3.3.1	Temperature modelling along the contact patch	27
3.3.2	Temperature modelling over all the tyre circumference	27
3.3.3	Heat transfer by convection to the ambient air	29
3.3.4	Heat transfer by conduction to the track	29
3.3.5	Heat generation due to friction	29
3.3.6	Heat generation due to hysteresis	30
4	How to build up a tyre in rFactor2	31
4.1	Introduction to the “.tgm” file	31
4.2	Step 1: data collection	35
4.3	Step 2: basic implementation	35
4.4	Step 3: QSA batch testing	40
4.5	Step 4: Realtime model batch testing	42
5	Optimisation algorithm based on a neural network	43
5.1	Introduction to the algorithm	43
5.2	Data recording	44
5.3	ANN implementation	52
5.4	Optimisation process	55
5.5	Validation procedure	56
5.5.1	Off-line tests	56
5.5.2	On-line tests	59
5.6	Final considerations	62

6	Thermodynamic aspect of the tyre	63
6.1	Formula Renault 2019 track tests	64
6.2	Comparison with the equivalent virtual tyres	65
6.3	Thermodynamic parameters tuning	67
6.4	Tyres warm-up training	71
7	Conclusions	73
7.1	Results	73
7.2	Future developments	75
	Bibliography	77

List of Figures

2.1	Collage of the main features of the single seater simulator [7].....	3
2.2	“R&D Driver” training approach [7].....	4
2.3	3D visualisation of the tyre model in “tTool”.....	6
3.1	rFactor2 tyre model [5].....	7
3.2	Brush model: reference system [1].....	8
3.3	Brush model: lateral sliding [1].....	9
3.4	Brush model: F_y and M_z trends function of the side slip angle α [1].....	13
3.5	Brush model: effective rolling radius and longitudinal sliding velocity [1].....	14
3.6	Brush model: lateral view in braking condition [1].....	15
3.7	Brush model: combined slip condition [1].....	16
3.8	Brush model: equivalent side slip angle α_{eq} [1].....	18
3.9	Brush model: $F_x(\alpha)$ [1].....	19
3.10	Brush model: $F_y(\kappa)$ [1].....	19
3.11	Brush model: $F_y(-F_x)$ [above], $M_z(-F_x)$ [below] [1].....	20
3.12	Brush model: flexible carcass [1].....	20
3.13	Brush model, flexible carcass: $M_z(-F_x)$ [normalized] [1].....	21
3.14	Rubber model: hysteresis and molecular adhesion [2].....	22
3.15	Indentation mechanism of grip generation at road-tire interface [6].....	23
3.16	Rubber model: storage modulus (E''), loss modulus (E'') and dissipation factor ($\tan \delta$) as a function of temperature [3].....	24
3.17	Hysteresis and modulus of tire rubber as function of temperature [6].....	25
3.18	Molecular adhesion mechanism of grip generation at road-tire interface [6].....	26
3.19	Friction coefficient as function of sliding velocity and surface temperature [6].....	26
3.20	Thermal model: heating and cooling mechanisms for the tread of a rolling tire [5].....	28

4.1	Virtual tyre .tgm file: [QuasiStaticAnalysis] section	32
4.2	Virtual tyre .tgm file: [Node] section.....	32
4.3	Cross section of a radial road tyre: nomenclature.....	33
4.4	Virtual tyre .tgm file: [Realtime] section.....	34
4.5	Virtual tyre .tgm file: [Lookup] section	34
4.6	“TGM Generator” spreadsheet: “General” section	36
4.7	“TGM Generator” spreadsheet: the tyre cross sectional geometry.....	37
4.8	“TGM Generator” spreadsheet: rubber material properties	37
4.9	“TGM Generator” spreadsheet: the ply material properties	38
4.10	“TGM Generator” spreadsheet: ply angles and thicknesses	38
4.11	“TGM Generator” spreadsheet: compound selection.....	39
4.12	“TGM Generator” spreadsheet: QSA tests boundary conditions.....	39
4.13	“tTool QSA Batch Tests” spreadsheet: “1_QSATest” boundary conditions.....	40
4.14	“tTool” window: QSA tests	41
4.15	“tTool QSA Batch Tests” spreadsheet: “1_AnalyseFlex” page	42
5.1	[QuasiStaticAnalysis] section of the front tyre .tgm file	45
5.2	“tTool Realtime Batch Tests” spreadsheet: Sweep Test boundary conditions..	46
5.3	Front tyre .tir file: boundary conditions.....	46
5.4	Normalised lateral force: real vs rF2 default	47
5.5	Normalised longitudinal force: real vs rF2 default	47
5.6	“Normalised self-aligning moment: real vs rF2 default	48
5.7	ANN setting.....	52
5.8	Bayesian regulation process performance	53
5.9	Outputs vs Targets: mean squared error of the lateral force	53
5.10	Outputs vs Targets: mean squared error of the self-aligning moment	54
5.11	Outputs vs Targets: delta of the longitudinal force peak values	54
5.12	Outputs vs Targets: means squared error of the longitudinal force	54
5.13	Objective functions domain: optimal solutions	55
5.14	Off-line validation test: a random optimal string is taken as reference.....	56
5.15	Off-line validation test: [Realtime] parameters modified in the .tgm file....	57
5.16	Off-line validation test: comparison between: a) predicted objective function; b) actual objective functions obtained with the optimised tyre; c) default configuration.....	57
5.17	Off-line validation test: normalised lateral force.....	58
5.18	Off-line validation test: normalised longitudinal force	58
5.19	Off-line validation test: normalised longitudinal force	59
5.20	Lateral acceleration comparison: default tyre vs the optimised one	61
5.21	Braking distance comparison: default tyre vs the optimised one.....	61

6.1	1 st day test at Cremona Circuit: Formula Renault instrumentation phase [7]..	64
6.2	Temperature profile comparison: real vs rF2 Formula Renault official suite ..	65
6.3	“StaticCurve” parameter: static friction as function of temperature.....	66
6.4	Surface temperature comparison: real tyres vs rF2 default tyres.....	67
6.5	Cross-sectional view of tire heat generation and transfer [9]	68
6.6	Surface temperature comparison: real tyres vs rf2 default tyres vs rF2 modified tyres (“GroundConductance”).....	69
6.7	Surface temperature comparison: real tyres vs rf2 default tyres vs rF2 modified tyres (“ExternalGasHeatTransfer”)	70
6.8	“StaticCurve” comparison: original vs modified trend.....	71
7.1	Surface temperature comparison: real tyres vs rf2 default tyres vs rF2 modified tyres.....	75

List of Tables

4.1	Front tyre off-line tests: boundary conditions.....	46
4.2	Front tyre .tgm file: data collection for the ANN	52
6.1	Example of optimisation process of the front tyre	74
6.2	Example of optimisation process of the rear tyre.....	74

Chapter 1. Introduction

The tyres are the only elements that allow every vehicle to grab the ground surface and transmit all the forces that are necessary to keep the desired trajectory.

In the everyday use the tyres play a very important role for what concerns safety, fuel economy and noise pollution issues. On the other hand, in motorsport applications, tyres are even more crucial for the final performance of the vehicle.

Although their fundamental importance, the tyres are the most unknown factor among the vehicle dynamics parameters and still today nobody has developed a physic and reliable model. This is due to the strong non-linear behaviour of rubber and its relationship with temperature. Even one of the most important tyre manufacturers, in the master motorsport competition, makes huge errors on the evaluation of the tyres' performances during a Grand Prix.

The key feature that distinguishes a winning racing team from the others is of course the capability to forecast the tyres' life during the entire duration of the race and this crucial aspect depends on many factors such as ambient and track conditions, car behaviour and mostly the driver's driving style.

On this last aspect nowadays more and more driving simulators come in help: from the amateur categories up to Formula1, these devices have reached a crucial importance for the drivers to get ready for the race.

1.1 Problem statement

Skydrive is an Italian start up, born in 2015, which realizes and sells professional driving simulators branded AVEHIL (acronym of Advance Vehicle Engineering Human In the Loop). After four years of R&D, in 2019 the first office, located in the grand stand of the Monza Eni Circuit, was opened to the public and just in few months it has become an essential place for many young drivers who are approaching for their first time the motorsport world.

There are actually two professional simulators, one is a GT simulator and the second one is a Formula simulator (more details will be given later on). My work will focus only on the second one, which is the spearhead of the company. The Formula simulator works with rFactor2, a commercial use video game. The reason why this software was adopted is the huge amount of customizable features that make it possible to build up your own model car under all the aspects: from brakes to chassis, from suspension geometry to the aerodynamic and so on. But the most complicated parts to develop on this software are of course the tyres. For the first time in a driving video game, somebody was able to implement a physic model of the tyre, increasing exponentially the level of accuracy but, at the same time, the complexity of the tyres' parameters set up.

Since rFactor2 was created to be user friendly for the majority of the customers, of course the tyre behaviour is very far from the real one: in particular the transient response is totally neglected in order to make the driving experience easier, but this goes against the Skydrive philosophy.

The aim of this master thesis will be an optimisation process in order to achieve the best compromise between the virtual tyres and the real ones, making the simulator even more realistic in order to help the young drivers to approach correctly a race weekend, from the free practices up to the highest step of the podium.

1.2 Thesis outline

I subdivided the following pages in six chapters, covering the main aspects behind my internship of the last six months.

In chapter two a brief introduction of Skydrive S.r.l. is given, focusing on the technical features of the Formula simulator and on the “Driver R&D” approach, widely applied with very interesting results.

In chapter three a detailed explanation of tyre physics implemented in rFactor2 is treated, in order to understand the main factors that affect the handling behaviour of the tyres.

In chapter four a step by step procedure of the tyre build up procedure is presented, starting from the preliminary design up to the final refinement.

In chapter five the optimisation procedure of the mechanical characteristics of the tyres is discussed. This is the central core of the thesis: a wide description of the implemented algorithm is provided with the annexed validation procedure.

In chapter six, an analytical approach of the thermodynamic behaviour of the tyres is covered through a comparison between the tyres surface temperatures, measured with infrared sensors on a Formula Renault 2019, and the corresponding temperatures coming from the telemetry of the simulator by varying the parameters which affect the thermal properties.

Finally, chapter seven summarizes the major findings of this thesis and presents possibilities for future work.

Chapter 2. Skydrive S.r.l.

In motorsport applications, even the smallest detail is not left to chance, and this occurs not only in the top end categories, but also starting from the amateur ones. Of course, the best thing to do in order to get ready for the competition would be make several track tests but this would lead to a huge investment of time and money. And even if the financial resources are not an issue, there are restrictions on the number of private tests in order to make more affordable that specific category.

The necessity to create a reference among the driving simulators, led Cristiano Giardina to found Skydrive in 2015, an innovative start up that received the seal of excellence by Horizon 2020 and the award of high quality project for its studies on the tyre behaviour in motorsport application. Skydrive realizes and sells professional simulators called “AVEHIL” (Advance Vehicle Engineering Human In the Loop): two of them are present in the field office located in the grandstand of the Monza Eni Circuit, which has become a technological hub in the North of Italy.

The two simulators located in Monza are designed to meet different demands in order to accommodate drivers registered in every championship. As suggested by the name itself, the GT simulator is reserved to covered wheels car drivers while the Formula simulator is intended for those who drive a single seater machine (**Figure 1.1**). Both software and hardware behind these devices are entirely realized and developed internally by Skydrive: in this way there are no third parties and compromises.



Figure 1.1 – Collage of the main features of the single seater simulator [7].

Each of them is built with a real tub (Lamborghini Huracan for the GT simulator and Dallara World Series for the single seater simulator), which is moved by brushless motors that allow 4 four degrees of freedom. Every detail is taken care in these machines: the dashboard, the seat, the pedal set and even the braking system (including master cylinder, brake calipers and disks) are the same that you would find on a real racing car, and this aspect underlines the maniacal research of perfection behind this ambitious project.

Last but not least, both of the simulators are provided with data collector and live telemetry in order to analyse and improve the driving style.

2.1 “Driver R&D” training approach

Driver R&D is a specific training method for those drivers who want to perform a true quantum leap in their professional career. This program was developed and widely adopted, receiving positive feedbacks all the times. It does not merely consist in driving at the simulator, but behind this special format there is a lot more (**Figure 1.2**).

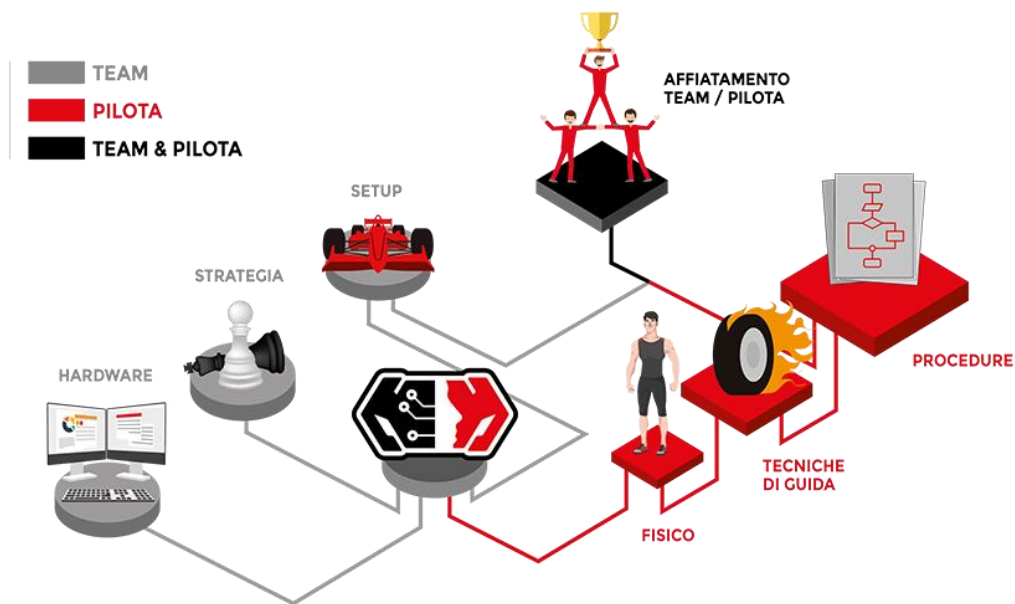


Figure 1.2 – “R&D Driver” training approach [7].

This package involves both the driver and his race engineer, when it is possible, in order to enhance the cooperation inside the team itself. It consists in more than one meeting, before and after every race weekend: in this way a strong correlation between the data from the real car and from the simulator is possible. The training sessions are not only intended to improve the driving skills, but also to make huge amount of set-up tests in order to save money and especially time: in this way 90% of the work is done out of the track and the driver can focus on the race pace.

Once the vehicle set-up is reasonably tuned, the “Driver R&D” approach really starts. During the training sessions the driver will be asked to simulate every salient moment of a race weekend, focusing mainly on the qualifying practice and on the tyre warm up. In particular, the driver will be put under pressure through very complicated manoeuvres in order to get used to rapidly analyse stressful situations and take the right decisions.

The driving skills are important as much as the awareness of what your body needs to perform at its best. A good physical condition is essential at every level of competition and is strictly related with the breathing quality during the agonistic activity. The use of a special t-shirt, provided with sensors, allows to collect several biometric data of the psycho-physical status of the driver: the heart rate, the respiratory rate and the breath-hold duration while braking are fundamental parameters on which it is possible to improve and make the difference.

2.2 rFactor1 & rFactor2 comparison

As said in the introduction, the work done during the internship was focused only on the single seater simulator. Initially the game platform implemented in the simulator was rFactor1, which is a well-known racing videogame among the drivers and the regular users for its ease to fine tuning. However, this peculiarity inevitably leads to neglect several physic aspects during the gameplay. The necessity to introduce something more accurate and reliable has involved the upgrade from rFactor1 to rFactor2. The second version cannot be seen as a simple evolution of the first one, but a drastic change in terms of implemented algorithms, like they were two completely different game platforms.

The main aspect that has undergone profound changes is the tyre model. In the first version of rFactor, the forces exchanged between the tyres and asphalt are calculated by a purely mathematical relationships based on Pacejka Magic Formula, which are standardized among all the tyres. Fictitious parameters are then listed in the tyre file and they adjust the static properties according the real time physical quantities. The relatively simple implementation of the tyre-road relationship, combined with a single contact point, is a smart way to reduce computation costs: this is beneficial in terms of response smoothness and driveability. On the other hand, the simpler the algorithm, the less accurate are the feelings felt by the driver. This is a reasonable compromise done by the developers with a double function: run the software at high frequencies and make easier the exploitation of the tyres, especially for non-professional users, by means of proper tuning of the fictitious parameters.

While, in the latest version of rFactor, the developers have introduced a totally renewed tyre based on a physical approach: the so-called brush model (**Figure 1.3**). This ambitious upgrade is the first attempt to use something different from a pure mathematical model among all the driving videogame. Indeed, the necessity to run in real time at high Hz leads inevitably the implementation of light and fast computer codes and this is not feasible with the complexity of the brush model. In order to match the computational effort, the creation of a lookup table is needed: by means of this procedure, it is possible to compute the values of the physical quantities, at different boundary conditions, during the offline mode.

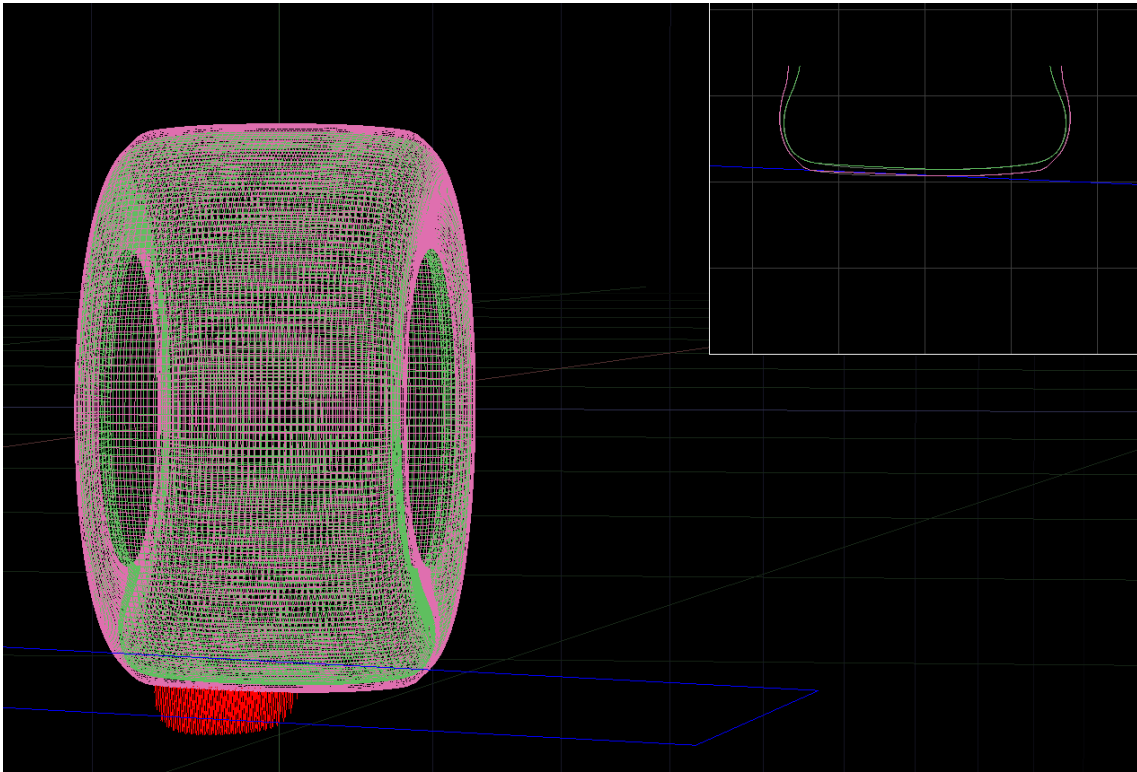


Figure 1.3 – 3D visualisation of the tyre model in “tTool”.

Once the lookup table of a tyre is compiled, the processors will no more compute the dynamic quantities at every clock rate but they will simply read their values at the actual condition of speed, vertical load, pressure, temperature and so on. Doing so, this powerful algorithm allows to perform operations that require high computational efforts, providing more reliable results with respect to a purely empirical-mathematical model. Nevertheless, this software architecture forces to update the lookup table at every modification of the tyre structure, slowing down the development phase.

The [Realtime] parameters come in help to tune correctly the final behaviour of the tyres, as they work as scaling factors. The optimization algorithm, explained in the fifth chapter, has been designed to give as output the combination of values of the most relevant parameters present in the [Realtime] section, in order to match the tyre response with the target curves derived from the “.tir” file of the same tyre: in this way, an empirical relationship between real data and fictitious parameters can be established.

Chapter 3. Tyre physics within rFactor2

In almost all driving simulators the tyre is one of the most complicated aspect to model, among all the subsets that affect the vehicle dynamics, and this is mainly due to the non-linear behaviour of the rubber and the arrangement of the internal plies. The necessity of a rapid response of the gameplay, leads to the simplification of the software code and this consequently induces some errors.

rFactor2 has introduced a completely renewed tyre model by adopting a physical approach with the aim of reducing approximations and make the driving experience more realistic. It consists in the combination of three sub models that are strictly correlated to each other (**Figure 3.1**): a brush model with a six DOFs rigid ring, a model that accounts for the intrinsic properties of the rubber compound and a thermal model.

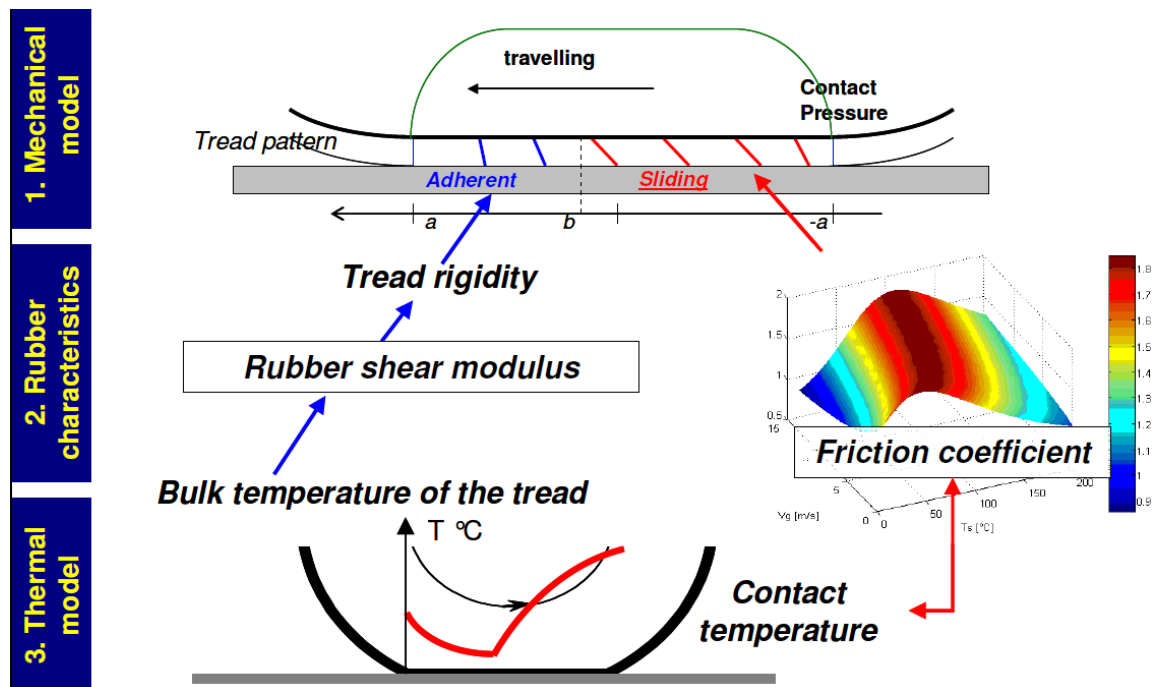


Figure 3.1 – rFactor2 tyre model [5].

The brush model allows to derive an analytical expression of the forces exchanged between the tyre and the ground, through the definition of the pressure distribution and the extension of the contact patch. The interaction between the belt and the tread is governed by the brush model too, while the interaction between the tread and the ground is governed by the rubber model which defines the friction characteristics: the latter depend on the sliding velocity, pressure distribution and surface temperature of the tyre. The rubber shear modulus affects the tread stiffness and therefore the shear force exchanged by the bristles.

Finally, the thermal model takes into account all the processes that affect the thermal aspect of the tyre (such as temperature build up and tyre cooling) and calculates the temperature at the interface tyre-ground along the whole contact patch.

3.1 Brush model

In the so-called brush model, the analysis is carried out in the mean longitudinal plane of the wheel, which assumes the shape of a disk with negligible thickness. The tyre is schematized as a rigid ring, on which an infinite number of elastic elements are radially connected. The ring represents the carcass and it can deform in radial direction, while the brushes represents the tread and they can deform only in the plane of contact (longitudinally and laterally). The brush-model developed by H.B. Pacejka in the textbook “Tire and Vehicle Dynamics” [1] has been used as guideline for the following presentation.

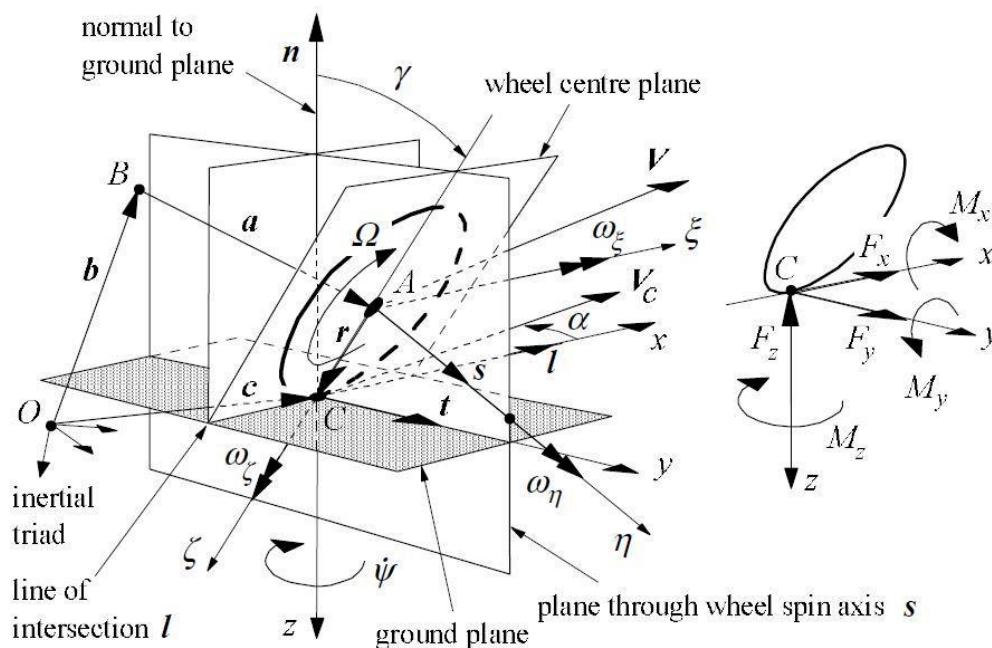


Figure 3.2 – Brush model: reference system [1].

In Figure 3.2 are represented the ground plane, the wheel centre plane e two other perpendicular planes with respect to the ground (normal-ground planes). Their intersection defines the contact point C between the tyre and the ground, which is taken as the origin of the reference system belonging to the tyre (axis n, y, x). A further local reference system has the origin A in the centre of the wheel (axis ξ, η, ζ). This arrangement allows to define the whole set of kinematic entities needed to derive forces and moments.

Having defined the reference system, it is necessary the introduction of the following assumptions:

- steady state conditions;
- non-deformable and flat ground surface;
- the rigid ring can deform only in radial direction;
- each bristle is independent from the others;
- linear bristle deformation;
- parabolic contact pressure distribution;
- isotropic behaviour of the bristles.

3.1.1 Pure lateral slip condition

The derivation of the forces exchanged by the tyre is made by considering the ideal condition of pure slipping, both lateral and longitudinal. The first condition, i.e. pure lateral slipping, happens when the tyre moves forward with a non-null side slip angle α , without longitudinal slippage. This hypothetical scenario allows to get an analytical formula of the lateral force F_y and the self-aligning moment M_z .

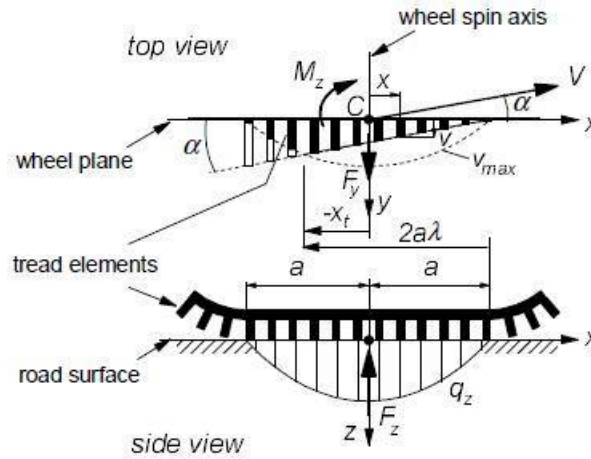


Figure 3.3 – Brush model: lateral sliding [1].

Analysing the contact zone, depicted in the **Figure 3.3**, it is possible to distinguish two areas:

- the adherence zone, where the bristle extremities describe a straight trajectory and parallel with respect to the velocity \vec{V} ;
- the sliding zone, where the bristle extremities describe a curved trajectory.

The second condition happens when the parabolic curve of the pressure distribution intercepts the linear curve of the force needed to deform the bristles: being the vertical load not sufficient to deform the bristles, they are not able to follow the moving direction and tend to return to their original position. This important observation leads to a different description of the two zones.

In the adherence zone, the sliding velocity V_g of a generic point belonging to the tread of a tyre that spins with an angular velocity φ and a certain side slip angle α , is defined as:

$$V_{gx} = V_c \cdot \left(y\varphi - \frac{\partial u}{\partial s} + \frac{\partial u}{\partial s} \right) \quad 3.1$$

$$V_{gy} = V_c \cdot \left(-tg\alpha - y\varphi - \frac{\partial v}{\partial x} + \frac{\partial v}{\partial s} \right) \quad 3.2$$

Where:

- u and v are the bristle deformations along x and y axis respectively;
- s is the travelled distance;
- V_c is the velocity of the centre wheel.

In adherence conditions, the relative velocity between the bristle tips and the ground is null ($V_g = 0$). By rearranging the lateral component V_{gy} , it is possible to derive the following relationship:

$$\frac{\partial v}{\partial x} - \frac{\partial v}{\partial s} = -tg\alpha - x\varphi \quad \mathbf{3.3}$$

Being in stationary conditions ($\frac{\partial v}{\partial s} = 0$) and with pure lateral slippage ($\varphi = 0$), you get:

$$\frac{\partial v}{\partial x} = -tg\alpha \quad \mathbf{3.4}$$

The variation of the linear lateral deformation of the bristles can be obtained by integrating the (3.4):

$$\frac{\partial v}{\partial x} = -tg\alpha \quad \mathbf{3.5}$$

The (3.5) allows to determine the lateral force F_y and the self-aligning moment M_z with the introduction of the cornering stiffness per unit length c_{py} of the single element:

$$F_y = \int_{-a}^a q_y(x) dx = c_{py} \int_{-a}^a (a-x)tg\alpha dx = 2c_{py}a^2tg\alpha \quad \mathbf{3.6}$$

$$M_z = - \int_{-a}^a q_y(x) \cdot x dx = -c_{py} \int_{-a}^a (a-x)tg\alpha \cdot x dx = -\frac{2}{3}c_{py}a^3tg\alpha \quad \mathbf{3.7}$$

where $q_y(x)$ is the distribution function of the lateral force. Once reached the maximum deformation v_{max} , the trend changes trend and becomes parabolic. In order to get a formulation of the lateral force in the sliding zone, it is necessary to define the vertical load that depends on the parabolic pressure distribution $q_z(x)$:

$$F_z = \int_{-a}^a q_z(x) dx \quad \mathbf{3.8}$$

$$q_z(x) = kx^2 + c \quad 3.9$$

The two coefficients can k and c can be determined by setting the boundary conditions of the vertical pressure distribution q_z . This step allows to write the pressure distribution function of the vertical load F_z :

$$q_z(x) = \frac{3F_z}{4a} \cdot \left[1 + \left(\frac{x}{a} \right)^2 \right] \quad 3.10$$

$$|q_{y,max}(x)| = \mu \cdot q_z(x) = \mu \frac{3F_z}{4a} \cdot \left[1 + \left(\frac{x}{a} \right)^2 \right] \quad 3.11$$

Where μ is the friction coefficient. By means of the cornering stiffness c_{py} , it is possible to obtain the maximum lateral deflection v_{max} that separates the adherence zone from the sliding one:

$$v_{max} = \frac{q_{v,max}}{c_{py}} \quad 3.12$$

$$\theta_y = \frac{2c_{py}a^2}{3\mu F_z} \quad 3.13$$

By imposing the parameter θ_y , (**3.13**) constant, you can determine the length of the contact patch a that depends quadratically on the vertical load.

$$a = \sqrt{\frac{3\mu F_z \theta_y}{2c_{py}}} \quad 3.14$$

In order to get the final expression of the lateral force F_y , included the contribution of the sliding zone, it is useful to introduce the dimensionless parameter λ , so that the transition point x_t is 2λ far from the point of attack:

$$(a - x_t) = 2a\lambda \quad 3.15$$

The transition between adherence and sliding zone occurs when the lateral load q_y equals the value of $q_{y,max}$:

$$|q_y| = c_{py}(a - x_t) \cdot |tg\alpha| = |q_{y,max}| = \frac{c_{py}}{2c_{py}\theta_y} (a - x_t)(a + x_t) \quad 3.16$$

From the (3.16) you get the expression of λ :

$$\lambda = 1 - \theta_y |tg\alpha| \quad \mathbf{3.17}$$

The (3.17) is fundamental for the derivation of the side slip angle in condition of total lateral slip (α_{sl}), obtained by imposing $\lambda = 0$:

$$tg\alpha_{sl} = \frac{1}{\theta_y} \quad \mathbf{3.18}$$

At this point it is possible to derive the complete expression of lateral force F_y and the self-aligning moment M_z , separating the adhesion zone ($a > x > x_t$) from the sliding zone ($x_t > x > -a$):

$$F_y = c_{py} \int_{x_t}^a (a-x)\sigma_y dx + c_{py} \int_{-a}^{x_t} \frac{(a^2 - x_t^2)}{2a\theta_y} dx \quad \text{if } |\alpha| < \alpha_{sl} \quad \mathbf{3.19}$$

$$F_y = c_{py} \int_{-a}^a \frac{(a^2 - x_t^2)}{2a\theta_y} dx \quad \text{if } |\alpha| > \alpha_{sl} \quad \mathbf{3.20}$$

$$M_z = c_{py} \int_{x_t}^a (a-x)\sigma_y \cdot x dx + c_{py} \int_{-a}^{x_t} \frac{(a^2 - x_t^2)}{2a\theta_y} \cdot x dx \quad \text{if } |\alpha| < \alpha_{sl} \quad \mathbf{3.21}$$

$$M_z = c_{py} \int_{-a}^a \frac{(a^2 - x_t^2)}{2a\theta_y} \cdot x dx \quad \text{if } |\alpha| > \alpha_{sl} \quad \mathbf{3.22}$$

where σ_y is the theoretical sliding slip. Then:

$$v = (a-x)\sigma_y \quad \mathbf{3.23}$$

By integrating the previous relationships, you get the analytical form of the lateral force F_y and the self-aligning moment M_z :

$$F_y = \mu F_z (1 - \lambda) sgn(\alpha) = 3\mu F_z \theta_y \sigma_y \cdot \left[1 - |\theta_y \sigma_y| + \frac{(\theta_y \sigma_y)^2}{3} \right] \quad \text{if } |\alpha| < \alpha_{sl} \quad \mathbf{3.24}$$

$$F_y = \mu F_z sgn(\alpha) \quad \text{if } |\alpha| > \alpha_{sl} \quad \mathbf{3.25}$$

$$M_z = \mu F_z \lambda^3 a (1 - \lambda) \operatorname{sgn}(\alpha) = -\mu F_z a \theta_y \sigma_y \left[1 - 3|\theta_y \sigma_y| + 3(\theta_y \sigma_y)^2 - |\theta_y \sigma_y|^3 \right] \quad \text{if } |\alpha| < \alpha_{sl} \quad \mathbf{3.26}$$

$$M_z = 0 \quad \text{if } |\alpha| > \alpha_{sl} \quad \mathbf{3.27}$$

Furthermore, it is possible to obtain the expression of the pneumatic trail t :

$$t = -\frac{M_z}{F_y} = \frac{1}{3} a \frac{\left[1 - 3|\theta_y \sigma_y| + 3(\theta_y \sigma_y)^2 - |\theta_y \sigma_y|^3 \right]}{1 - |\theta_y \sigma_y| + \frac{(\theta_y \sigma_y)^2}{3}} \quad \text{if } |\alpha| < \alpha_{sl} \quad \mathbf{3.28}$$

$$t = 0 \quad \text{if } |\alpha| > \alpha_{sl} \quad \mathbf{3.29}$$

In **Figure 3.4** it is possible to observe the general trend of the physical quantities calculated previously.

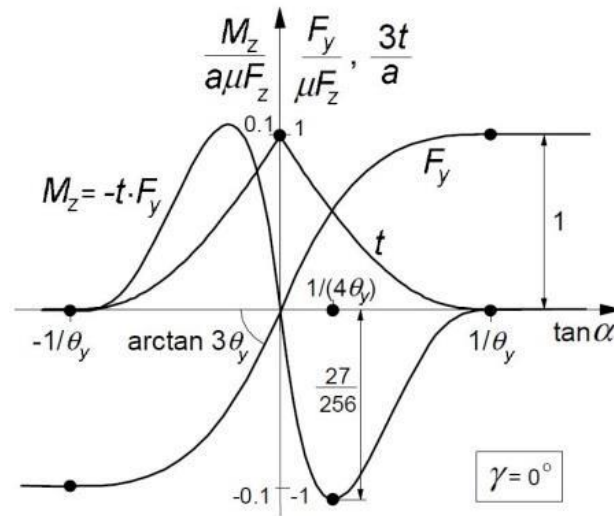


Figure 3.4 – Brush model: F_y and M_z trends function of the side slip angle α [1].

3.1.2 Pure longitudinal slip condition

The procedure to obtain the analytical expression of the longitudinal force F_x is similar to that one discussed before for the lateral force F_y and the self-aligning moment M_z . Now the case of pure longitudinal slippage is considered ($\alpha = 0$), which implies that the vector \vec{V} is directed as the x axis ($V = V_x$). It is necessary to introduce of some of the physical quantities that characterize the longitudinal motion of the tyre.

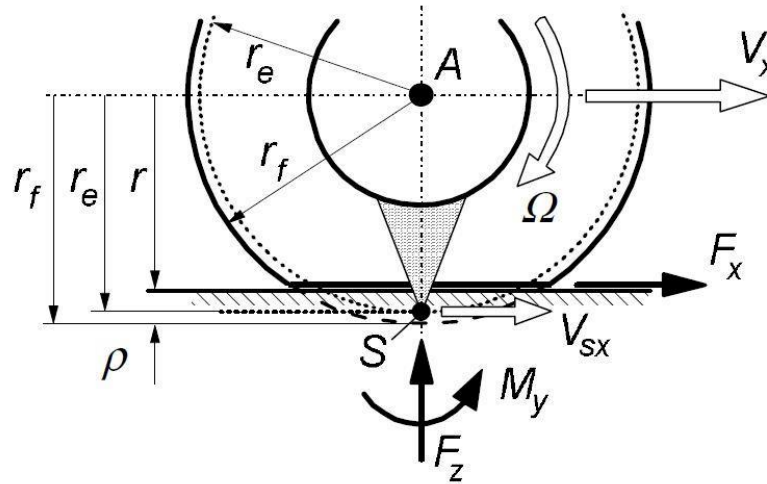


Figure 3.5 – Brush model: effective rolling radius and longitudinal sliding velocity [1].

Figure 3.5 shows the difference between the undeformed rolling radius r_f and the effective rolling radius r_e : this is induced by the vertical load applied on the tyre even when there are no torques applied. Since the contact area is extended rather than point-like, also circumferential deformations occur. The effective rolling radius r_e is defined as:

$$r_e = \frac{V_x}{\Omega_0} \tag{3.30}$$

where Ω_0 is the angular speed in pure rolling condition. The driving and the traction torques applied on the tyre induce a further deformation of the bristles, leading to a sliding velocity V_{sx} in the contact zone:

$$V_{sx} = V_x - \Omega \cdot r_e \tag{3.31}$$

A different speed profile in proximity of the ground leads to a longitudinal slip s :

$$s = -\frac{V_{sx}}{V_x} = -\frac{V_x - \Omega \cdot r_e}{V_x} = \frac{\Omega}{\Omega_0} - 1 \tag{3.32}$$

The longitudinal slip defined in (3.30) is taken positive during traction and negative during braking. Now it is possible to analyse the brush model in pure longitudinal slip condition, using as reference the **Figure 3.6**.

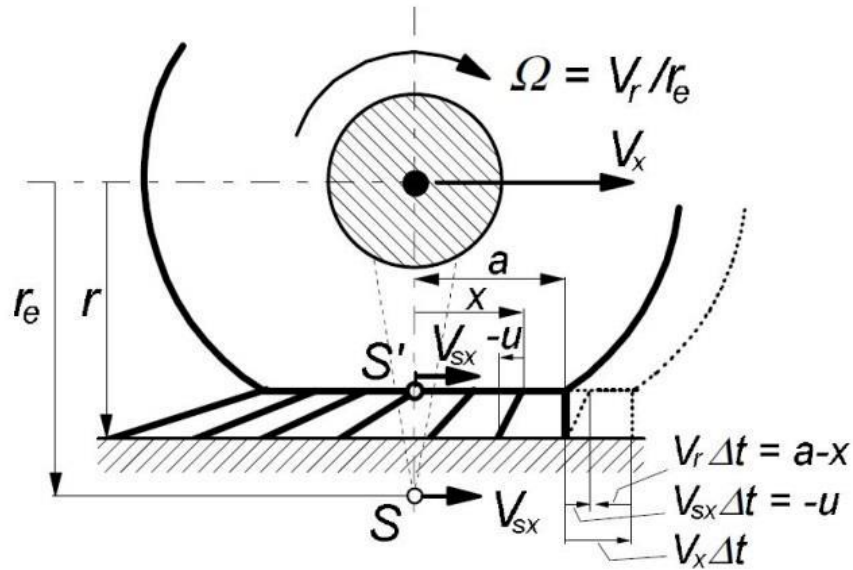


Figure 3.6 – Brush model: lateral view in braking condition [1].

The bristles are rigidly connected to the ring and enter vertically in the contact region. In the absence of longitudinal slip ($V_{sx} = 0$), they remain perpendicular to the ground and the longitudinal force is null. Instead, when a braking or traction force is applied, a relative velocity between the bristle tips and the ground occurs. The peripheral speed of the bristles is defined as follows:

$$V_r = \Omega \cdot r_e = V_x - V_{sx} \quad \mathbf{3.33}$$

The adherence condition is ensured when the bristle is subjected to a deformation u in the longitudinal direction:

$$u = -V_{sx} \cdot \Delta t = -V_{sx} \cdot \frac{a - x}{V_r} = -(a - x) \cdot \frac{V_{sx}}{V_x - V_{sx}} = (a - x) \frac{s}{1 + s} \quad \mathbf{3.34}$$

By rearranging the deformation in the longitudinal direction in the same way as the lateral case (3.21), you get to the following relationship:

$$\sigma_x = -\frac{V_{sx}}{V_r} = \frac{s}{1 + s} \quad \mathbf{3.35}$$

$$u = (a - x) \cdot \sigma_x \quad \mathbf{3.36}$$

The parameter θ_x is introduced in order to derive the limit longitudinal slip s_{sl} , that determines the transition phase from adherence to sliding:

$$\theta_x = \frac{2c_{px}a^2}{3\mu F_z} \tag{3.37}$$

$$s_{sl} = -\frac{1}{1 \pm \theta_x} \tag{3.38}$$

And finally, the longitudinal force F_x expression:

$$F_x = 3\mu F_z \theta_x \sigma_x \cdot \left[1 - |\theta_x \sigma_x| + \frac{(\theta_x \sigma_x)^2}{3} \right] \quad \text{if } s < s_{sl} \tag{3.39}$$

$$F_x = \mu F_z \operatorname{sgn}(s) \quad \text{if } s > s_{sl} \tag{3.40}$$

At this point it is possible to consider the combined case with both longitudinal and later slippage, as illustrated in **Figure 3.7**.

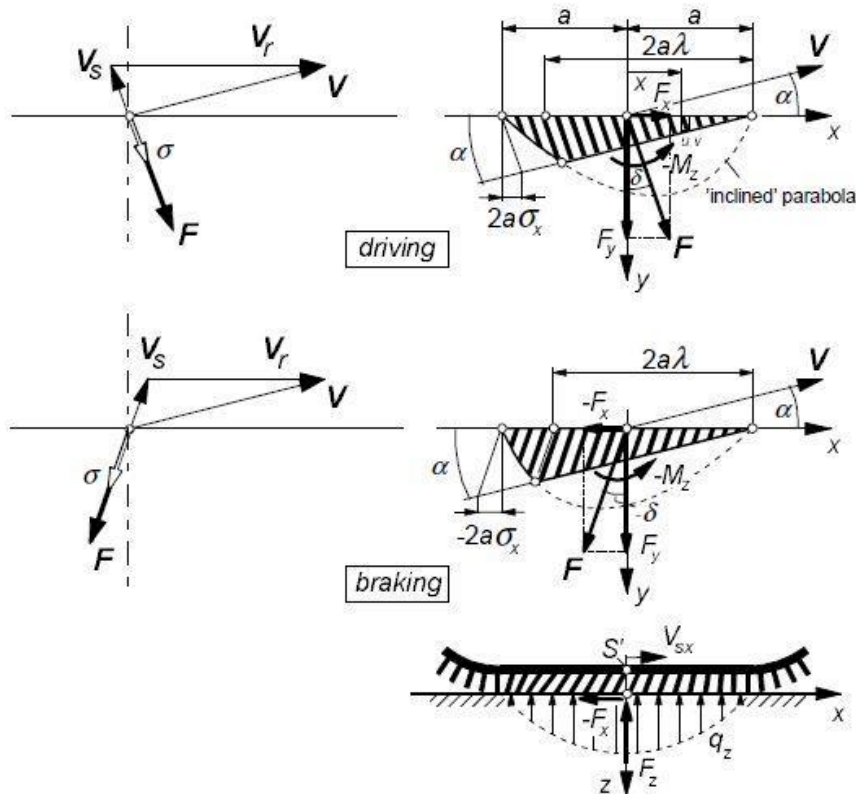


Figure 3.7 – Brush model: combined slip condition [1].

3.1.3 Combined slip condition

If the tyre exchanges simultaneously longitudinal and lateral force with the ground, as matter of fact the adherence in both the directions is lower with respect to the pure slip condition. In order to go deeper in the description, it is necessary to make some assumptions on the isotropic behaviour of the tyre:

- same brush stiffness in both the directions:

$$c_p = c_{py} = c_{px}$$

- uniform and constant friction coefficient:

$$\mu = \mu_x = \mu_y$$

Given these hypotheses, the bristle deformation is split along the two directions, with u and v components. In **Figure 3.10**, the velocity triangles that link the forward velocity V , the sliding velocity V_s and the rolling velocity V_r are illustrated. Since the following analysis takes into account two different directions, it is necessary to adopt vector quantities.

The deflection in the adherence zone (**3.39**) and the theoretical slip (**3.40**) are written in vector form:

$$\vec{e} = \begin{pmatrix} u \\ v \end{pmatrix} = \vec{V}_s \cdot \Delta t = -\frac{\vec{V}_s}{V_r} \cdot (a - x) \quad \mathbf{3.41}$$

$$\vec{\sigma} = \begin{pmatrix} \sigma_x \\ \sigma_y \end{pmatrix} = \frac{\vec{V}_s}{V_r} = -\frac{\vec{V}_s}{V_r} \cdot \begin{pmatrix} V_{sx} \\ V_{sy} \end{pmatrix} \quad \mathbf{3.42}$$

The theoretical slippages are then introduced in order to simplify the computations:

$$\sigma_x = \frac{s}{1 + s} \quad \mathbf{3.43}$$

$$\sigma_y = \frac{tg\alpha}{1 + s} \quad \mathbf{3.44}$$

The (**3.41**) and the (**3.42**) allow to express the longitudinal and lateral deflection as function of the corresponding slips. Even the horizontal load needs to be written in vector form:

$$\vec{q} = c_p \cdot (a - x) \cdot \vec{\sigma} \quad \text{if } q < \mu q_z \quad \mathbf{3.45}$$

$$\vec{q} = -\frac{\vec{V}_s}{V_s} \cdot \mu q_z = \frac{\vec{\sigma}}{\sigma} \cdot \mu q_z \quad \text{if } q \geq \mu q_z \quad \mathbf{3.46}$$

where $q = \sqrt{q_x^2 + q_y^2}$, $V_s = \sqrt{V_{sx}^2 + V_{sy}^2}$ and $\sigma = \sqrt{\sigma_x^2 + \sigma_y^2}$.

At this point it is necessary the transition condition coordinates, as seen in the previous formulations:

$$c_p \cdot (a - x) \cdot \sigma = \frac{3}{4} \mu F_z \cdot \frac{a^2 - x_t^2}{a^3} \rightarrow x_t = a \cdot (2\theta\sigma - 1) \quad \mathbf{3.47}$$

Thanks to the isotropy hypothesis, the definition of the parameter λ is equivalent to the (3.17):

$$\lambda = 1 - \theta\sigma \quad \mathbf{3.48}$$

Now it is possible to determine the limit slip expression σ_{sl} , that indicates the transition from adherence to sliding zone:

$$\sigma_{sl} = \frac{1}{\theta} \quad \mathbf{3.49}$$

Finally, the derivation of the final expression of the force F is made possible:

$$F = \mu F_z (1 - \lambda^3) = \mu F_z \cdot [3\theta\sigma - 3(\theta\sigma)^2 + (\theta\sigma)^3] \quad \text{if } \sigma < \sigma_{sl} \quad \mathbf{3.50}$$

$$F = \mu F_z \quad \text{if } \sigma \geq \sigma_{sl} \quad \mathbf{3.51}$$

$$\vec{F} = F \cdot \frac{\vec{\sigma}}{\sigma}; \quad F_x = F \cdot \frac{\sigma_x}{\sigma}; \quad F_y = F \cdot \frac{\sigma_y}{\sigma} \quad \mathbf{3.52}$$

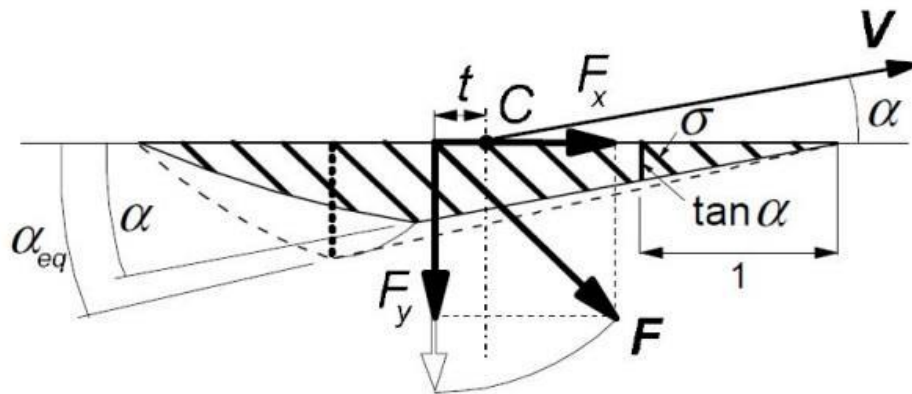


Figure 3.8 – Brush model: equivalent side slip angle α_{eq} [1].

For what concerns the self-aligning moment M_z in combined slip situations, it can be derived by multiplying the lateral force F_y and the pneumatic trail t . The expression of t is the same of the pure lateral slip conditions, except for the equivalent side slip angle α_{eq} (represented in **Figure 3.8**) which takes into account also the longitudinal slip such that $tg(\alpha_{eq}) = \sigma$:

$$t = \frac{1}{3} a \frac{1 - 3|\theta\sigma| + 3(\theta\sigma)^2 - |\theta\sigma|^3}{1 - |\theta\sigma| + \frac{(\theta\sigma)^2}{3}} \rightarrow M_z = -t(\sigma) \cdot F_y \tag{3.53}$$

For demonstration purposes, the characteristic behaviour of the brush model is represented below in combined sliding condition, with reference to the textbook “Tire and Vehicle Dynamics” [1].

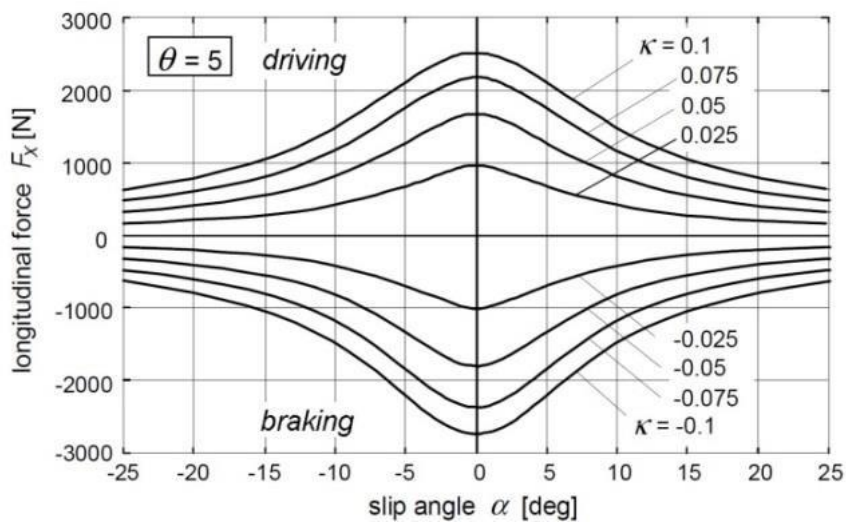


Figure 3.9 – Brush model: $F_x(\alpha)$ [1].

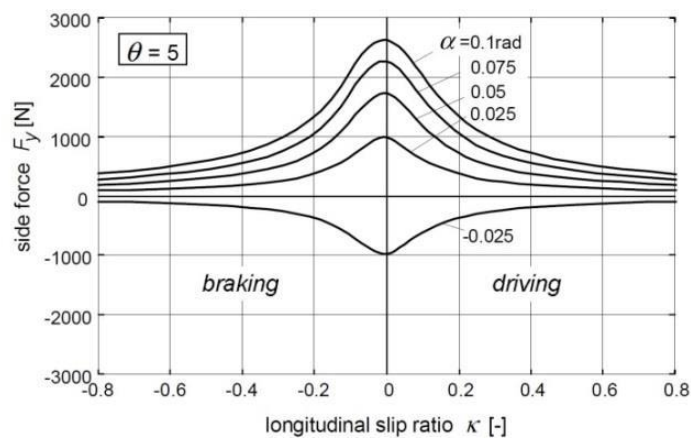


Figure 3.10 – Brush model: $F_y(\kappa)$ [1].

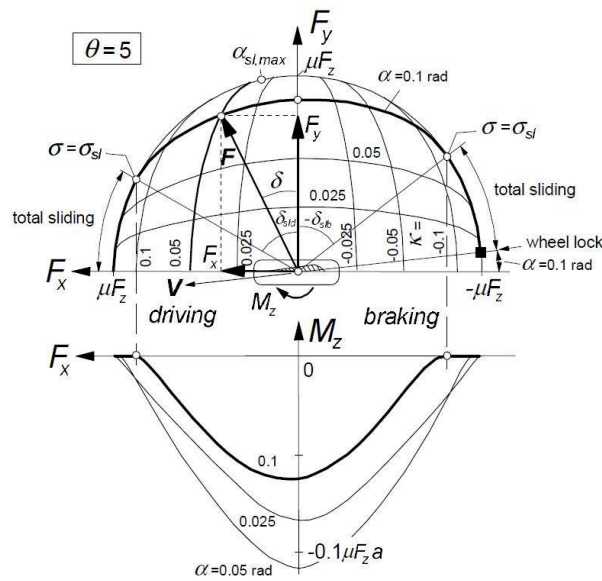


Figure 3.11 – Brush model: $F_y(-F_x)$ [above], $M_z(-F_x)$ [below] [1].

3.1.4 Carcass flexibility

The brush model is able to predict the tyre behaviour with a good approximation. The deviation from the experimental data is due to the strong assumptions made at the beginning. Despite the presented model presents some limitations, it is possible to introduce other features to the model in order to get more reliable data, increasing consequently its complexity.

By introducing the flexibility of the carcass, a more realistic trend of the self-aligning moment M_z can be obtained, coherently with the experiments. The new carcass can be schematized as a line parallel to the contact zone, as shown in Figure 3.13.

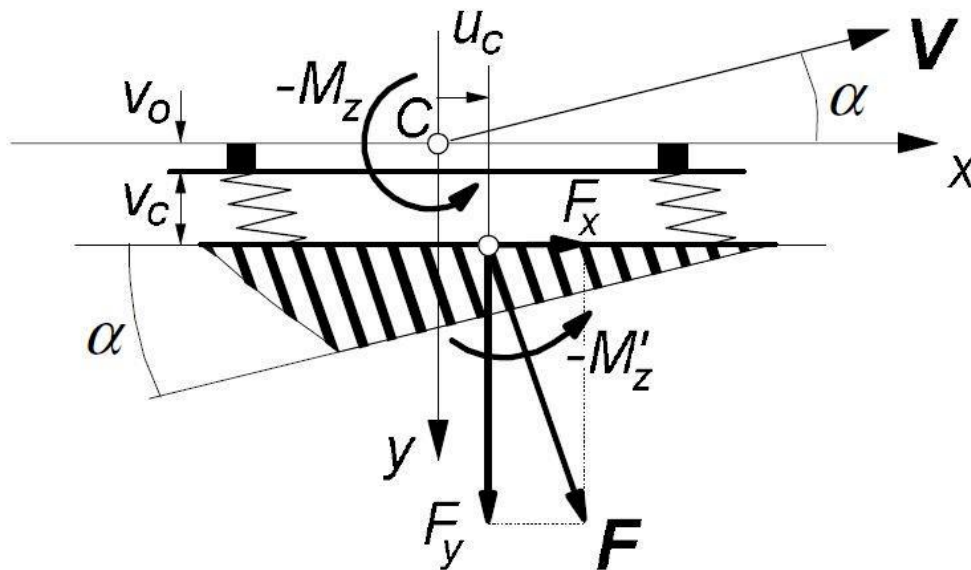


Figure 3.12 – Brush model: flexible carcass [1].

The introduction of the longitudinal and lateral stiffness of the carcass, defined respectively C_{cx} and C_{cy} (with $C_{cx} \gg C_{cy}$), allow to determine the deformations u_c and u_v in both the directions:

$$u_c = \frac{F_x}{C_{cx}}; \quad u_v = \frac{F_y}{C_{cy}} \tag{3.54}$$

The resulting moment is equals to the sum of the self-aligning moment of the previous model (M'_z in **Figure 3.15**) and the contributions due to F_x and F_y . Because of the carcass flexibility, the longitudinal and the lateral forces do no more act in the contact point C , but in a second point that takes into account the carcass deformations u_c and u_v :

$$M_z = M'_z - F_x \cdot (v_0 + v_c) + F_y \cdot u_c \tag{3.55}$$

The behaviour of (3.53) is shown in **Figure 3.13**.

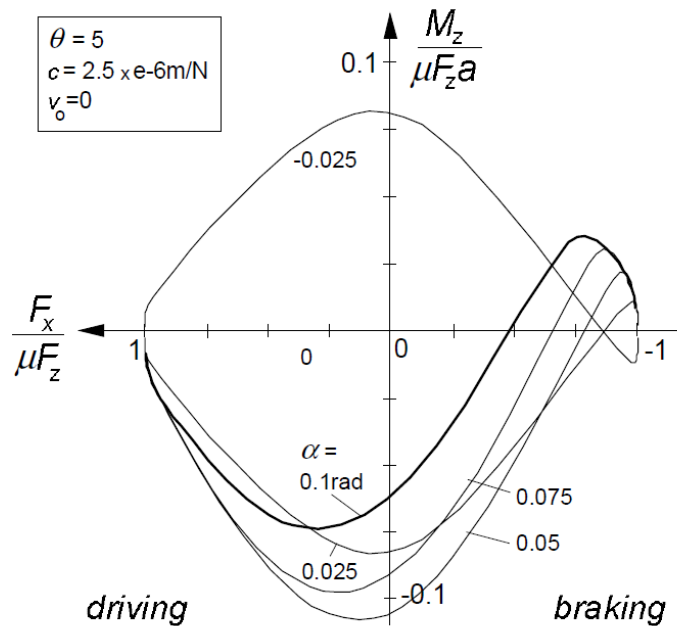


Figure 3.13– Brush model, flexible carcass: $M_z(-F_x)$ [normalized] [1].

It is important to underline that in the literature [1], the brush model is deeper analysed with the addition of more complex features, leading to a very consistent prediction of the tyre response subjected to a wide range of boundary conditions. The introduction to the brush model, reported in this chapter, describes the physical phenomena of the tyre-road interaction with a basic approach, in order to better understand the algorithm adopted in rFactor2.

3.2 Rubber friction model

Tread rubber characteristics play an important role in the tyre force generation as they govern the tread stiffness, the friction properties and the heat generation.

As pointed out in [2], the friction force generated between the tread and the ground is mainly composed by two contributions: the hysteresis and the molecular adhesion. The first one comes from the intrinsic visco-elastic properties of the rubber: when the tyre slides, the asperities of the asphalt exert oscillating forces on the tread surface (“indentation”), leading to cyclic deformations and to energy dissipation because of the damping of the rubber. The second contribution, instead, is due to the molecular bonding between the rubber chains and the molecules of the track (“molecular adhesion”): this strongly depends on the average roughness of the ground and plays an important role during sliding. The adhesion and hysteresis phenomena are represented in **Figure 3.14**.

A brief explanation of the friction mechanism is presented, with reference to [3], [4] and [9].

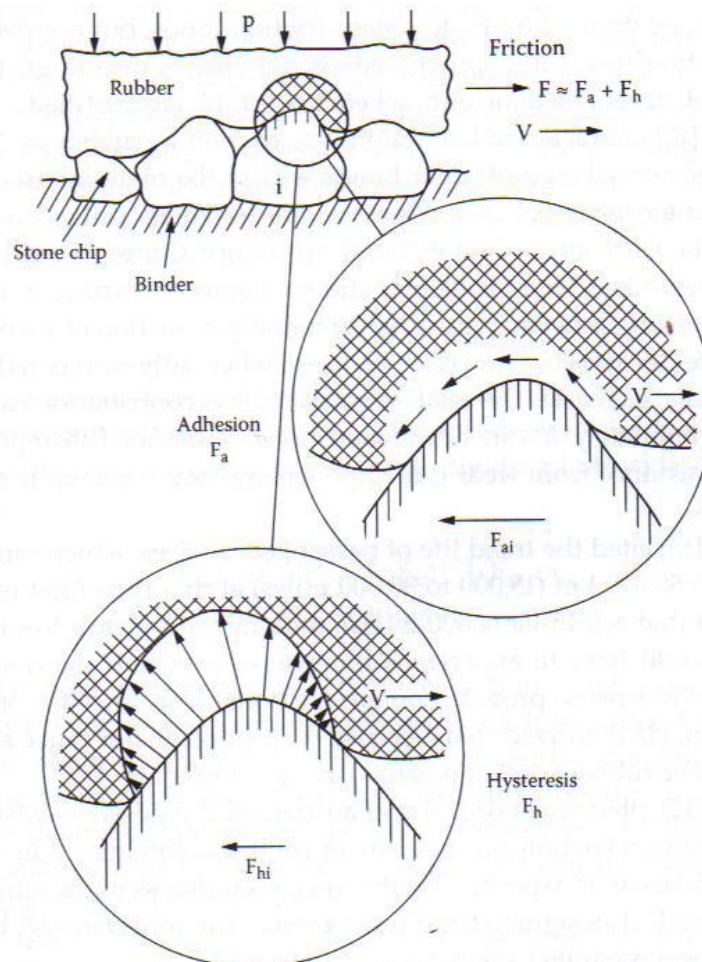


Figure 3.14 –Rubber model: hysteresis and molecular adhesion [2].

3.2.1 Indentation

The indentation mechanism is due to the contact between the tyre tread and the road roughness topology: when sliding, the rubber is subjected to a compression-relaxation cycles (**Figure 3.15**).

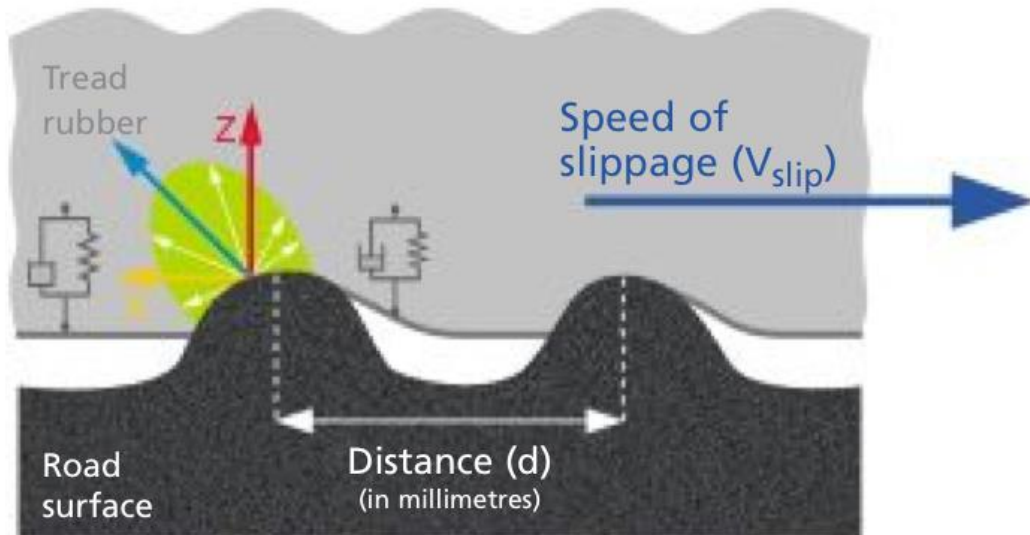


Figure 3.15 – Indentation mechanism of grip generation at road-tire interface [6].

Since the stress-strain behaviour of rubber compounds is not reversible, the constitutive laws for large strains cannot be used. When rubber is dynamically stretched and released the returned energy is less than the energy provided to the rubber. The visco-elastic properties of the rubber mainly depend on the temperature and on the external excitations (amplitude and frequency). The relationship between the stress σ and the strain ε is the following:

$$\sigma = E^* \cdot \varepsilon = (E' + iE'')\varepsilon \quad 3.56$$

E^* represents the complex modulus and consists of two components: the storage modulus E' , that relates to the energy storage involved by the stress component proportional to the strain, and the loss modulus E'' , that relates to the energy dissipation involved by the stress component proportional to the strain rate. The dissipation factor, that describes the proportion between the viscous and the elastic behaviour, is defined as follows:

$$\tan \delta = \frac{E''}{E'} \quad 3.57$$

As result of DMA measurements [3], it is observed a monotonic decreasing trend of both energies with the increase of the temperature. However, the different gradient of the two curves assumes a relevant meaning in the dissipation factor behaviour: in fact, it manifests a peak value that shifts toward higher temperature when the rubber element is subjected at higher excitation frequencies. **Figure 3.16** summarises the trend of the three functions.

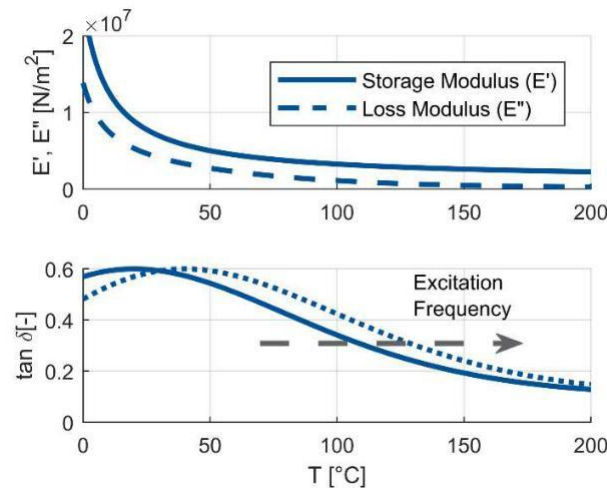


Figure 3.16 – Rubber model: storage modulus (E'), loss modulus (E'') and dissipation factor ($\tan \delta$) as a function of temperature [3].

The so-called glass transition temperature T_g is a fundamental parameter that indicates the limit temperature under which a polymer shows a glassy behaviour. It is possible to see experimentally that if the frequency of the test is increased, the temperature at which it is possible to observe the glassy transition shifts towards higher values [5]. In the same way if the frequency is reduced, the temperature of the maximum decreases. This means that exciting the material at higher frequencies is equivalent to excite it at lower temperatures and vice-versa.

Race compounds are designed to express their maximum performance in terms of grip coefficient in a very narrow range of temperatures (about 5 °C wide), where the hysteresis and the flexibility of the rubber are simultaneously maximized (**Figure 3.17**). Once beyond the transition temperature T_g , the tread tears itself apart causing blistering, graining and premature wear.

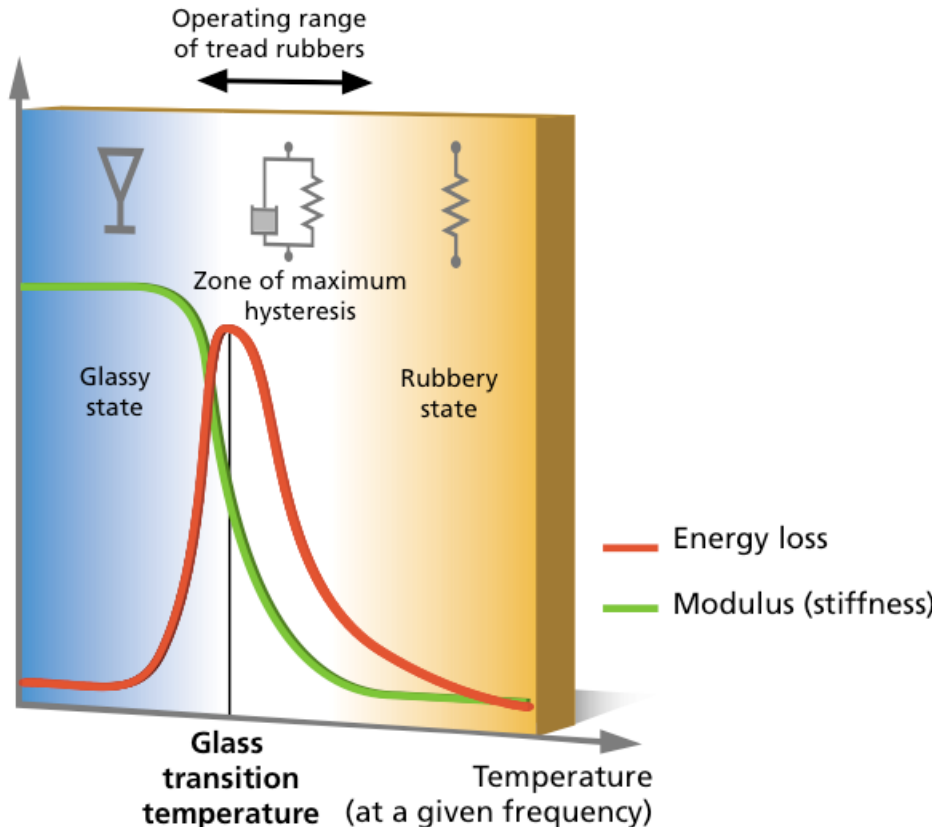


Figure 3.17 – Hysteresis and modulus of tire rubber as function of temperature [6]

The WLF law (3.56) describes the relationship between the rubber properties as function of temperature and frequency. It provides a powerful frequency-temperature equivalence principle enabling to correlate mechanical behaviour over wide ranges of frequency with temperature:

$$T - T_{ref} = \frac{C_2 \log \frac{f}{f_{ref}}}{C_1 - \log \frac{f}{f_{ref}}} \tag{3.58}$$

where C_1 and C_2 are empirical constants.

3.2.2 Molecular adhesion

The molecular adhesion between the rubber is due to the Van der Waals bonding at the road-rubber interface and it is strictly related to the average roughness of the road. The forces generated by the molecular bonding act tangentially with respect to the contact surface: in contrast to the indentation mechanism, the adhesion is emphasized with smooth road surfaces that allow a larger contact area (**Figure 3.18**). Furthermore, the surface temperature and the sliding velocity strongly affect the bonding energy: the friction coefficient trend is shown in **Figure 3.19**.

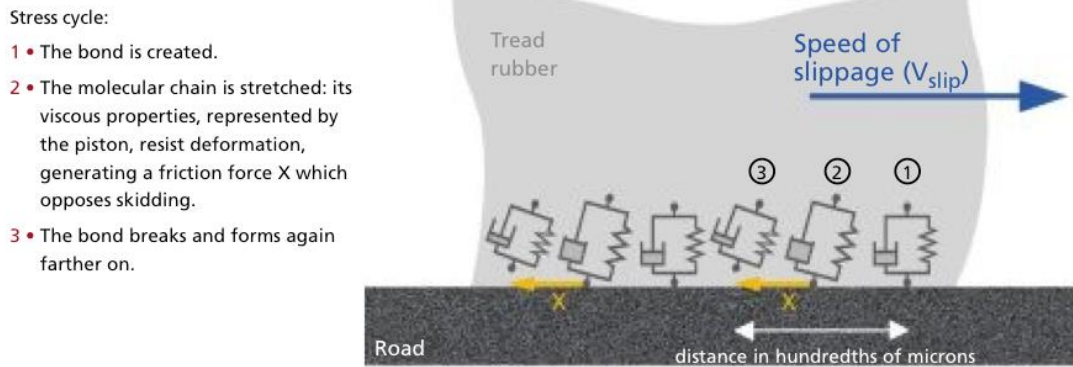


Figure 3.18 – Molecular adhesion mechanism of grip generation at road-tire interface [6].

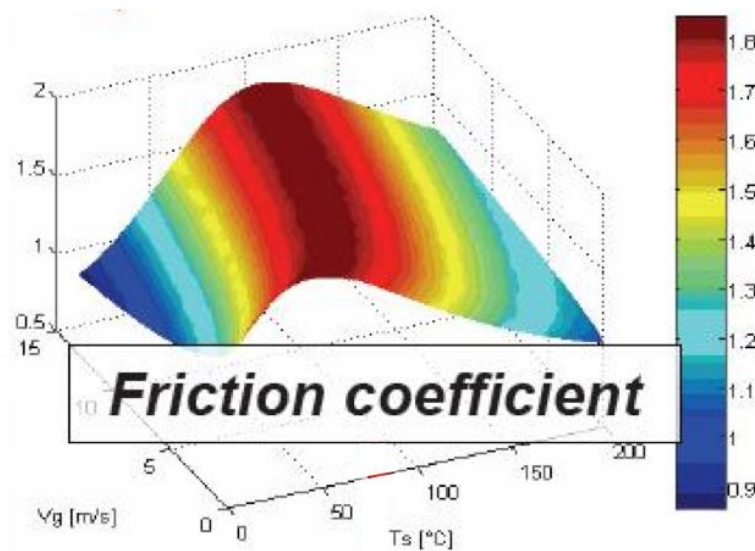


Figure 3.19 – Friction coefficient as a function of sliding velocity and surface temperature [6].

3.3 Thermal models

The way a tyre receives and exchanges heat during its rolling motion is a very complicated aspect to be modelled. The sources of heat generation in a tyre are several and it is quite difficult to predict the right percentage of relevance of each component. In order to simplify the treatment of the topic, a superimposition principle is adopted: with this assumption, it is possible to consider separately each aspect.

In the following pages the thermal model adopted by rFactor2 is presented, with reference to the “TameTire” model developed by Michelin [5]. The following thermal model is subdivided in three main sections: temperature modelling along the contact patch, over the tyre circumference and heat exchange with the ambient air.

3.3.1 Temperature modelling along the contact patch

In the sliding area of the contact patch the dissipated energy due to friction action leads to a rise of the surface temperature of the tyre. In order to get a reasonable estimation of the heat flux between the tread and the contact patch, the theory of the thermal equilibrium between two uniform-semi infinite media can be adopted.

The generic heat flux Q can be written as:

$$Q(t) = \alpha \mu p V_g \quad 3.59$$

where α is the splitting flux between the road and rubber due to friction, μ is the local friction coefficient, p is the contact pressure and V_g is the sliding speed (x, y components). The contact temperature along the contact patch is defined as:

$$T_c(t) = T_0 + \int_0^t \frac{\alpha}{e_r} Q(\xi) \sqrt{\frac{1}{\pi \xi}} d\xi \quad 3.60$$

where $T_0 = \frac{T_s e_{rubber} + T_{track} e_{track}}{e_{rubber} + e_{track}}$ (e is the effusivity) and T_s is the surface temperature of the tread.

3.3.2 Temperature modelling over all the tire circumference

Once derived the analytical expression of the external surface temperature of the tyre along the contact patch, it is possible to get an estimation of the internal core temperature. In order to get this quantity, it is necessary to calculate the heat transfer across the rubber layer starting from an average external temperature that takes into account the whole tyre circumference over a period of rotation. The final result is the combination of different phenomena that occur simultaneously (**Figure 3.20**): heat transfer by conduction with the track in the adherence zone, by friction in the sliding zone and by convection with the ambient air. Additional heating is generated in the tread core due to hysteresis effect.

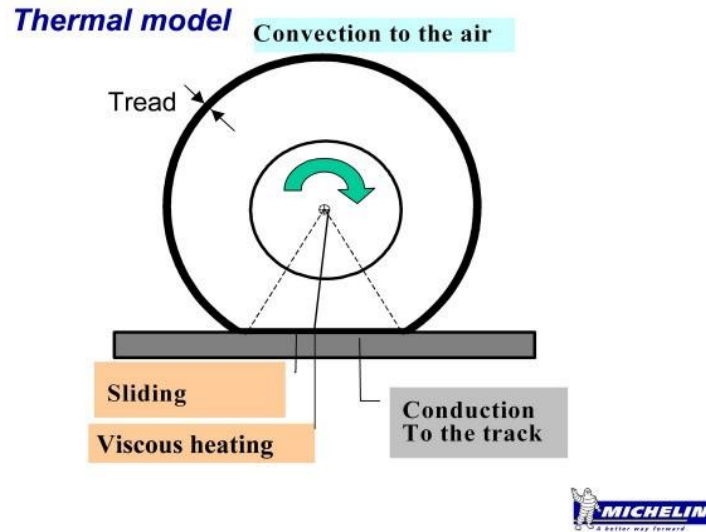


Figure 3.20 –Thermal model: heating and cooling mechanisms for the tread of a rolling tyre [5].

The following model is able to predict the thermal state of the tyre and work in closed loop with tyre force models. It is based on a physical approach, but at the same time it must be light enough to be integrated in real time applications: a trade-off is necessary in this case. Particularly, it is obtained by averaging the equations that govern the heat flux through the tread thickness only in radial direction, neglecting lateral and longitudinal heat transfer. The equation of the heat transfer, based on the Fourier diffusive law, is the following:

$$\frac{\partial T}{\partial t} = \frac{\lambda}{\rho c_p} \frac{\partial^2 T}{\partial X^2} + \frac{\dot{q}}{\rho c_p} \tag{3.61}$$

where X is the radial coordinate.

The previous mentioned contributions are scaled with respect to the effective time frame in which they occur during a complete revolution of the tyre. So, the average through the thickness heat flux over the complete circumference of the tyre is defined as:

$$\varphi = \frac{\varphi_{slide} t_{slide} + \varphi_{track} t_{adc} + \varphi_{air} t_{Hadc}}{t_{adc} + t_{Hadc}} \tag{3.62}$$

where:

- t_{adc} is the time spent by an element of rubber into the contact patch during one period of rotation;
- t_{slide} is the time in the sliding zone of the contact patch;
- t_{Hadc} is the time outside the contact patch.

In the following paragraphs the analytical expression of φ_{slide} , φ_{track} and φ_{air} is provided.

3.3.3 Heat transfer by convection to the ambient air

Convective heat transfer is usually modelled through the use of experimentally determined relationships as functions of the Prandtl and Reynolds numbers. Considering that the wheel rotation induces a turbulent air flow, then the convective heat flux is given by:

$$\varphi_{air} = C_{air} h_{air} (T_S - T_{air}) \quad \mathbf{3.63}$$

where:

- $h_{air} = 0.025 Re_D^{0.8} Pr^{0.33} \frac{D}{\lambda}$
- $Re_D = \frac{\omega D^2}{2\nu}$.

The coefficient C_{air} is a correction factor that refers to the interaction wheel-air ($C_{air} = 1$ for covered wheels car, otherwise for formula cars $C_{air} > 1$ because it takes into account the addition heat exchange due to the oncoming air stream).

3.3.4 Heat transfer by conduction to the track

For what concern the heat transmitted through conduction with the track the relationship is similar to the (3.61):

$$h_{air} = -2 \frac{e_{rubber} e_{track}}{e_{rubber} + e_{track}} \frac{1}{\sqrt{t_{adc} \pi}} \quad \mathbf{3.64}$$

$$\varphi_{track} = h_{track} (T_S - T_{track}) \quad \mathbf{3.65}$$

3.3.5 Heat generation due to friction

The heat generation due to the friction in the sliding zone can be analysed according to the theory of thermal balance between two semi-infinite media. The energy dissipated in the contact patch is:

$$\varphi_{slide} = \frac{V_g F_{slide}}{S_{slide}} \quad \mathbf{3.66}$$

where:

- F_{slide} is the tire force component due to friction;
- S_{slide} is the area of sliding in the contact patch.

The energy dissipated turns into heat which is spread across the two surfaces in contact: the tread rubber and the asphalt. The coefficient α indicates the percentage of heat flux that comes into the tyre.

3.3.6 Viscous heating due to rubber shearing and compression

The hysteresis is the capability of the rubber to returns less force with respect to the one used to deform it and the energy stored generates heat. Temperature and excitation frequency strongly affect this phenomenon. So, the periodical compression and shearing of the tread during its rolling motion leads to temperature built up across the whole thickness of the rubber. Considering W_f the maximum deformation energy of the rubber in the contact patch and Λ the percentage of energy dissipated due to hysteresis, then it is possible to derive the expression of the specific internal heating power \dot{q} at excitation frequency f :

$$\varphi_{slide} = \frac{V_g F_{slide}}{S_{slide}} \quad \mathbf{3.67}$$

where W_f is calculated from the brush model.

Chapter 4. How to build up a tyre in rFactor2

rFactor2 is a wide-spread racing video game greatly appreciated by the users for the possibility to customize or build up your own vehicle, covering every aspect. This is one of the main reasons why Skydrive adopted this virtual platform.

The main problem to deal with is the data collection in order to tune correctly the features of the car. Through the “Driver R&D” program, a close cooperation with the engineers of the racing teams is established: this allows to have access to the car manual and therefore an accurate model of the car can be obtained.

The tyres can be modelled from scratch too, but in this case the data about their physical characteristics are quite impossible to obtain from the manufactures. This leads to a very complex procedure that might give totally off results. In order to obtain reliable results, rFactor2 provides a powerful tool that gives the chance to the users to test their own tyres, called “tTool”. Once launched, it is possible to get a tri-dimensional view of the prototypal tyre and then do some basic tests in order to verify if the final results are coherent.

In this chapter an overview of the “.tgm” file structure and the step by step procedure of the tyre built up is provided.

4.1 Introduction to the “.tgm” file

Every tyre in rFactor2 has its own “.tgm” file that accounts for all the properties needed to run correctly in the gameplay. It is subdivided in four main sections, respectively in this order: [QuasiStaticAnalysis], [Node], [Realtime] and [Lookup]. In this paragraph an overview of the “.tgm” file structure is given: further information about each parameter effect are widely described in [8].

The [QuasiStaticAnalysis] (QSA) section (**Figure 4.1**) accounts for the nominal data (such as mass, inertia, number of nodes and so on) and the set of boundary conditions at which the QSA tests are intended to run: during this process, the tyre is subjected to the nominal lateral and longitudinal forces (“LateralTestForce” and “LongitudinalTestForce”) in every combination of inflation pressure (“GaugePressure”), temperature (“Carcass Temperature”) and angular speed (“RotationSquared”). These tests are carried out through the tyre model introduced in the previous chapter: this is the reason why they last several hours, but the results are very accurate. During the QSA tests the calculation of the contact patch properties are also performed (contact area, pressure distribution, coordinates of the point where the forces act and so on).

```
[QuasiStaticAnalysis]
NumLayers=2
NumSections=238
RimVolume=0.01838
DisplaceBulkMassWithPly=1
PlyCompressionTensionTransition=(-0.00034,0.00105)
UserDTMultiplier=0.2
RealtimeCamberLimit=32
CalcPointAccel=0.72
LateralTestForce=7400
LongitudinalTestForce=3400
GaugePressure=46332.72
GaugePressure=110316
GaugePressure=137895
GaugePressure=177971
GaugePressure=218047
CarcassTemperature=283.15
CarcassTemperature=353.15
CarcassTemperature=416.15
RotationSquared=0
RotationSquared=10191.8
RotationSquared=30560.2
RotationSquared=45840.26
NumNodes=85
TotalMass=7.678073292529414
TotalInertiaStandard=(0.523762938273423,0.3319543475878489,0.33195434758785053)
RingMass=5.761998922205789
RingInertiaStandard=(0.4491896864794103,0.26268298301978255,0.2626829830197779)
```

Figure 4.1 – Virtual tyre “.tgm” file: [QuasiStaticAnalysis] section.

The tyre transversal profile is subdivided in nodes. Each node has its own [Node] section (**Figure 4.2**) that accounts for: node coordinates (“Geometry”), mechanical and thermal properties of the bulk and of the tread (“BulkMaterial” and “TreadMaterial”) and the plies properties (“PlyParams” and “PlyMaterials”). Depending on the position along the profile, the nodes have to comply with the different layers which characterize the tyre construction. In **Figure 4.3** a cross section of the tyre is illustrated: during the definition of the properties of each node this schema must be followed. In fact, these sections affect the intrinsic mechanical and thermal behaviour of the tyre and the QSA tests allow to check if the overall tyre structure give reasonable results in term of vertical, lateral and longitudinal stiffnesses.

```
[Node] // 35
Geometry=(0.040398,-0.287255,0.009644)
BulkMaterial=(273.15,1148,4650000,0.46,1,1250,0.3)
BulkMaterial=(373.15,1126,3490000,0.46,1,1290,0.28)
AnisoCarcassConductivityMult=(2.057,1.753,2.387)
TreadDepth=0.0036
TreadMaterial=(273.15,1180,3822000,0.47,1,1870,0.185)
TreadMaterial=(323.15,1168,3058000,0.47,1,2060,0.181)
TreadMaterial=(373.15,1156,2351000,0.47,1,2250,0.178)
TreadMaterial=(423.15,1145,1556000,0.47,1,2450,0.173)
RingAndRim=(1,0)
PlyParams=(77.01,0.0002264,3)
PlyMaterial=(273.15,1144,3110000000,0.3,0.09,1695,0.25)
PlyMaterial=(373.15,1131,2950000000,0.3,0.09,1715,0.24)
PlyParams=(102.99,0.0002264,3)
PlyMaterial=(273.15,1144,3110000000,0.3,0.09,1695,0.25)
PlyMaterial=(373.15,1131,2950000000,0.3,0.09,1715,0.24)
PlyParams=(26.05,2.729e-005,3)
PlyMaterial=(273.15,7907,106000000000,0.3,0.29,465,26)
PlyMaterial=(373.15,7879,103000000000,0.3,0.29,484,25)
PlyParams=(153.95,2.729e-005,3)
PlyMaterial=(273.15,7907,106000000000,0.3,0.29,465,26)
PlyMaterial=(373.15,7879,103000000000,0.3,0.29,484,25)
```

Figure 4.2 – Virtual tyre “.tgm” file: [Node] section.

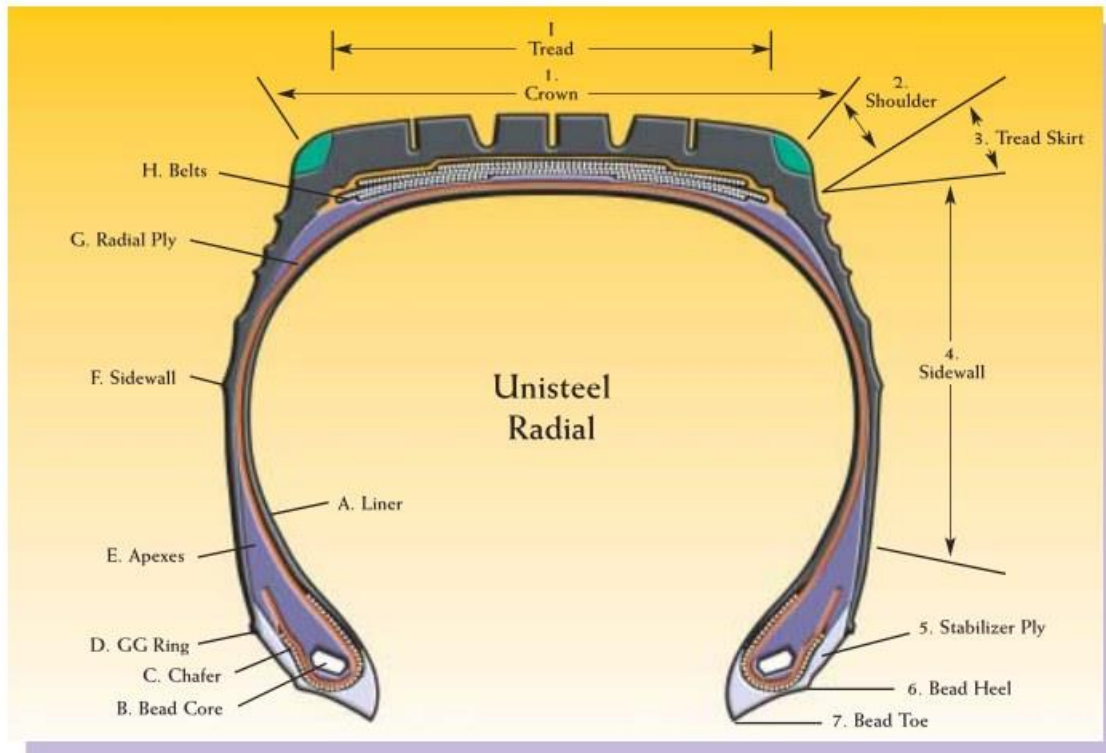


Figure 4.3 – Cross section of a radial road tyre: nomenclature.

Once defined and tested with positive results the tyre structure, the compilation of the [Realtime] section takes place (**Figure 4.4**). As suggested by the name itself, this section of the “.tgm” file accounts for those parameters that affect the behaviour of the tyres during the gameplay: in this way the final adjustments can be tested immediately, without performing again the QSA tests. The optimisation process, widely discussed in the next chapter, is focused only on this part of the file “.tgm” for reasons of time and lack of data, with the assumption that the material properties of the nodes are correctly compiled.

```
[Realtime]
StaticBaseCoefficient=3.2657
SlidingBaseCoefficient=2.2857
StaticDiffusiveAdhesion=(0.001, 4800, 0.5)
SlidingDiffusiveAdhesion=(0.001, 800, 0.5)
AbrasionCurveWLFStartStep=(-8.5, 0.5)
AbrasionVolumePerUnitEnergy=(1.15E-9, 9.8e-10, 8.43e-10, 7.25e-10, 6.1
DegradationPerWearFraction=(0.99, 1, 0.999, 0.9976, 0.9966, 0.9957, 0.99
DegradationCurveParameters=(346.15, 2550)
DegradationPerUnitHistory=(1, 0.985, 0.971, 0.963, 0.958, 0.955, 0.9525, (
MassInertiaMultiplier=(1, 1, 1, 1)
SizeMultiplier=(1, 1)
LoadVsDeflectionMultiplier=1
InclinationExtrapolation=0
LateralDistributionMultiplier=0.95
LongitudinalDistributionMultiplier=0.7
RingStiffnessMultiplier=(1, 1, 1, 0.3, 1, 1)
TemporaryRingDamper=(0.037, 0.055, 0.055, 0.133, 0.087, 0.087)
SpringConditions=(0, 0, 0)
BeltSpringX=(1.166e6, 1.9393, -1219.8507, 2.0394)
BeltSpringZ=(1.308e6, 2.6818, -785.9425, 0.1542)
TemporaryBeltDamper=(31.189, 41.1)
TreadSpringXPerUnitArea=(9.153e8, 105.1865, -1.379e6, -1523.546)
TreadSpringZPerUnitArea=(1.299e9, -732.9861, -1.4741e6, -408.1029)
BaseDamperPerUnitArea=(1355.4, 0.8, 2162.6)
HystereticVerticalDamperPerUnitArea=12000
VerticalDampingMultiplier=(1.6, 1.15, 0.99, 0.98, 0.99, 1.15, 1.6)
MarbleEffectOnEffectiveLoad=-0.1
TerrainWeightOnContactTemperature=0.1
StaticRoughnessEffect=-0.2
WLFParameters=(247.15, 50, -8.86, 51.5)
```

Figure 4.4 – Virtual tyre “.tgm” file: [Realtime] section.

At the end of the “.tgm” file there is the [Lookup] section (Figure 4.5), which contains the numerical results of the QSA tests. These lines are encrypted, so it is not possible to modify them unless repeating the entire test procedure. The lookup table contains all the information about the physics of the tyre under all the possible combinations of load, pressure, temperature and rotational speed: during the gameplay, no calculations are needed to derive the tyre response since they are performed previously by the QSA tests. So, the software simply scans the lookup table and read the information about the tyre in that specific circumstance: in this way it is possible to have a solid and reliable tyre model based on a physical approach and, at the same time, a light algorithm that can run at 2400 Hz.

```
[LookupV2]
Version=1.104
P=UYf7K>W0Z**MQ*M>Ur]_svLC.>Ur]^cqUQp>6^H7hU*>Yg/AM6YQ1:b>Vb@f791jJf>UJ;O/1k/O>UJ;O5kbpZ>Pf7dZq8Yyg
P=>u`kq>Vtqxr@aef<|K>|nW]U)OEJ>\Pd68fWp|>fHNL<[TFO>KVpTQMq>Zgu{K1ya1Yq>t3k|8B>gM>kb~*7V~N~>\1Fpc
P=@FTDQg_zA1\n^pO>Xc.(A,b{>Se,U4Npz->S^U]0mr, Pg`,{fTNjp>X_<gyX}7D>T[m:h0Q+>S`HWtBCP2g`2~*060.v>
P=g`9Lr-;hUs>XPuL`*6e|>V31}.RbaD>SeSBddK?cg`?mAo7{cm>XSRBtmzpp>U{BIgdh>n>Sgjjz:Qu:kg`F;p-sTD|>XUOs3
P==YF>0>XWc6aY4;=>Ubv=_)CD>\>SkzT,8wDXg`S<FBOxo>X{c^mE4N+>UG0zE08K+>SmVGLdTUTg`Yw{RF2<1>X_qasv9|N>
P=>Xc5@Hmlv|>S|]v4qncS>So@hF+45=g`gpBI:_] \>Xd{v[-.e>Qzq?YfC>k>SoZZHO05Mg`n^f2^Ng1>Xer8ylsN`>M0Jz-
P=ne@HJg^5Ub8cjhI>SnsINE7Ilg`|I,-K\cL>Xa-hnQ{z,g`.?}6UJN?>Sm.=GN`SAGA~/6kCkS>X\@;uSC7qga2GDZzG;A>
P=gaVR>5h.+e>ShgTL]142ga71<@003+>XR3E[7|]Vgarg>Kdtr\>SfP/^PVz:ga9pN^ELS4>XOXV:|{u{gb+*4Ln?o.>ScjM=
P=ze4->S`A:l;+0Bga>N7/VHe>X.Rrv4uungc0`[h~xA,>S[pO;=?16gaBgIM=s9[>WN62=8]sZgcfS^Yi1j>SP]<Nj2JKG
P=>SD,j.GF0`gaEnUy{xRm>Uyg/abE*mgdC{6F-Ine>S7<YOMxg`gaFn^qUQ^Y>U0554@>r/gdMR\Ds1?L>R~y.k_x_ltggaGJPl
P=EA56+gaGg..EXzM>RnRSA)tnsgdTq>*Mn^.>Rd5Xcp_`^*gaH,kUvhu9>RV+LwnM>IgdU3Z[|<Qw>RvE1L3h.[7gaHC0YtXv@>
P=gaHV[fB2rY>Qq0o`esyqgdU`HFGAa4>R;q={4y\gaHfiKltp*>QC1n24c/kgdUnHP.:TA>R.MVBd1TBgaHt@4o`@M>Po?X2
P=Am{vs>PKI?/DjlagdV+B00W:W>Q]1F,h9p-gaI3Q+ZG]_>Ow+143x:BgdV0V1HO`e>QBD-ryy-+gaI:pGyNKm>OC-,Lz8?Dg
P=>NkMf-Cs)qgdV6ad;qS>Pan4G)EgpgaIEG`;zT3>N=^],{9lgdV8@/pEK;>PG0-B>2=RgaIH>QzC1^>MUD17[pi<gdV9Ez
P=JyzMtgdV:+)XN|M>0@B;+KR_(gaImNwaPeQ>L-)[tja0HgDv:NqWX2]>N_u>fM;-<gaIOAs10k.>K>Hf|K~*DgdV:cF^j*mx>
P=gdV:oh0Vc`>Kq~<?7|q0gaIPvlX8Z1>Hm+~6:f?PgDv:uNn|S4={o8M?Mz=UgaIQ;K*PIlg<hpu0?1|XgdV:woa~@LgWbY1;
P=qJvOngYIffp5V01?gaIPA1R)|kgUymxE;<v?gdV:o[q`6pgZPPie?K8mgaIOAl\Z51gW.yk|@*oogdV:cDsm8Cg|0rf|9jfKg
P=g{fApIPVNDgaIKJChL|^gXfT>JnNa9gdV:~p^w8Lg\7`W@IN;-gaIH~SydM,gYEuB7Y4{JgdV9ENeGx6g\RI_F8L07gaIEGc
P=Zg.1*gaI@fL)BrIgz[~+.5q<tgdV6aJj;iTg]2tXr6kX3gaI:pIbPhgg[3]7Nw-d;gdV46X^EzYg]Map-9@>QgaI3QId]fWg
P=gaI`JDkA;5g\yB6huW-gdV+B/fXang]s-;G^fXMGaHt@62j,mq\_oJ?nc`AgdUxhgUL2*g^,Lg2:4v4gaHfjV\OFag]3aPE
P=DZNJ-g]a`5K^:LngdU`HrqB{3g^@vIW[6AgaHCJF9Yh=g]}2GVkc+;gdUMaz^MD7g^Tf,8WT9xgaH,1FH4N-g^FX=R@:FEg
P=g^^@e?durgdQDRH^E>g^oUBt4*x<gaGJQ]seR-g`WfDh\,M/gdSGQ3{43jg^|m3NP`^9gaFn]@_a9Dg`uhoLkLLFGdMRKp
P=7fEUNgdCz]S>T-g`_AbhWJ-g-gaDQp4v,c3gbRD9L[MzWgd6LF,gbgng.LK{>3<ZkgaBgI,1J>-gc>Fckpq~bgcfS30R/bq
P=gc0*WM/vt7g_TEx<IGJbga=0f]yet`gd93Sf4J+cgBh5xCYm2Pg_w+Z]3o.ega9pNdtBhgD@4M]?kx3gb+*. *06D;g_YC*K
P=MpeNyg`_Ihkq-fga3oKcFjr?gdGelG[A-|gaVR>|<wf]g_]gHgqyza--/`CT^gdLpeY]Cm0ga2GG-dY=ig_/?P[C2Xg
P=...>
```

Figure 4.5 – Virtual tyre “.tgm” file: [Lookup] section.

After this preview of the “.tgm” file structure, the step by step procedure of the file compilation is presented.

4.2 Step 1: Data collection

The “.tgm” file compilation is made possible thanks to three spreadsheets released by rFactor2 to the developers. They are subdivided in sequential pages that must be filled out with the appropriate information: the procedure is intuitive and widely commented on, but it requires a lot of data.

So, it all starts from the data collection of the geometrical and mechanical properties of the tyre that you want to model: its physical presence is highly recommended in order to have a good degree of accuracy of the measurements. First of all you need to calculate the mass and obtain the cross sectional geometry and the construction material properties. Except for the first information, the other two require to literally dissect the tyre: so, before that, it is recommended to take several times the necessary measurements and perform some qualitative vertical deflection tests that could come in handy for the later validation phase.

For what concern the determination of the tyre profile shape, the best would be a CAD model or a three-dimensional scan. If not possible, the complete listing of overall dimensions (section width, radius, rim width and rim diameter, etc) can be qualitatively measured with high resolution photographs.

Instead, for what concern the construction properties, a powerful magnet could come in handy to detect if the tyre belts are whether steel or not. Especially in open wheeler tyres with tall sidewalls, steel chafer plies are used in order to stiffen the tyre structure which must sustain high lateral loads. The plies thickness and angle can be determined by means of an x-ray machine or, most likely, by literally pulling the plies apart. Once determined the number of plies and their material composition, the mechanical and thermal properties of such materials can be drawn on a pre-compiled form provided in the “TGM Generator” spreadsheet. If the angles of the plies can not be measured, some typical ranges used by the manufacturers are outlined in the spreadsheet.

4.3 Step 2: Basic implementation

The data collection phase is the most difficult part of the entire tyre build up process. Once finished, it is necessary to rearrange correctly the data within the “TGM Generator” spreadsheet cells. The procedure is time consuming but quite straightforward: the spreadsheet is divided in pages that must be filled in that specific order, since some values are linked to the previous pages.

So, starting from the “General” page, you need to define the overall size and shape of the tyre first and then to provide some basic properties. This part is quite fast and does not require too much effort, however the data must be very accurate before being inserted, since they highly affect all the subsequent sections (**Figure 4.6**).

WIP! This page is primarily intended for beginners and amateurs. I strongly suggest to use the advanced pages, and if you can't understand them, find someone who does to help you. Most of

General / Easy		Offset		Imperial		SI		Size	
Section Width [mm]	277	43.436	0.5089	10.906 in	0.277	10.906 in	0.277	Circumference	1.598756501
Profile [%]	32.4%			20.0354 in	0.25445	20.0354 in	0.25445	Apply	
Construction	R	Radial							
Rim Diameter [in]	13	0	329.4 mm	0.1647 m Rim Lip	0.182	0.1647 m Rim Lip	0.182		
Rim Width [in]	10J	0	254 mm			0.254 m			
Metric Code	275/30 R13								
Target Weight [kg]	5.5		5.50 kg	12.13 lbs	5.5 kg				
Max Pressure [PSI]	26		179.3 kPa	26 PSI	179264 Pa			Hot Approx.	206154 29.9 PSI Rot ²
Speed Rating	Cust325	-15	310 km/h	192.6 mph	86.1 m/s			Rotation	338.42 rad/s 3231.7 rpm
Load Rating	80		450 kg	992.1 lbs	4413 N			Peak Load ~	8384.69 N Corner 14354.6
Tread Depth [in]	16/95		4.28 mm	0.1684 in	0.004278 m				
Tread Width [mm]	235		9.173 in	0.233 m					
Tyre Construction	Quantity	Material	Quantity	Material	Quantity	Material	Quantity	Material	Quantity
Sidewall Ply	4	Polyamide - Aramid Hybrid							
Tread Ply	4	Nylon - 70s							
Type	1		0		0		0		0
Tread Volume	1								
Performance Scale	0.9	Estimated G's		2.14					
UTQG (Unused thus far)									
Tread Wear	100			1					
Traction	AA			0.54	0.44				
Temperature	A								
Fuel Rating	E	Crr Approximation.		0.0109					
Wet Grip	C								
Static Loaded Radius	0.244	0.01045 ~Spring Rate		422295.93 (@ Max Load and Inflation).					
Revolutions Per Mile	888	Effective Rolling Radius		0.28844 m					
Starting Temp. [°C]	20			293.15					
~Optimum Temp. [°C]	80			353.15					
Starting Pressure [psi]	16.5	113.763		113763					
Warm Pressure [psi]	22	151.685		151685					
Car Specifications			Force						
Weight [kg]	650		6374.3225 Wheel Static Load						
Distribution [x:1]	0.388		2473.23713	1236.618565					
Patch Area (tTool) [m ²]	0.01236	Average contact pressure		100050					
Tyre Name	Brand	Size-Rim	Compound	Type	Year	Combined			
G		9.2-20.0-13x10	Soft	Slick	1975	G 9.2-20.0-13x10 Soft Slick 1975.tqm			

Figure 4.6 – “TGM Generator” spreadsheet: “General” section.

The second page is called “Geometry” and it accounts for the tyre shape: basically, you need to insert the coordinates of the nodes (X,Y), with respect to the tyre transversal plane centred in the wheel middle point, and the thickness of the profile along the perimeter: once given these 3 values, the spreadsheet calculates automatically the coordinates of the internal profile. If the tyre construction is symmetric, only half of the nodes are necessary. It is important to underline that the coordinates of the nodes are intended as the tyre is mounted on the wheel, but not inflated. The more the nodes, the better is the potential accuracy of the model, at the expense of longer table generation times. The computational effort increases in a linear way with respect to the number of nodes and it is preferable to add circumferential sections (“NumSections”) to match the higher number of nodes. This procedure lasts for long time because it is very complicated to get reasonable values of the node coordinates: a useful plot projects instantaneously the tyre profile in order to assess qualitatively the overall geometry. In **Figure 4.7** a screenshot of the “Geometry” page is illustrated: in red there are the cells of the coordinates of the nodes, while in blue there are the cells of the tread bounds.

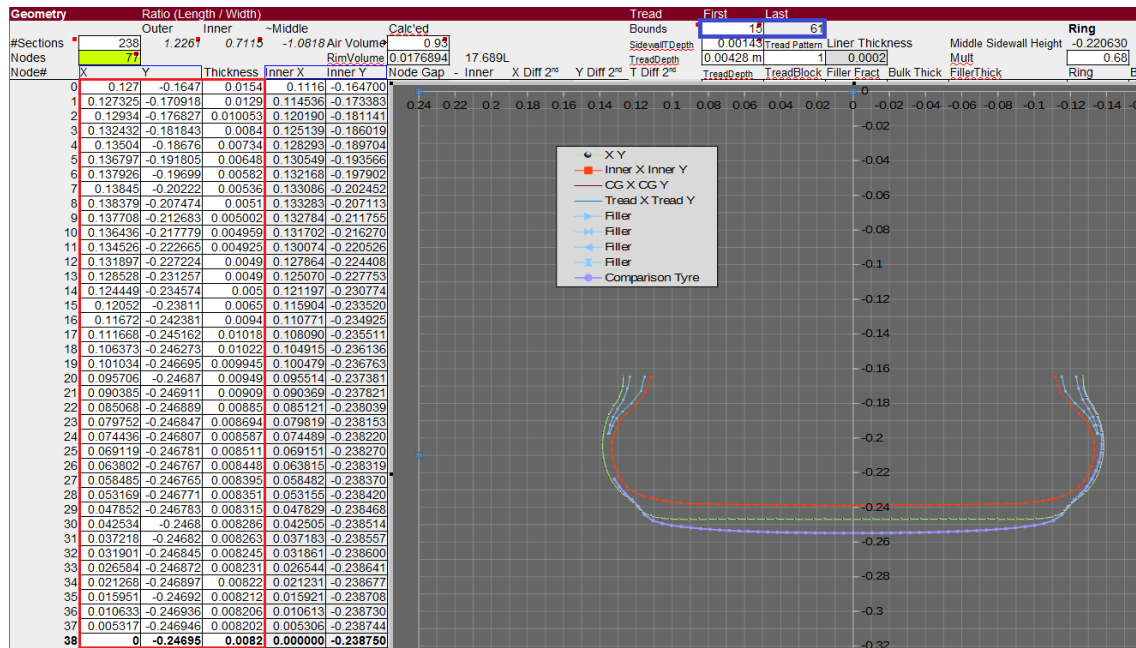


Figure 4.7 – “TGM Generator” spreadsheet: the tyre cross sectional geometry.

When the tyre profile assumes a satisfying shape, it is necessary to implement the material construction properties in terms of rubber and plies by compiling the “Construction” section. For what concern the selection of the rubber properties, the spreadsheet indicates by default the different rubber layers that must be used for the tyre “assembly”: “Tread”, “Tread Sidewall”, “Bulk Bead/Filler”, “Bulk Sidewall” and “Bulk Belt”. Different rubber properties are already implemented and can be selected from the drop-down menu, as illustrated in Figure 4.8. The bounds of each type of rubber are automatically generated in the “Geometry” section (rows L, M, N O, P).

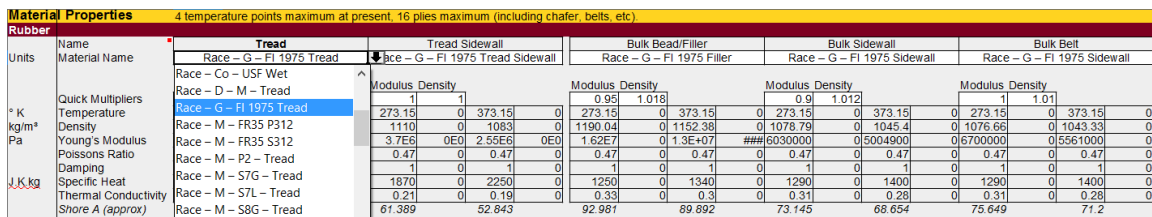


Figure 4.8 – “TGM Generator” spreadsheet: rubber material properties.

A separate discussion must be done for the bead and ply materials: in this case the tyre developer indicates which type of ply material from the drop-down menu, the boundary nodes, the ply thickness and the ply angle. For sure this part is the least intuitive of the overall process and requires experience. Anyway, several comments are provided and some instantaneous plies visualiser are present. In Figure 4.9 and Figure 4.10 illustrate a part of the procedure just described.

Fibre / Ply Materials																
Name	Ply1				Ply2 (Opposite of 1)				Ply3 (turnup)				Ply4 (Opposite of 3)			
Material Name	Nylon - 70s				Nylon - 70s				Nylon - 70s				Nylon - 70s			
Type Section (Min / Max)	Keivar - 70s				Keivar - 70s				Keivar - 70s				Keivar - 70s			
Quick Multipliers	Keivar - Stranded - Outside Dian				Keivar - Stranded - Outside Dian				Keivar - Stranded - Outside Dian				Keivar - Stranded - Outside Dian			
Temperature	Nylon - 66 - Modern				Nylon - 66 - Modern				Nylon - 66 - Modern				Nylon - 66 - Modern			
Density	Nylon - 70s				Nylon - 70s				Nylon - 70s				Nylon - 70s			
Young's Modulus	Nylon - Modern				Nylon - Modern				Nylon - Modern				Nylon - Modern			
Poissons Ratio	Nylon - Old				Nylon - Old				Nylon - Old				Nylon - Old			
Compression-to-Tension Ratio	Nylon - Soft				Nylon - Soft				Nylon - Soft				Nylon - Soft			
Specific Heat	Polyamide - Aramid Hybrid				Polyamide - Aramid Hybrid				Polyamide - Aramid Hybrid				Polyamide - Aramid Hybrid			
Thermal Conductivity	Polyester - Modern - Common				Polyester - Modern - Common				Polyester - Modern - Common				Polyester - Modern - Common			
Conductivity Longitudinal	Polyester - Modern - Common				Polyester - Modern - Common				Polyester - Modern - Common				Polyester - Modern - Common			
Left Length	0.20518612				0.20518612				0.20518612				0.205186119			
Start	0				0				0				0			
End	38				38				38				38			
Modulus	0.875				0.875				0.875				0.875			
Density	1.01				1.01				1.01				1.01			
273.15	0				0				0				0			
1161.5	0				0				0				0			
2.01E9	0E0				0E0				0E0				0E0			
0.3	0				0				0				0			
0.09	0				0				0				0			
1695	0				0				0				0			
0.25	0				0				0				0			
0.9	0				0				0				0			

Figure 4.9 – “TGM Generator” spreadsheet: the ply material properties.

Ply Angle Visualiser, and thickness calculator																		
Whether ply exists	Ply1-2	Ply3-4	Ply5-6	Chafer1	Chafer2	Shoulder	Belt1-2	Belt3-4	Undercap	(1 single ply, 2-add opposing ply (only partially implemented) this is derived from the next sheet 'TGM' Diameter Calculator								
Strand Diameter	0.00064	0.00064	0.00064	0.00064	0.00064	0.00012	0.00012	0.00012	0.00012	28.4444444	Density	1986	Diameter * 0.003868					
Strand Spacing	0.00099	0.00099	0.00099	0.00099	0.00099	0.00099	0.00099	0.00099	0.00099	25.95959	Denier	210	Diameter * 0.008205					
Strand Cross Section	3.21699087728E-07	3.2E-07	3.2E-07	3.2E-07	3.217E-07	0.1313E-08	0	0	0	~Relative Strength Ply Vs Belt	TEX	193	Diameter * 0.008205					
Relative Area	0.5977	0.5977	1.0000	0.5977	0.5977	1.0000	1.0000	1.0000	1.0000	22990.7462	2.3E-05							
Ply Thickness	0.00032494857348	0.00032	0.00032	0.00032	0.00032495	0.1142E-05	0	0	0	22990.7462	2.3E-05							
Relative Thickness	Ply1-2	Ply3-4	Ply5-6	Chafer1	Chafer2	Shoulder	Belt1-2	Belt3-4	Undercap									
Thick Mult	1.04	1.04	1	1.04	1.04	1.04	1.04	1.04	1.04									
Angle Mult	153	153	153	153	153	153	153	153	153									
Min Angle	27	27	27	27	27	27	27	27	27									
0	53.08	0.000268	53.08	0.000268	0	0.000000	53.08	0.000325	126.92	0.000325	0	0.000000	53.08	0.000004	0	0.000000	0	0.000000
1	50.59	0.000263	50.59	0.000263	0	0.000000	50.59	0.000325	129.41	0.000325	0	0.000000	50.59	0.000002	0	0.000000	0	0.000000
2	48.29	0.000260	48.29	0.000260	0	0.000000	48.29	0.000325	131.71	0.000325	0	0.000000	48.29	0.000002	0	0.000000	0	0.000000
3	46.8	0.000260	46.8	0.000260	0	0.000000	46.8	0.000325	133.2	0.000325	0	0.000000	46.8	0.000001	0	0.000000	0	0.000000
4	45.65	0.000260	45.65	0.000260	0	0.000000	45.65	0.000325	134.35	0.000325	0	0.000000	45.65	0.000001	0	0.000000	0	0.000000
5	44.42	0.000260	44.42	0.000260	0	0.000000	44.42	0.000325	135.58	0.000325	0	0.000000	44.42	0.000001	0	0.000000	0	0.000000
6	43.01	0.000261	43.01	0.000261	0	0.000000	43.01	0.000325	136.99	0.000325	0	0.000000	43.01	0.000002	0	0.000000	0	0.000000
7	41.48	0.000263	41.48	0.000263	0	0.000000	41.48	0.000325	138.52	0.000325	0	0.000000	41.48	0.000002	0	0.000000	0	0.000000
8	39.88	0.000265	39.88	0.000265	0	0.000000	39.88	0.000325	140.12	0.000325	0	0.000000	39.88	0.000003	0	0.000000	0	0.000000
9	38.22	0.000269	38.22	0.000269	0	0.000000	38.22	0.000325	141.78	0.000325	0	0.000000	38.22	0.000005	0	0.000000	0	0.000000
10	36.55	0.000273	36.55	0.000273	0	0.000000	36.55	0.000325	143.45	0.000325	0	0.000000	36.55	0.000006	0	0.000000	0	0.000000
11	34.92	0.000278	34.92	0.000278	0	0.000000	34.92	0.000325	145.08	0.000325	0	0.000000	34.92	0.000008	0	0.000000	0	0.000000
12	33.37	0.000285	33.37	0.000285	0	0.000000	33.37	0.000325	146.63	0.000325	0	0.000000	33.37	0.000010	0	0.000000	0	0.000000
13	31.98	0.000292	31.98	0.000292	0	0.000000	31.98	0.000325	148.02	0.000325	0	0.000000	31.98	0.000013	0	0.000000	0	0.000000
14	30.69	0.000299	30.69	0.000299	0	0.000000	30.69	0.000325	149.31	0.000325	0	0.000000	30.69	0.000015	0	0.000000	0	0.000000
15	29.46	0.000307	29.46	0.000307	0	0.000000	29.46	0.000325	150.54	0.000325	0	0.000000	29.46	0.000018	0	0.000000	0	0.000000
16	28.32	0.000311	28.32	0.000311	0	0.000000	28.32	0.000325	151.78	0.000325	0	0.000000	28.32	0.000019	0	0.000000	0	0.000000
17	28.55	0.000313	28.55	0.000313	0	0.000000	28.55	0.000325	151.45	0.000325	0	0.000000	28.55	0.000011	0	0.000000	0	0.000000
18	28.25	0.000315	28.25	0.000315	0	0.000000	28.25	0.000325	151.75	0.000325	0	0.000000	28.25	0.000011	0	0.000000	0	0.000000
19	27.96	0.000317	27.96	0.000317	0	0.000000	27.96	0.000325	152.04	0.000325	0	0.000000	27.96	0.000012	0	0.000000	0	0.000000
20	27.66	0.000320	27.66	0.000320	0	0.000000	27.66	0.000325	152.34	0.000325	0	0.000000	27.66	0.000012	0	0.000000	0	0.000000
21	27.45	0.000321	27.45	0.000321	0	0.000000	27.45	0.000325	152.55	0.000325	0	0.000000	27.45	0.000013	0	0.000000	0	0.000000
22	27.35	0.000322	27.35	0.000322	0	0.000000	27.35	0.000325	152.85	0.000325	0	0.000000	27.35	0.000013	0	0.000000	0	0.000000
23	27.29	0.000323	27.29	0.000323	0	0.000000	27.29	0.000325	152.71	0.000325	0	0.000000	27.29	0.000013	0	0.000000	0	0.000000
24	27.26	0.000323	27.26	0.000323	0	0.000000	27.26	0.000325	152.74	0.000325	0	0.000000	27.26	0.000013	0	0.000000	0	0.000000
25	27.23	0.000323	27.23	0.000323	0	0.000000	27.23	0.000325	152.77	0.000325	0	0.000000	27.23	0.000014	0	0.000000	0	0.000000
26	27.21	0.000323	27.21	0.000323	0	0.000000	27.21	0.000325	152.79	0.000325	0	0.000000	27.21	0.000014	0	0.000000	0	0.000000
27	27.19	0.000323	27.19	0.000323	0	0.000000	27.19	0.000325	152.81	0.000325	0	0.000000	27.19	0.000014	0	0.000000	0	0.000000
28	27.16	0.000324	27.16	0.000324	0	0.000000	27.16	0.000325	152.84	0.000325	0	0.000000	27.16	0.000014	0	0.000000	0	0.000000
29	27.14	0.000324	27.14	0.000324	0	0.000000	27.14	0.000325	152.86	0.000325	0	0.000000	27.14	0.000014	0	0.000000	0	0.000000
30	27.12	0.000324	27.12	0.000324	0	0.000000	27.12	0.000325	152.88	0.000325	0	0.000000	27.12	0.000014	0	0.000000	0	0.000000
31	27.09	0.000324	27.09	0.000324	0	0.000000	27.09	0.000325	152.91	0.000325	0	0.000000	27.09	0.000014	0	0.000000	0	0.000000
32	27.07	0.000324	27.07	0.000324	0	0.000000	27.07	0.000325	152.93	0.000325	0	0.000000	27.07	0.000014	0	0.000000	0	0.000000
33	27.05	0.000325	27.05	0.000325	0	0.000000	27.05	0.000325	152.95	0.000325	0	0.000000	27.05	0.000014	0	0.000000	0	0.000000
34	27.04	0.000325	27.04	0.000325	0	0.000000	27.04	0.000325	152.96	0.000325	0	0.000000	27.04	0.000014	0	0.000000	0	0.000000
35	27.02	0.000325	27.02	0.000325	0	0.000000	27.02	0.000325	152.98	0.000325	0	0.000000	27.02	0.000014	0	0.000000	0	0.000000
36	27.01	0.000325	27.01	0.000325	0	0.000000	27.01	0.000325	152.99	0.000325	0	0.000000	27.01	0.000014	0	0.000000	0	0.000000
37	27	0.000325	27	0.000325	0	0.000000	27	0.000325	153	0.000325	0	0.000000	27	0.000014	0	0.000000	0	0.000000
38	27	0.000325	27	0.000325	0	0.000000	27	0.000325	153	0.000325	0	0.000000	27	0.000014	0	0.000000	0	0.000000

Figure 4.10 – “TGM Generator” spreadsheet: ply angles and thicknesses.

In the next page it is required to select the compound and the size of the tyre: this section has a huge impact on the tyre final behaviour because to each compound corresponds a specific combination of values that will fill out the “Realtime” section. As usual, a large database is already implemented and it comes in handy for the tyre developer. Of course, there is the possibility to insert a new compound with its proper specifics.

The selection of the compound determines the degradation curve in terms of abrasion and thermal fraction: two useful plots help the tyre developer to make the right choice. In **Figure 4.11** a screenshot of the “Compound” page is illustrated (some columns have been hidden for reasons of space): it is worth to notice the [Realtime] parameters accounted for each compound.

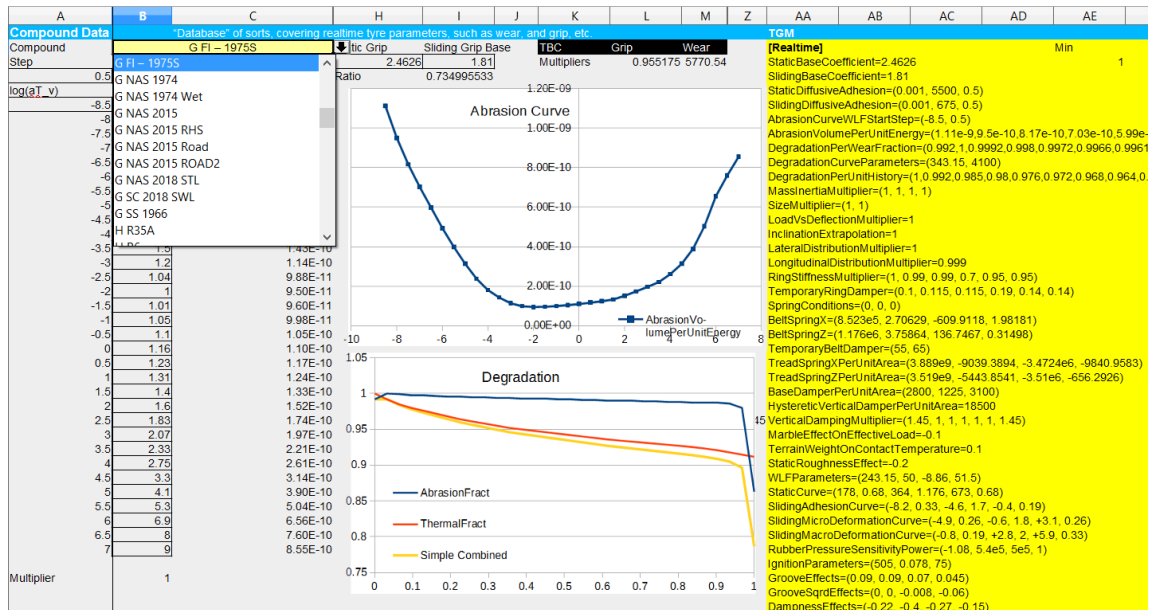


Figure 4.11 – “TGM Generator” spreadsheet: compound selection.

At this point the “.tgm” file is almost complete: the last step consists in the definition of the boundary conditions at which you want to run the QSA tests in the “TGM” section (Figure 4.12). In the preliminary phase of the tyre development, it is recommended to run the QSA tests in just few operating conditions in order to save time. As last step, you simply click on the button “Generate TGM” and it will appear in the folder “pTool” selected in the first page.

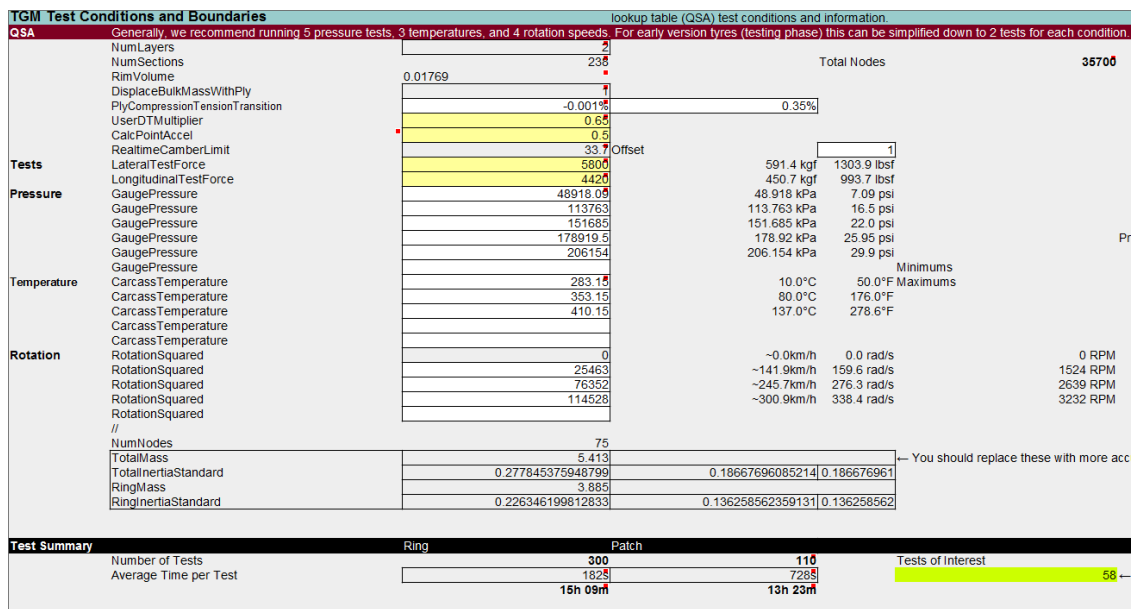


Figure 4.12 – “TGM Generator” spreadsheet: QSA tests boundary conditions.

4.4 Step 3: QSA Batch testing

Once generated the first attempt of the “.tgm” file, it is necessary to verify if it works correctly. Instead of running the whole set of QSA tests (more than 400 iterations), rFactor2 allows to test separately the different tyre characteristics (such as shape, stiffness, growth or contact patch pressure distribution) through a second spreadsheet called “tTool QSA Batch Tests”. In the same way of the “TGM Generator” spreadsheet, you must follow the sections order: as usual several comments are provided.

In the first page (“Input”), you have essentially to fill-out the cells with the sensible information regarding the optimal operating conditions of the real tyre that you want to virtualize.

Then the validation procedure can start. Proceed to “o_PreTest”: this should be preloaded with some minor tests to ascertain some values required to create more relevant tests in “1_QSATest”, where the most important part of the validation phase begins. Through this page you can create your own cycle test in order to verify the main characteristics of the tyre: in **Figure 4.13** a sample screenshot is reported. After that, it is necessary generate the test file by press the button “Generate Remaining” in the “Input” page.

V0.28	Symmetric	DT Multiplier	AVD (0/1)	AmbientPres [kPa]	ConstPress	Press [kPa]	Temp [C]	Rotation (rad/s)	Load [N]	Deflection (m)	Camber [°]	Sections (#)	PatchGoalCG	PatchGoalCG
Start	0		1	101.325	1	115	25	0.1	-1	0.00382979	1	2	-0.00957447	-0.00382979
Step	0				0	33	50	289.9		0.00344681	0	6	-0.00641489	-0.00256596
Step*2						0	0	0		0	0	0	0.00160372	0.00064149
# of Steps	2	1	1	0	1	2	2	2	3	3	2	3	6	6
Max Value	0	0	1	101.325	1	148	75	290	-1	0.0107234	1	14	-0.01598936	-0.00639574
Step Count	1	1	1	1	1	24	12	6	1	1	2	1	1	1
DisableBefore	0	0	0	0	0	0	0	0	0	0	0	0	0	3
DisableAfter	1	256	256	256	256	256	256	256	256	256	256	256	2	5
Notes														Automated
Fall-back														0
Range														0.000385
48	Symmetric	DT Multiplier	AVD	AmbientPres	ConstPress	CavityPress	CarcasTemp	RotationX	Load	Deflection	Camber	PatchSections	PatchGoalCG	PatchGoalCG
0	0		1	101325	1	216325	298.15	0.1	-1	0.00383037	1	2	-0.00957447	
1	0		1	101325	1	216325	298.15	0.1	-1	0.0072777	1	8	-0.01438564	
2	0		1	101325	1	216325	298.15	0.1	-1	0.01072504	1	14	-0.01598936	
3	0		1	101325	1	216325	298.15	0.1	-1	0.00383037	1	2		-0.00382979
4	0		1	101325	1	216325	298.15	0.1	-1	0.0072777	1	8		-0.00575426
5	0		1	101325	1	216325	298.15	0.1	-1	0.01072504	1	14		-0.00639574
6	0		1	101325	1	216325	298.15	290	-1	0.00383037	1	2	-0.00957447	
7	0		1	101325	1	216325	298.15	290	-1	0.0072777	1	8	-0.01438564	
8	0		1	101325	1	216325	298.15	290	-1	0.01072504	1	14	-0.01598936	
9	0		1	101325	1	216325	298.15	290	-1	0.00383037	1	2		-0.00382979
10	0		1	101325	1	216325	298.15	290	-1	0.0072777	1	8		-0.00575426
11	0		1	101325	1	216325	298.15	290	-1	0.01072504	1	14		-0.00639574
12	0		1	101325	1	216325	348.15	0.1	-1	0.00383037	1	2	-0.00957447	
13	0		1	101325	1	216325	348.15	0.1	-1	0.0072777	1	8	-0.01438564	
14	0		1	101325	1	216325	348.15	0.1	-1	0.01072504	1	14	-0.01598936	
15	0		1	101325	1	216325	348.15	0.1	-1	0.00383037	1	2		-0.00382979
16	0		1	101325	1	216325	348.15	0.1	-1	0.0072777	1	8		-0.00575426
17	0		1	101325	1	216325	348.15	0.1	-1	0.01072504	1	14		-0.00639574
18	0		1	101325	1	216325	348.15	290	-1	0.00383037	1	2	-0.00957447	
19	0		1	101325	1	216325	348.15	290	-1	0.0072777	1	8	-0.01438564	
20	0		1	101325	1	216325	348.15	290	-1	0.01072504	1	14	-0.01598936	
21	0		1	101325	1	216325	348.15	290	-1	0.00383037	1	2		-0.00382979
22	0		1	101325	1	216325	348.15	290	-1	0.0072777	1	8		-0.00575426
23	0		1	101325	1	216325	348.15	290	-1	0.01072504	1	14		-0.00639574
24	0		1	101325	1	249325	298.15	0.1	-1	0.00383037	1	2	-0.00957447	
25	0		1	101325	1	249325	298.15	0.1	-1	0.0072777	1	8	-0.01438564	
26	0		1	101325	1	249325	298.15	0.1	-1	0.01072504	1	14	-0.01598936	
27	0		1	101325	1	249325	298.15	0.1	-1	0.00383037	1	2		-0.00382979
28	0		1	101325	1	249325	298.15	0.1	-1	0.0072777	1	8		-0.00575426
29	0		1	101325	1	249325	298.15	0.1	-1	0.01072504	1	14		-0.00639574

Figure 4.13 – “tTool QSA Batch Tests” spreadsheet: “1_QSATest” boundary conditions.

In order to start the validation procedure, you need to launch rFactor2 in “DevMode” and open the “tTool” window. Then you need to load both the “.tgm” file and the test file and then press “Run Automated” (Figure 4.14): by doing so the QSA tests will start and it will take some hours.

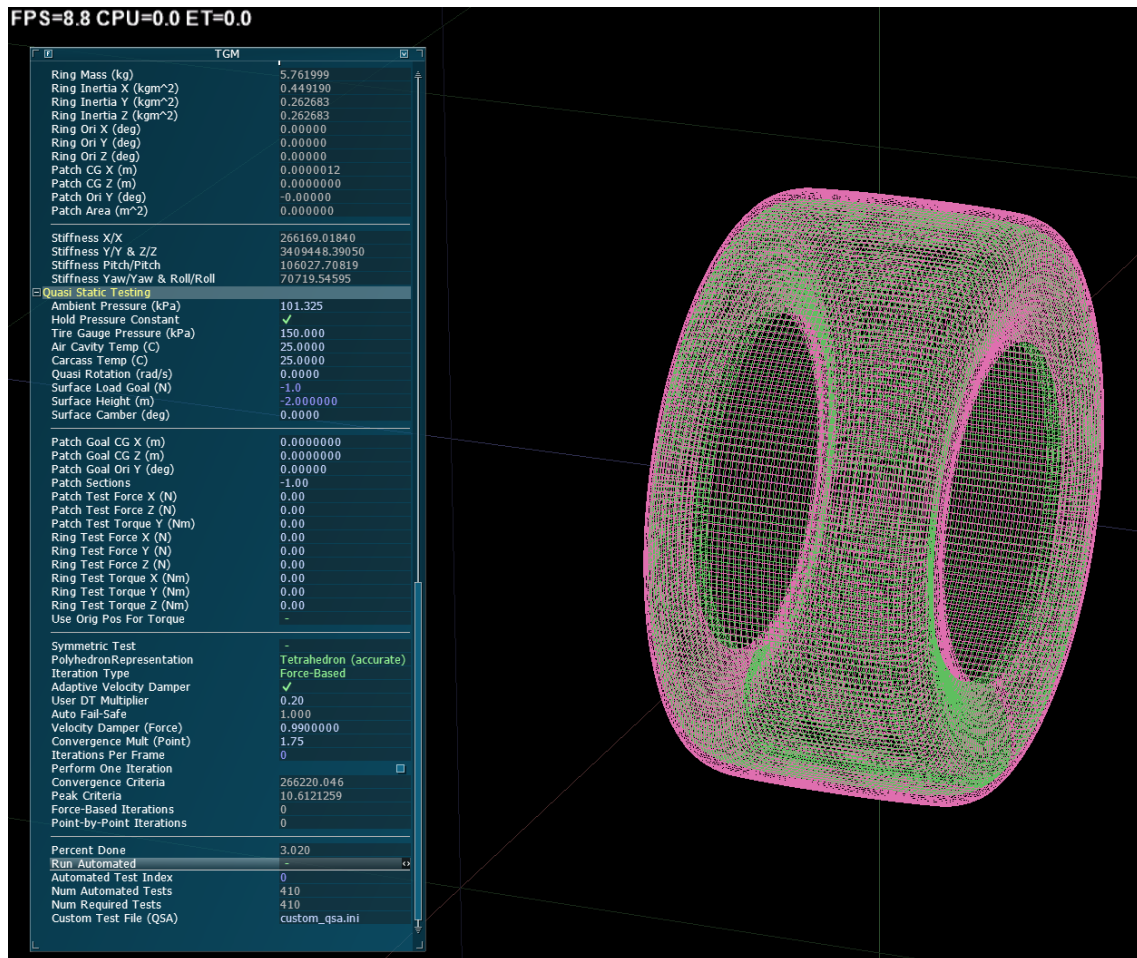


Figure 4.14 – “tTool” window: QSA tests.

The results of the previous test must be copied and pasted in the page “1_QSAResult”. Then they will be automatically analysed in the next page “1_AnalyseFlex”, where the lateral and longitudinal stiffnesses of the tyre subject to different boundary conditions are plotted (Figure 4.15). If the prototypal tyre satisfies the stiffness requirements, it is necessary to perform all the QSA tests (defined previously in the ‘TGM Generator’ spreadsheet) in order to provide a provisional lookup table, needed to perform, this time, the “Realtime” tests.

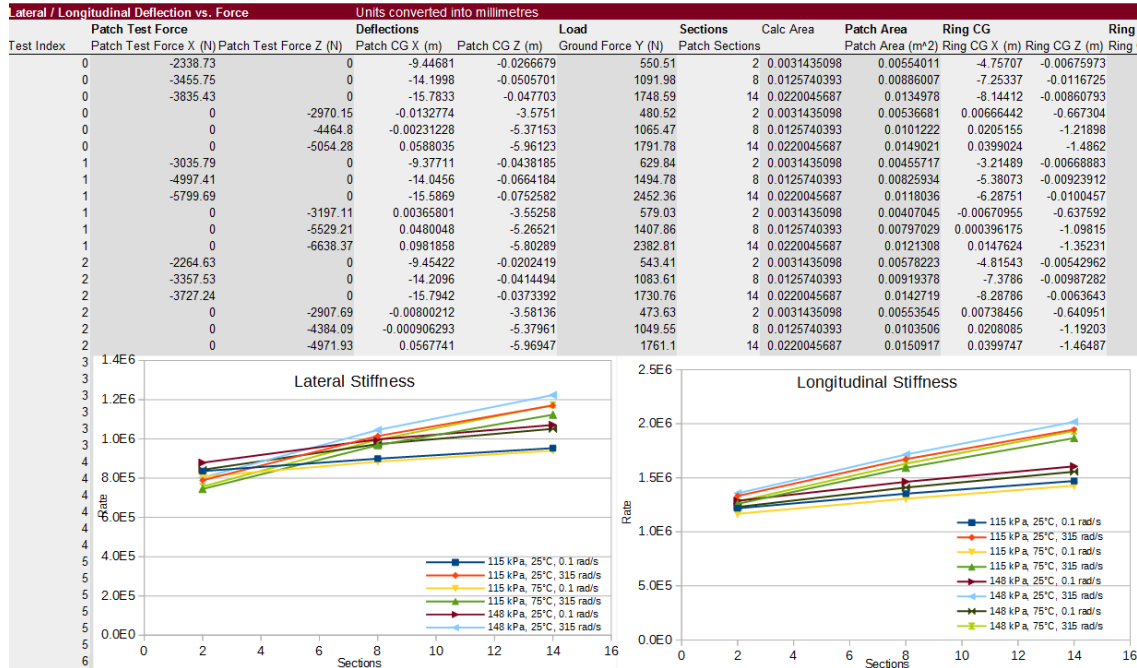


Figure 4.15 – “tTool QSA Batch Tests” spreadsheet: “1_AnalyseFlex” page.

Once the whole set of QSA tests has been run, the lookup table is automatically generated: it must be copied and pasted in the “.tgm” file, below the [Realtime] section. Now the tgm file is complete: the tyre can be used in the on-line mode, but it is recommended to do further refinements through the third and last spreadsheet, called “tTool Realtime Batch Tests”.

4.5 Step 4: Realtime model batch tests

Essentially the procedure is quite the same as the one seen in the previous step. The difference is that now you act to the [Realtime] parameters in order to match the correct tyre behaviour.

In the “General” sections, as usual, the main data about the tyre must be inserted: they are very important because they define the utilisation range of the tests. Then it is possible to analyse those tyre characteristics that are typically felt directly by the driver: slip curve plots, rolling resistance plots, aligning moment plots, deflection tests can be derived easily and eventually modified by changing the [Realtime] parameter values.

Once the parameters are adjusted and the tyre behaves correctly, the very last operation to do is to go back to the “TGM Generator” spreadsheet, increase the number of operating conditions of the QSA tests and recalculate the complete lookup table in order to avoid bugs during the gameplay. Now the tyre is finally ready to be used. Anyway, this final part of the tyre design phase is better analysed and developed in the next chapter, since it is the section on which the thesis is focused on.

Chapter 5. Optimisation algorithm based on a neural network

In the last two chapters the physical model of the tyre implemented in rFactor2 and the procedure to build up from scratch a “.tgm” file are widely discussed. This chapter represents the consequent development of the tyres, which is the main focus of the thesis.

The [Realtime] parameters provided by default in the “TGM Generator” spreadsheet are standardised and intended for amateur users: the resulting behaviour of the tyre is quite far from the real one and this leads to the necessity of a refinement process. The main issue is the correlation between the fictitious parameters and their impact on the overall tyre dynamics: the “TGM Tyre Tool Quick Start” [8] contains a detailed description of each parameter role, but only few mathematical expressions are provided. So, it is very difficult to appreciate the effective influence of the parameter on the tyre performance: the driver feedbacks and the telemetry data are the only means of assessing the tyre response, but they are not repeatable. On the other hand, the off-line tests performed in “tTool” allow to derive some minor information, but they are the only way to get accurate and reliable results.

The idea is to compare the characteristic curves (lateral force, longitudinal force and self-aligning moment) of two equivalent tyres: the first one is the real tyre, described by the “.tir” file directly released by the tyre manufacturer, and the second one is the virtual tyre, described by the “.tgm” file. The purpose of this procedure is to develop an algorithm capable of giving as output the combination of values to be assigned to the selected [Realtime] parameters, in order to match as much as possible the three curves. Being these data strictly reserved, the specific tyre model is not cited and all the plots are normalized. Anyway, it is important to state that the considered tyre is a racing slick and intended for an open wheels car.

5.1 Introduction to the algorithm

Due to the complexity of the tyre model behind rFactor2 and the lack of mathematical expressions that relate the fictitious parameter to the final response of the tyre, the implementation of an Artificial Neural Network (ANN) represents a smart way to create a correlation between input and output: it is like a black box that is able to predict how the tyres will behave as a result of the parameter changing. Essentially, it works like a human brain, as suggested by the name itself: the hidden neurons, implemented in the algorithm, adapt to the system evolution according to the input variation through a set of input-output data used for the training phase. A certain percentage of these data is then used for the validation phase: so, by doing the reverse operation, a certain output is analysed by the neurons and their capability to predict the correct input is measured.

A fundamental aspect is the quality of the data used to train and validate the ANN: in order to not contaminate the final behaviour of the tyre, only one parameter at a time is changed with a constant step and the corresponding output values have been recorded.

For what concern the output variables, the choice fell on the mean squared errors (mse) between the three couples of curves.

The following premise is necessary in view of the overall optimisation process that is illustrated in this chapter: the ANN is trained at each iteration with random data and this leads to slightly misleading results. Furthermore, during the optimisation process, the trained network is asked to find the best combination of values to be assigned to the parameter, in order to obtain an overall decrease of the mse from the target curves. However, the ANN is trained by changing only one parameter at a time with the assumption of the superimposition principle between the different outputs. The set of optimal values, provided by the algorithm, has been tested several times through both off-line and on-line tests, obtaining most of the times the expected feedbacks.

This approach has been used two times, respectively for the front and for the rear tyres: the overall behaviour of the objective functions, in relation to the input parameter changing, turned out to be quite the same despite the totally different implementation of the tyre construction made by the tyre developers. This important aspect confirms the independency among the fictitious parameters and the possibility to adapt this method for every tyre supplied with target data, for example provided by the “.tir” file.

5.2 Data recording

The tyre testing is a mandatory step done by every tyre manufacturer in order to verify if their own product satisfy certain requirements, before the commercialization phase. This procedure is made possible through the use of a Flat Track machine, on which the tyres undergo to the most critical conditions in terms of vertical load, camber angle, slip angle and so on: in such way it is possible to measure the forces exchanged by the tyres at different boundary conditions. The overall procedure allows to fill out the so called “.tir” file, which contains the whole set of parameters needed to interpolate the correct shape of the tyre force functions, through the Pacejka Magic Formula.

So, the very first step was to reconstruct the characteristic curves of both tyres. The provided “.tir” files work according to the “MF-Tyre 5.2” version, whose equations are listed in the textbook “Tire and Vehicle Dynamics” [1]: a MatLab code has been implemented in order to generate the tyre characteristic curves at the desired condition. For the sake of simplicity, the target curves have been generated with 0° of camber angle and in pure slip condition; for what concern the vertical load a trade-off was made, based on the data contained in the “.tgm” file of the equivalent tyres. In particular, it was defined according to the “LateralTestForce” and “LongitudinalTestForce” values, contained in the [QuasiStaticAnalysis] section, which represents the maximum admissible force sustainable by the tyre (**Figure 5.1**).


```
[QuasiStaticAnalysis]
NumLayers=2
NumSections=238
RimVolume=0.01838
DisplaceBulkMassWithPly=1
PlyCompressionTensionTransition=(-0.00034,0.00105)
UserDTMultiplier=0.2
RealtimeCamberLimit=32
CalcPointAccel=0.72
LateralTestForce=7400
LongitudinalTestForce=3400
GaugePressure=46332.72
GaugePressure=110316
GaugePressure=137895
GaugePressure=177971
GaugePressure=218047
CarcassTemperature=283.15
CarcassTemperature=353.15
CarcassTemperature=416.15
RotationSquared=0
RotationSquared=10191.8
RotationSquared=30560.2
RotationSquared=45840.26
NumNodes=85
TotalMass=7.678073292529414
TotalInertiaStandard=(0.523762938273423,0.3319543475878489,0.33195434758785053)
RingMass=5.761998922205789
RingInertiaStandard=(0.4491896864794103,0.26268298301978255,0.2626829830197779)
```

Figure 5.1 – [QuasiStaticAnalysis] section of the front tyre “.tgm” file.

Once defined the three target curves of both the tyres, it was necessary to perform the analogous tests for the virtual tyre through the “tTool Realtime Batch Tests” spreadsheet: the Lateral Force (F_y) and the Self-Aligning Moment (M_z) have been obtained through the “Sweep Test”, while the Longitudinal Force (F_x) through the “Longitudinal Test”. In **Figure 5.2** a screenshot of the boundary conditions setting is illustrated: the highlighted cells represent the most important data to insert (Load [N], Velocity [m/s], Pressure [kPa] and Temperature [°C]). Velocity and inflation pressure must correspond to the ones indicated in the “.tir” file (**Figure 5.3**).

Sweep Test	ConvAngle [°]	Deflection [m]	Load [N]	FreeRoll [0/1]	Velocity [m/s]	LatVel [m/s]	Rotation [rad/s] or [m/s]	Radius [m]	Camber [°]	Pressure [kPa]	Temp [°C]
Start		0.013	2500	1	22.22			0.28937	0	124	80
Step		0	0	0	0			0	0	30	55
Step²		0	0	0	0			0	0	0	0
# of Steps	50	1	1	1	1	1	1	1	1	1	1
Max Value	0	0.013	2500	1	22.22	0	0	0	0	124	80
Step Count	1	1	1	1	1	1	1	3	1	34	17
Disable Before	0	0	0	0	0	0	0	0	0	0	0
Disable After	999	999	999	999	999	999	999	999	999	999	999
Notes	Overrides LatRatio & LatVel		Overrides Defle		Overrides Rotation						
Fall-back					Max [km/h]				0	127	0
Range					79.992						
100	SlipAngle	Deflection	Load	FreeRoll	LongVel	LatVel	RotAngular	Radius	Camber	Pressure	Temperature
0	0.00000	0.013	2500	1	22.22000	0	76.78750	0.290554	0	124000	353.15
1	0.23663	0.013	2500	1	22.21981	0.0917686	76.78685	0.290554	0	124000	353.15
2	0.48817	0.013	2500	1	22.21919	0.1893144	76.78472	0.290554	0	124000	353.15
3	0.75461	0.013	2500	1	22.21807	0.2926374	76.78084	0.290554	0	124000	353.15
4	1.03596	0.013	2500	1	22.21637	0.4017376	76.77495	0.290554	0	124000	353.15
5	1.33225	0.013	2500	1	22.21399	0.516615	76.76675	0.290554	0	124000	353.15
6	1.64347	0.013	2500	1	22.21086	0.6372696	76.75592	0.290554	0	124000	353.15
7	1.96964	0.013	2500	1	22.20687	0.7637014	76.74214	0.290554	0	124000	353.15
8	2.31079	0.013	2500	1	22.20193	0.8959104	76.72506	0.290554	0	124000	353.15
9	2.66694	0.013	2500	1	22.19593	1.0338966	76.70433	0.290554	0	124000	353.15
10	3.03810	0.013	2500	1	22.18877	1.17766	76.67958	0.290554	0	124000	353.15
11	3.42432	0.013	2500	1	22.18033	1.3272006	76.65041	0.290554	0	124000	353.15
12	3.82562	0.013	2500	1	22.17049	1.4825184	76.61640	0.290553	0	124000	353.15
13	4.24204	0.013	2500	1	22.15913	1.6436134	76.57714	0.290553	0	124000	353.15
14	4.67364	0.013	2500	1	22.14612	1.8104856	76.53218	0.290553	0	124000	353.15
15	5.12046	0.013	2500	1	22.13133	1.983135	76.48106	0.290552	0	124000	353.15
16	5.58256	0.013	2500	1	22.11461	2.1615616	76.42330	0.290552	0	124000	353.15
17	6.06001	0.013	2500	1	22.09683	2.3457654	76.35841	0.290552	0	124000	353.15
18	6.55287	0.013	2500	1	22.07484	2.5357464	76.28585	0.290551	0	124000	353.15
19	7.06123	0.013	2500	1	22.05147	2.7315046	76.20510	0.290551	0	124000	353.15
20	7.58518	0.013	2500	1	22.02557	2.93304	76.11559	0.29055	0	124000	353.15
21	8.12481	0.013	2500	1	21.99697	3.1403526	76.01675	0.290549	0	124000	353.15

Figure 5.2 – “tTool Realtime Batch Tests” spreadsheet: Sweep Test boundary conditions.

COMMENT :	Nom. section width (m)	0.25
COMMENT :	Nom. aspect ratio (-)	0.57
COMMENT :	Infl. pressure (Pa)	124000
COMMENT :	Rim radius (m)	0.1651
COMMENT :	Measurement ID	
COMMENT :	Test speed (m/s)	22.2222
COMMENT :	Road surface	Unknown
COMMENT :	Road condition	Dry

Figure 5.3 – Front tyre “.tir” file: boundary conditions.

In the following table all the data regarding the sweep test and the longitudinal tests are summarized for both the tyres (Table 5.1).

		LongRatio [%]	SlipAngle [°]	FreeRoll [0/1]	Load [N]	Velocity [m/s]	Pressure [kPa]	Temp [°C]
Front	Sweep Test	-	0 ÷ 30	1	2500	22.22	124	80
	Longitudinal Test	0 ÷ -30 (braking)	-	0	1800	22.22	124	80
Rear	Sweep Test	-	0 ÷ 30	1	3000	22.22	124	80
	Longitudinal Test	0 ÷ 30 (driving)	-	0	4000	22.22	124	80

Table 5.1 – Front tyre off-line tests: boundary conditions.

The procedure to run the Realtime tests is similar to the one discussed in the previous chapter for the QSA tests. The results must be copied and pasted in the spreadsheet page “3 Ana”, then in the page “3 Res” the characteristic curves are automatically generated. The following plots were obtained from the front tyre with the default configuration: they present a slightly different behaviour with respect to the target curves in terms of initial slope and peak value (Figures 5.4, 5.5, 5.6).

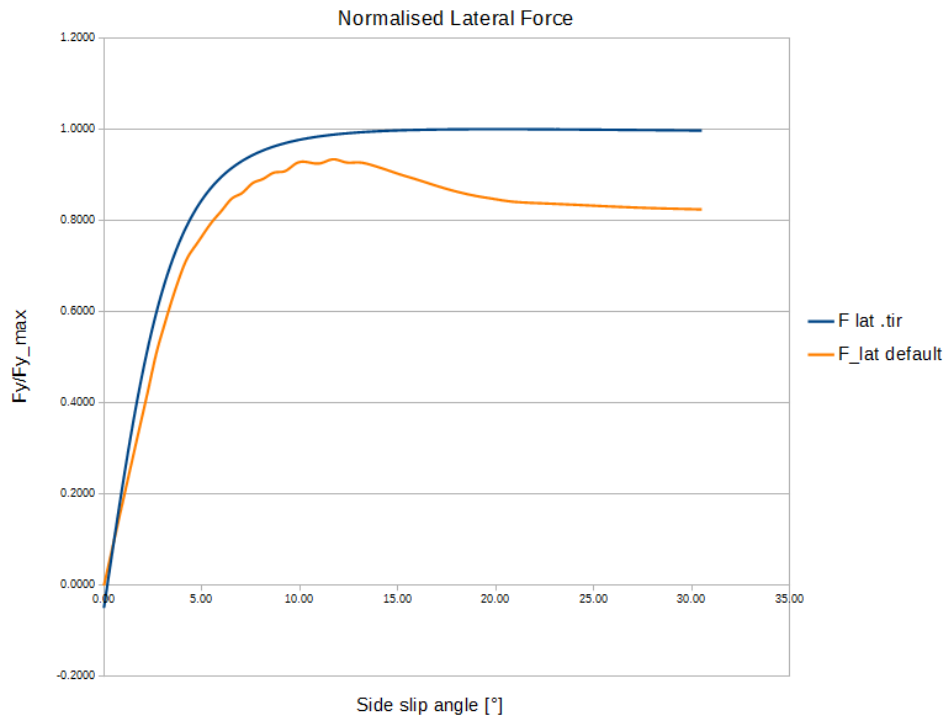


Figure 5.4 – Normalised lateral force: real vs rF2 default.

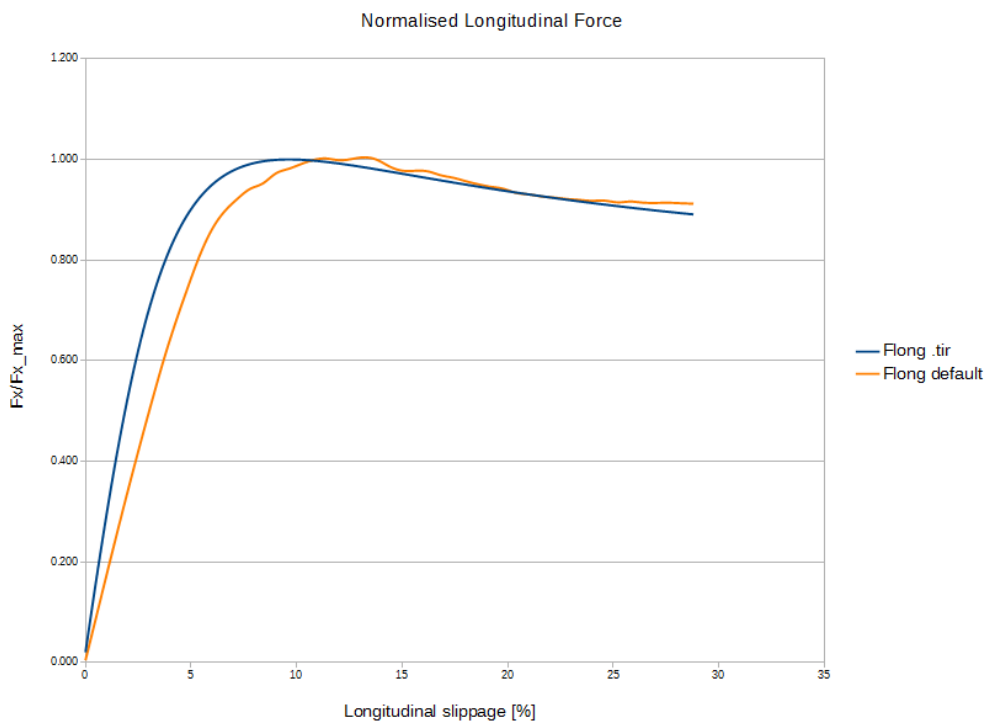


Figure 5.5 – Normalised longitudinal force: real vs rF2 default.

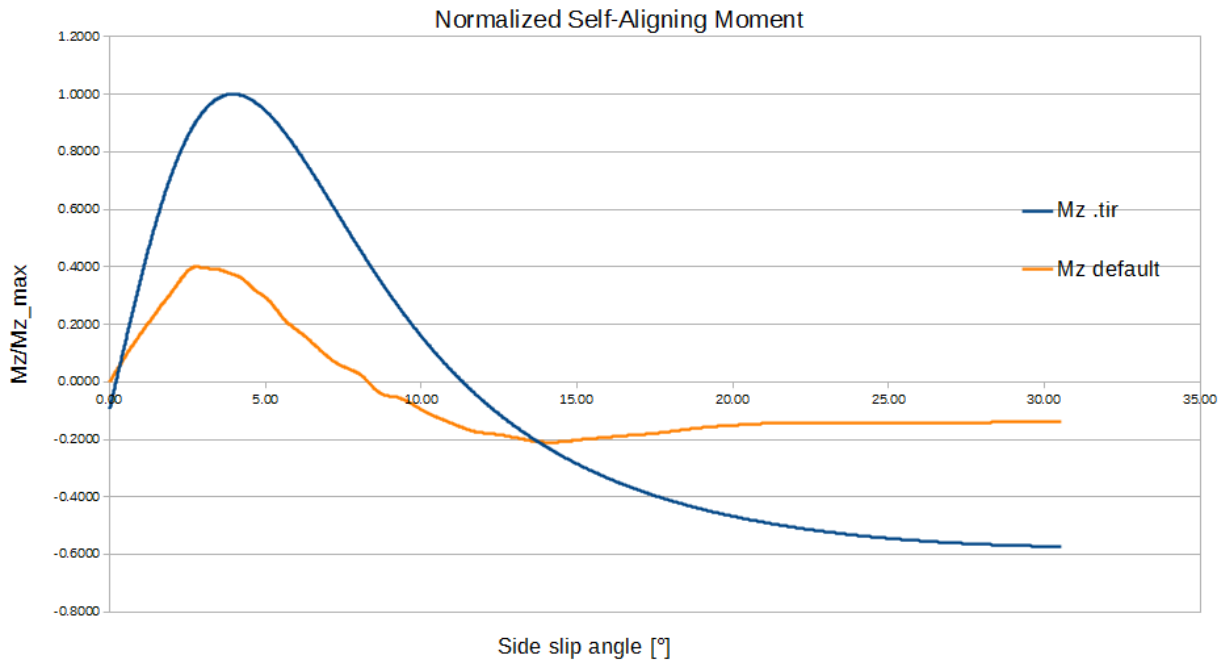


Figure 5.6 – Normalised self-aligning moment: real vs rF2 default.

The self-aligning moment trend, instead, looks very different from the one obtained through the “.tir” file: by rearranging the (3.26), the self-aligning moment can be simply written as the product between the lateral force F_y and the pneumatic trail t . Being F_y close to the target, this means that the pneumatic trail t should be drastically revised: since it depends on the contact patch properties (contained in the Lookup table), a complete redesign of the tyre structure in terms of plies arrangement must be done. Due to time and data limitations, this part of the tyre design has been neglected and a compromise has been made, with the objective to optimize the tyre by acting only on the [Realtime] parameters.

The aim of the optimization algorithm is to make the curves obtained by the virtual tyre as close as possible to the target ones. So, some performance indices must be defined in order to measure the degree of improvement among the different parameters; the region of interest of the optimization process is about the first part of the curve up to the peak value, i.e. the range of utilisation of the tyre itself. The indices adopted are the mean squared errors between the three pairs of curves; a fourth index has been introduced in order to limit the difference between the peak values of the longitudinal force F_x , since it can assume bigger values.

The four indices represent the final objective functions that must be minimized (equalled to zero for what concern the fourth). Instead, as for the selection of the parameters to optimise, it takes into consideration some practical aspects: firstly, the choice fell on those ones with the greater relevance on the tyre behaviour; the second aspect takes in consideration how the parameter is defined within the “.tgm” file, since some of them depend on more than one value.

For example:

BeltSpringX=(1.166e6, 1.9393, -1219.8507, 2.0394)

- the first value is the constant base of the “BeltSpringX” parameter;
- the remaining ones are multipliers of variable quantities (the inflation pressure [Pa], the surface temperature [K] and the square of the angular speed of tyre $[\frac{rad^2}{sec^2}]$).

The total value of “BeltSpringX” accounts for the summation of the four contributes. In order to limit the system complexity, only the “base” values are considered. The third criterion is to consider only those ones that affect the purely mechanical behaviour in terms of belt and tread stiffnesses and grip coefficient.

In total 8 parameters have been selected as the most relevant in terms of tyre response:

- StaticBaseCoefficient=3.2657
- SlidingBaseCoefficient=2.2857
- LoadVsDeflectionMultiplier=1
- BeltSpringX=(**1.166e6**, 1.9393, -1219.8507, 2.0394)
- BeltSpringZ=(**1.308e6**, 2.6818, -785.9425, 0.1542)
- TreadSpringXPerUnitArea=(**9.153e8**, 105.1865, -1.379e6, -1523.546)
- TreadSpringZPerUnitArea=(**1.299e9**, -732.9861, -1.4741e6, -408.1029)
- RubberPressureSensitivityPower=(-8.8, **3e6**, 5e5, 1)

In order to appreciate significantly the influence of the parameters on the four objective functions, they have been changed one at a time within a certain percentage and with a constant step. This procedure is quite simple but very time consuming: the more the samples provided as input, the more accurate the ANN will be. In the following table (**Table 5.2**), the iterations computed for each parameter and the respective objective functions of the front tyre are listed:

	delta	Fy mse [N]	Mz mse [Nm]	ΔFx peak [N]	Fx mse [N]
StaticBaseCoefficient	+9%	286.599	47.785	106.859	347.053
	+7.5%	296.372	48.057	93.676	347.896
	+6%	305.513	48.282	82.514	348.974
	+4.5%	315.739	48.534	58.816	350.703
	+3%	326.280	48.748	47.332	352.863
	+1.5%	337.652	49.015	36.595	355.615
	+0%	348.802	49.266	15.844	358.597
	-1.5%	359.184	49.540	-2.017	361.758
	-3%	369.110	49.808	-12.183	365.222
	-4.5%	379.185	50.001	-30.139	369.261
	-6%	389.088	50.205	-47.973	373.220
	-7.5%	400.084	50.351	-63.717	377.545
-9%	410.477	50.590	-81.453	382.006	

SlidingBaseCoefficient	+9%	279.753	46.368	207.925	363.308
	+7.5%	287.906	46.900	176.404	359.621
	+6%	297.369	47.392	143.799	357.009
	+4.5%	308.294	47.881	111.851	355.616
	+3%	320.568	48.343	80.004	355.375
	+1.5%	333.749	48.793	47.492	356.360
	+0%	348.802	49.266	15.844	358.597
	-1.5%	364.542	49.754	-16.496	361.986
	-3%	381.010	50.187	-47.357	366.479
	-4.5%	397.135	50.667	-79.265	372.107
	-6%	414.569	51.137	-112.277	378.712
	-7.5%	432.630	51.592	-144.068	386.504
-9%	450.953	52.071	-175.880	395.289	

BeltSpringX	+15%	211.222	53.364	15.794	358.590
	+12.5%	227.965	52.756	15.782	358.591
	+10%	248.544	52.085	15.767	358.590
	+7.5%	270.034	51.376	15.643	358.584
	+5%	293.118	50.678	15.878	358.583
	+2.5%	320.287	50.009	15.764	358.591
	+0%	348.802	49.266	15.844	358.597
	-2.5%	377.676	48.598	15.684	358.601
	-5%	409.770	47.941	15.676	358.604
	-7.5%	444.810	47.278	15.649	358.604
	-10%	479.463	46.633	15.543	358.600
	-12.5%	517.158	46.065	15.537	358.605
	-15%	557.626	45.513	15.521	358.595

BeltSpringZ	+15%	353.265	48.435	18.155	257.017
	+12.5%	352.458	48.562	10.813	272.583
	+10%	351.752	48.695	16.994	288.544
	+7.5%	351.065	48.848	12.126	305.086
	+5%	350.279	48.987	20.989	322.224
	+2.5%	349.626	49.146	18.965	339.915
	+0%	348.802	49.266	15.844	358.597
	-2.5%	347.815	49.410	17.114	377.422
	-5%	347.328	49.552	15.650	397.036
	-7.5%	346.497	49.719	15.301	417.051
	-10%	345.413	49.866	15.701	438.468
	-12.5%	344.896	50.014	10.673	460.371
	-15%	344.199	50.166	15.323	482.727

TreadSpringXPerUnitArea	+15%	327.595	49.850	15.876	358.590
	+12.5%	330.459	49.761	15.875	358.591
	+10%	333.070	49.679	15.885	358.596
	+7.5%	336.535	49.610	15.887	358.589
	+5%	340.292	49.498	15.887	358.600
	+2.5%	344.243	49.377	15.871	358.598
	+0%	348.802	49.266	15.844	358.597
	-2.5%	353.917	49.143	15.733	358.604
	-5%	359.032	49.004	15.693	358.602
	-7.5%	364.816	48.878	15.685	358.599
	-10%	371.550	48.709	15.682	358.599
	-12.5%	379.348	48.532	15.681	358.602
	-15%	388.503	48.329	15.680	358.604

TreadSpringZPerUnitArea	+15%	349.334	49.167	18.973	338.947
	+12.5%	349.167	49.187	17.470	341.649
	+10%	349.094	49.205	15.225	344.531
	+7.5%	349.060	49.208	12.827	347.563
	+5%	348.944	49.227	11.478	350.991
	+2.5%	348.907	49.245	13.041	354.602
	+0%	348.802	49.266	15.844	358.597
	-2.5%	348.528	49.291	19.151	362.914
	-5%	348.390	49.313	20.261	367.654
	-7.5%	348.140	49.347	19.704	372.808
	-10%	348.122	49.375	16.664	378.475
	-12.5%	347.765	49.417	13.287	385.015
	-15%	347.685	49.435	11.701	392.406

RubberPressureSensitivityPower	+15%	285.080	47.590	172.906	359.744
	+12.5%	292.073	47.870	149.400	357.674
	+10%	300.408	48.128	119.480	356.062
	+7.5%	310.179	48.395	95.605	355.252
	+5%	322.126	48.659	75.178	355.342
	+2.5%	334.908	48.938	49.142	356.498
	+0%	348.802	49.266	15.844	358.597
	-2.5%	363.866	49.595	-18.110	361.942
	-5%	380.199	49.946	-42.515	366.249
	-7.5%	397.918	50.274	-72.606	372.439
	-10%	416.971	50.627	-114.378	380.309
	-12.5%	438.263	50.965	-150.909	389.788
	-15%	462.189	51.322	-183.487	401.155

LoadVsDeflectionMultiplier	+0%	348.802	49.266	15.844	358.597
	-1.5%	334.283	49.157	28.020	343.292
	-3%	319.564	49.035	51.337	326.979
	-4.5%	305.049	48.875	76.291	310.715
	-6%	290.384	48.764	95.841	294.300
	-7.5%	276.511	48.648	117.728	278.726
	-9.0%	262.019	48.543	138.874	263.012

Table 5.2 – Front tyre “.tgm” file: data collection for the ANN.

The same procedure must be carried out for the rear tyre. By analysing the results, it is possible to observe that “BeltSpringZ” and “TreadSpringZPerUnitArea” do not affect so much the tyre response, so they can be neglected in order to reduce the computational effort and the algorithm complexity.

5.3 ANN implementation

Once collected the entire data set, it is possible to start the implementation of the ANN through the “Deep Learning Toolbox” provided by MatLab.

Once reduced the number of variables involved, you can definitively proceed to the implementation of the ANN, that has been set as illustrated in **Figure 5.7**.

```
net=feedforwardnet(15,'trainbr'); % define Neural network architecture and training algorithm
net.layers{1}.transferFcn= 'tansig'; % set the activation function of the j-th hidden layer of my network
net.divideParam.trainRatio = 0.85;% divide training and validation sets randomly
net.divideParam.valRatio = .15;
net.divideParam.testRatio = 0;
net.trainparam.epochs=1000; % set max. number of epochs
net.trainParam.max_fail= 10;% set max. validation fails
```

Figure 5.7 – ANN setting.

The algorithm is based on the Bayesian regulation process ('trainbr'): “the training working function updates the weight and bias values according to Levenberg-Marquardt optimization. It minimizes a combination of squared errors and weights, and then determines the correct combination so as to produce a network that generalizes well” [10].

For what concern the percentage of the data used for the training and the validation processes, reasonable values could be respectively 85% and 15%: the validation set is used to check the generalization error and when it increases, the training is stopped and the net weights returned are the ones that minimize the generalization error. In this way overtraining is avoided and the training process drops out before the maximum number of epochs is reached. The data used to train the ANN is random and at each iteration slightly different results could appear. The overall performance of the ANN is illustrated in **Figure 5.8**.

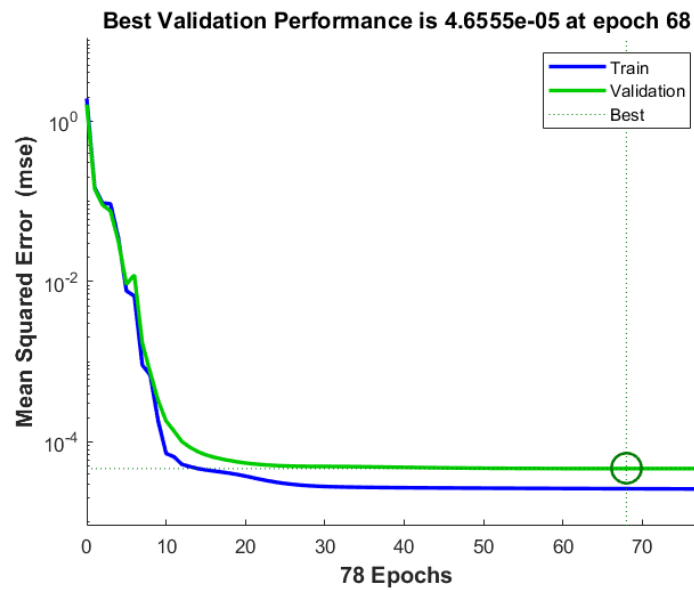


Figure 5.8 – Bayesian regulation process performance.

In the following figures (Figures 5.9, 5.10, 5.11, 5.12) the relationship between the four objective functions and those ones calculated by the ANN is shown: as you can see, the ratio is almost one and this indicates a close correlation between the approximated model created by the ANN and the objective functions provided as input.

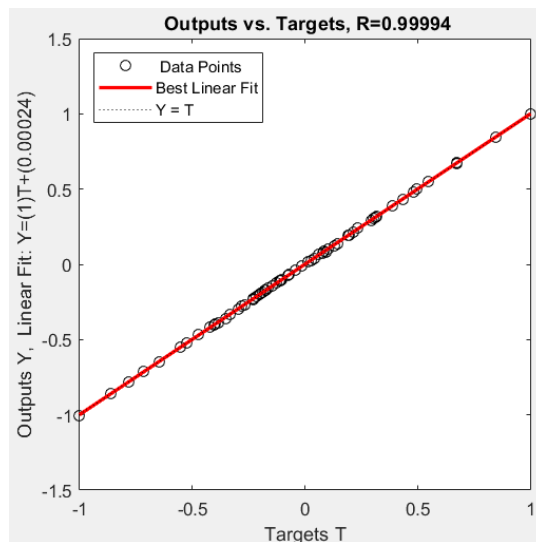


Figure 5.09 – Outputs vs Targets: mean squared error of the lateral force.

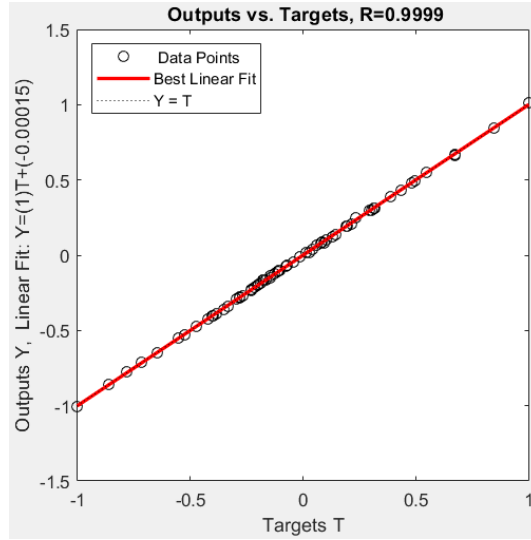


Figure 5.10 – Outputs vs Targets: mean squared error of the self-aligning moment.

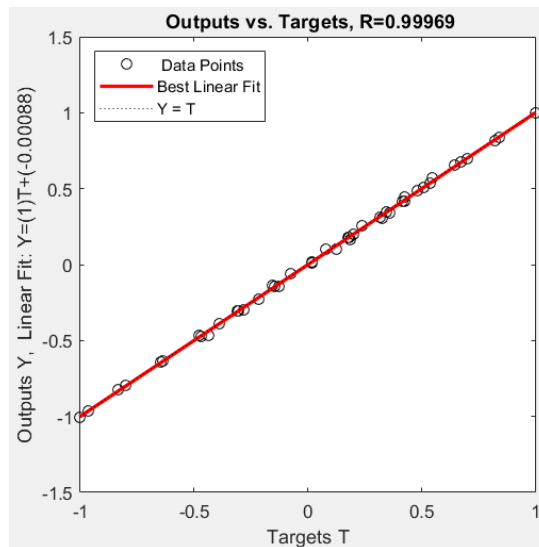


Figure 5.11 – Outputs vs Targets: delta of the longitudinal force peak values.

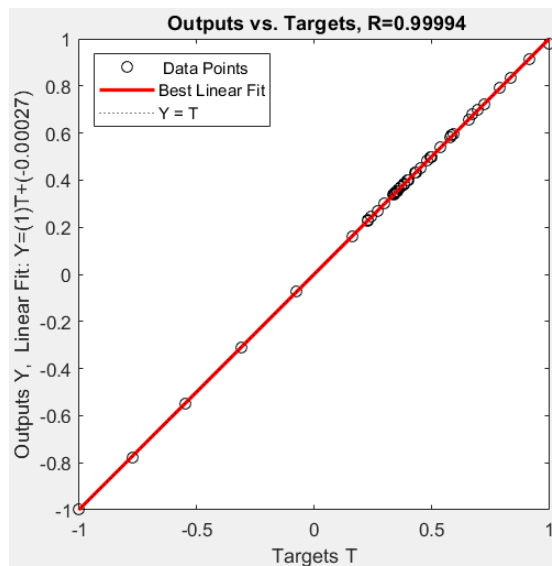


Figure 5.11 – Outputs vs Targets: means squared error of the longitudinal force.

5.4 Optimisation process

The trained network is then used for the optimisation process. First of all, it is necessary to create a uniform grid of samples of the input variables, evaluated in the range used to train the ANN: for each of the six [Realtime] parameters, eight samples were considered. For each of the 6^8 combinations, the network created by the ANN provides the approximated values of the four objective functions. Finally, the optimisation algorithm evaluates the whole domain of the objective functions and selects the Pareto optimal set (**Figure 5.13**).

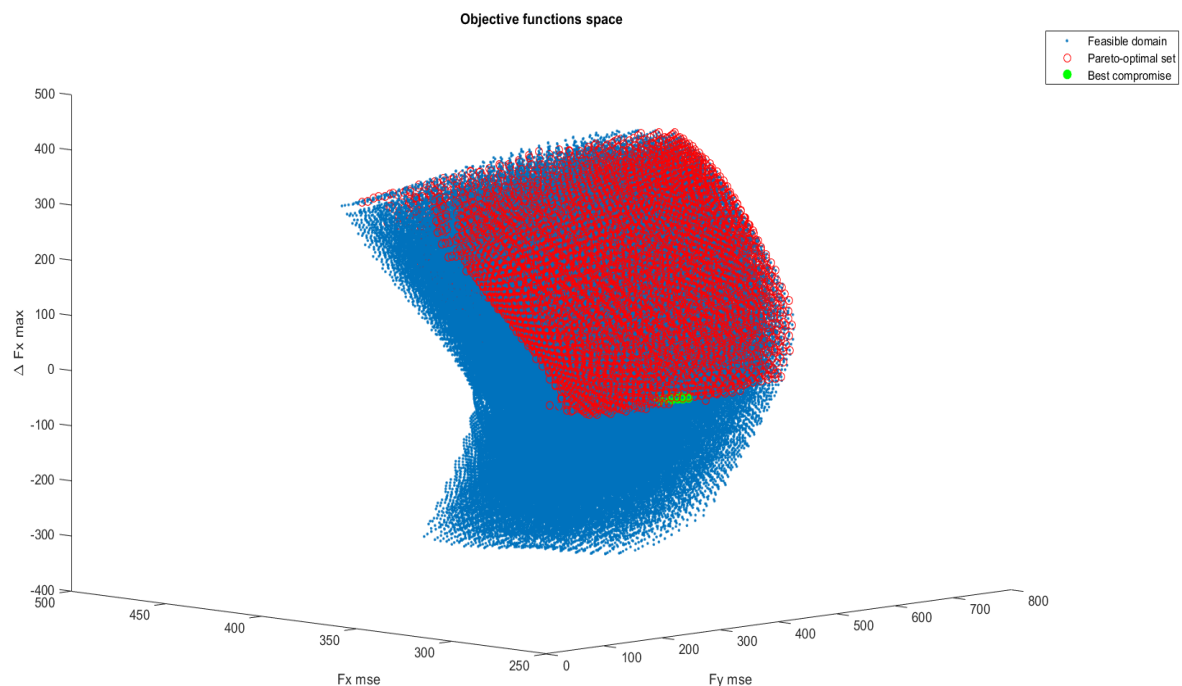


Figure 5.13 –Objective functions domain: optimal solutions.

The Pareto optimal solutions correspond to those combinations of parameters that optimise one of the four objective functions without worsening the others.

The Pareto optimal set includes the combinations of parameters that minimize only in one direction the tyre behaviour and this is not the aim of the algorithm. In order to get round this, a further selection was implemented: among the Pareto optimal set, only the combinations that contemporary reduce the four objective functions, with respect to the original setting, are saved (green circles in **Figure 5.13**). The result is a short list of the optimal combinations, but the final choice will be up to the tyre developer according to his necessities.

5.5 Validation procedure

As said in the introduction, the ANN selects randomly the data set for the training process: this involves in different networks every time the script is run, and therefore different relationships between the parameter combinations and the resulting objective functions: so, an accurate validation procedure must be carried out. The optimal combinations provided by the algorithm have been tested several times, firstly with the off-line tests (i.e. by means of “tTool”) and secondly with the on-line tests with the simulator.

5.5.1 Off-line tests

The off-line tests have been carried out by adopting the reverse procedure used for the compilation of the training data. In details, a random combination is selected among the optimal ones and the corresponding parameters are adjusted within the “.tgm” file (Figures 5.14, 5.15).

1	3.5270	2.2726	0.9883	1.1843e+06	8.7215e+08	2.7643e+06	318.8532	49.1678	10.5433	341.0829
2	3.5270	2.3216	1	1.1843e+06	9.0092e+08	2670000	321.2114	49.1465	6.7060	352.2457
3	3.5270	2.2237	0.9767	1.1843e+06	8.4338e+08	2.8586e+06	322.0397	49.2057	15.2005	328.3741
4	3.5270	2.2726	0.9533	1.1477e+06	9.5845e+08	2670000	323.3831	49.0399	10.9889	311.3728
5	3.4570	2.3216	0.9767	1.1843e+06	8.7215e+08	2670000	324.0458	49.2038	6.1286	335.4990
6	3.5270	2.3216	1	1.1843e+06	8.7215e+08	2670000	326.7272	48.9587	6.4677	352.6094
7	3.4570	2.3216	0.9767	1.1477e+06	1.0160e+09	2670000	327.3409	49.2022	7.9766	334.8141
8	3.5270	2.2237	0.9417	1.1477e+06	9.2968e+08	2.7643e+06	327.6582	49.0888	14.9400	298.0513
9	3.5270	2.2726	0.9883	1.1843e+06	8.4338e+08	2.7643e+06	327.9344	48.9773	10.2473	341.2694
10	3.5270	2.2726	0.9883	1.1477e+06	1.0160e+09	2.7643e+06	329.1394	49.1961	8.8314	341.6247

Figure 5.14 – Off-line validation test: a random optimal string is taken as reference. In blue, the values to assign to the [Realtime] parameters. In red, the expected objective functions calculated by the ANN.

```
[Realtime]
StaticBaseCoefficient=3.527 //StaticBaseCoefficient=3.2657
SlidingBaseCoefficient=2.2726 //SlidingBaseCoefficient=2.2857
StaticDiffusiveAdhesion=(0.001, 4800, 0.5)
SlidingDiffusiveAdhesion=(0.001, 800, 0.5)
AbrasionCurveWLFStartStep=(-8.5, 0.5)
AbrasionVolumePerUnitEnergy=(1.15E-9,9.8e-10,8.43e-10,7.25e-10,6.17e-10,5.1e-10,4.12e-10,3.23e-10,2.45e-10,1.
DegradationPerWearFraction=(0.99,1,0.999,0.9976,0.9966,0.9957,0.9949,0.9942,0.9936,0.993,0.9925,0.992,0.9915,
DegradationCurveParameters=(346.15, 2550)
DegradationPerUnitHistory=(1,0.985,0.971,0.963,0.958,0.955,0.9525,0.9501,0.9478,0.9456,0.9435,0.9415,0.9396,0
MassInertiaMultiplier=(1, 1, 1, 1)
SizeMultiplier=(1, 1)
LoadVsDeflectionMultiplier=0.9883 //LoadVsDeflectionMultiplier=1
InclinationExtrapolation=0
LateralDistributionMultiplier=0.95
LongitudinalDistributionMultiplier=0.7
RingStiffnessMultiplier=(1, 1, 1, 0.3, 1, 1)
TemporaryRingDamper=(0.037, 0.055, 0.055, 0.133, 0.087, 0.087)
SpringConditions=(0, 0, 0)
BeltSpringX=(1.1843e6, 1.9393, -1219.8507, 2.0394) //BeltSpringX=(1.166e6, 1.9393, -1219.8507, 2.0394)
BeltSpringZ=(1.308e6, 2.6818, -785.9425, 0.1542)
TemporaryBeltDamper=(31.189, 41.1)
TreadSpringXPerUnitArea=(8.7215e8, 105.1865, -1.379e6, -1523.546) //TreadSpringXPerUnitArea=(9.153e8, 105.18
TreadSpringZPerUnitArea=(1.299e9, -732.9861, -1.4741e6, -408.1029)
BaseDamperPerUnitArea=(1355.4, 0.8, 2162.6)
HystereticVerticalDamperPerUnitArea=12000
VerticalDampingMultiplier=(1.6, 1.15, 0.99, 0.98, 0.99, 1.15, 1.6)
MarbleEffectOnEffectiveLoad=-0.1
TerrainWeightOnContactTemperature=0.1
StaticRoughnessEffect=-0.2
WLFParameters=(247.15, 50, -8.86, 51.5)
StaticCurve=(183, 0.61, 373, 1.176, 673, 0.61)
SlidingAdhesionCurve=(-5.7, 0.4, -3.3, 1.7, -0.9, 0.2)
SlidingMicroDeformationCurve=(-3.3, 0.3, -0.9, 1.8, +1.7, 0.3)
SlidingMacroDeformationCurve=(-0.9, 0.2, +1.7, 2, +4.3, 0.4)
RubberPressureSensitivityPower=(-8.8, 2.7643e6, 5e5, 1) //RubberPressureSensitivityPower=(-8.8, 3e6, 5e5, 1)
```

Figure 5.15 – Off-line validation test: [Realtime] parameters modified in the “.tgm” file.

Once modified, the new tyre is tested through the “tTool”, under the same boundary conditions. Finally, the results obtained are compared with the approximated objective functions provided by the optimisation process together with the parameter combination, in order to evaluate the goodness of the algorithm (Figure 5.16).

a)	318.8532	49.1678	10.5433	341.0829
b)	Fy mse [N]	Mz mse [Nm]	ΔFx peak [N]	Fx mse [N]
	325.031	49.228	0.132	339.312
c)	Fy mse [N]	Mz mse [Nm]	ΔFx peak [N]	Fx mse [N]
	348.802	49.266	15.844	358.597

Figure 5.16 – Off-line validation test: comparison between: a) predicted objective functions; b) actual objective functions obtained with the optimised tyre; c) default configuration.

The objective functions predicted by the algorithm are pretty close the ones generated by the off-line test: the overall tyre performance has been improved in terms of standard deviation of the longitudinal force, lateral force and self-aligning moment and the difference of longitudinal force peaks is reduced.

In **Figures 5.17, 5.18 and 5.19** the characteristics curves of the front tyre are illustrated: it is possible to observe a defined reduction of the gap from the target in the ascending phase up to the peak value, i.e. the region where we are looking for a better response.

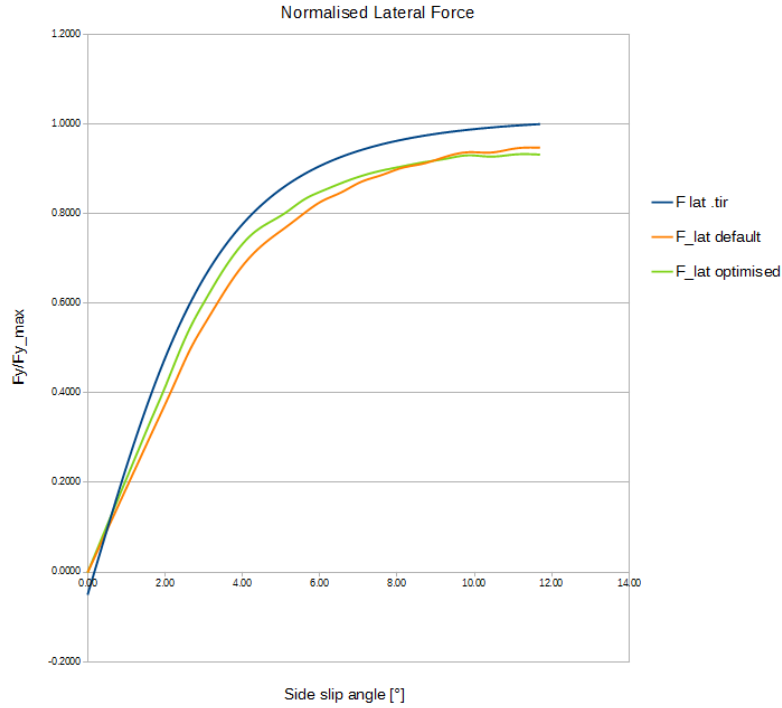


Figure 5.17 – Off-line validation test: normalised lateral force.

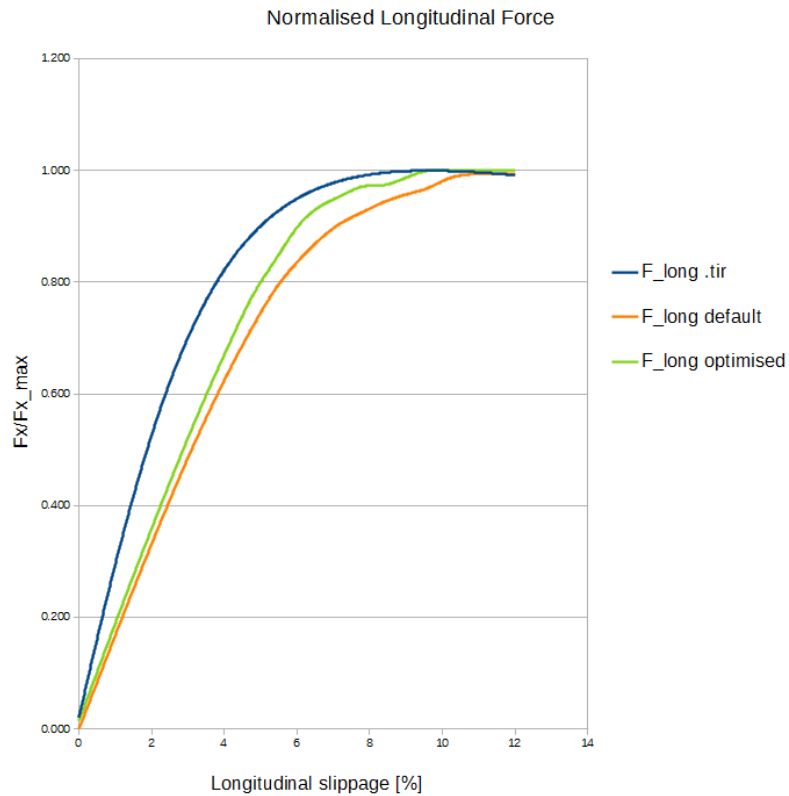


Figure 5.18 – Off-line validation test: normalised longitudinal force.

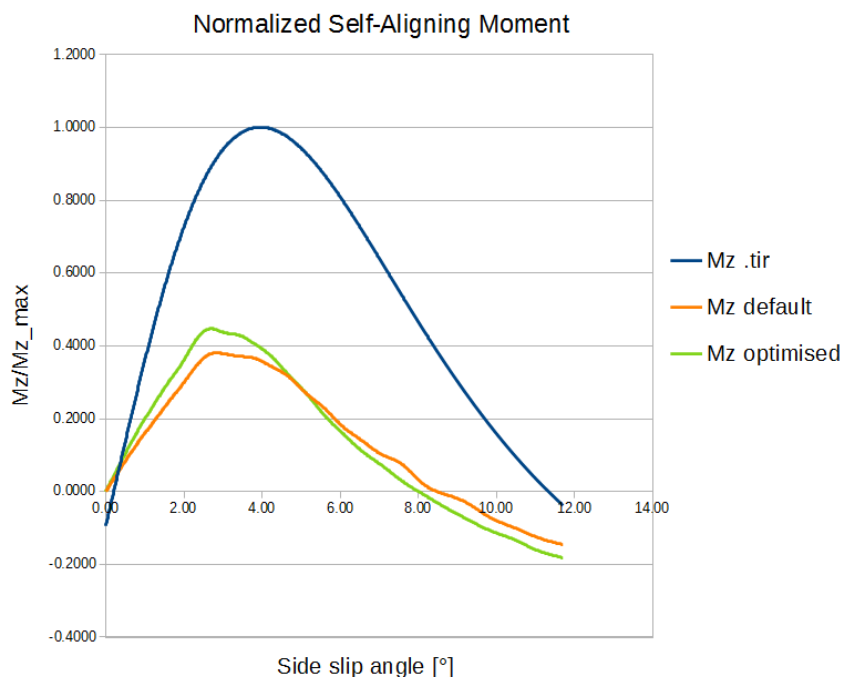


Figure 5.19 – Off-line validation test: normalised self-aligning moment.

The off-line tests have been carried out by a random selection among the possible optimal combinations obtaining most of the times coherent results with the predicted ones. The differences encountered between the objective functions are due to the fact that the network is trained with one change at a time, while the simulations carried out for the optimisation process involve the contemporary modification of the whole set of parameters. Anyway, the algorithm works in the right direction and the results obtained are always beneficial for the optimisation purpose of the objective functions.

5.5.2 On-line tests

The results obtained until now with the off-line tests are only partially positive: the goal of the optimisation process is to reduce the gap from the characteristic target curves of the tyre, but, at the same time, the tyre must not show a fake behaviour.

So, the litmus test must be carried out directly on board the simulator. In order to provide realistic feedbacks, the on-line tests were carried out by Alessio Rovera, who is the actual champion of the Italian GT Championship, as well as the test driver of both the simulators. The first test consists only in driving the vehicle in the Valencia Circuit before and after the tyre modifications: despite the opportunity to analyse the telemetry data, this type of test was based only on the personal feelings of the driver, because it is very complicated to extrapolate such information from the crude numbers: in fact, due to the multitude of factors at stake, it is quite impossible to make accurate comparisons between two different laps.

The tyres were tested in three different conditions:

- default tyres;
- both tyres optimized for the maximum lateral performance;
- both tyres optimized for the maximum longitudinal performance.

In both the optimized conditions the difference is tangible, but always without incurring in totally misleading tyre behaviour. The tyres in the second configuration (lateral force optimised) seem to be qualifying tyres: they slip less allowing to reduce the lap time. While, in the third configuration (longitudinal force optimised), the tyres improved the braking and the traction: while exiting by the corners you can push the throttle pedal more safely and the braking is more generous.

The feedbacks obtained are in line with the expectations of the results provided by the off-line tests. Of course, during these tests the tyre behaviour was extremized in only one direction, worsening the other, and this was necessary in order to validate the accuracy of the algorithm at first instance. So, a trade-off in the final selection of the optimal combination is therefore compulsory.

Once established a realistic behaviour of the tyres, some more reliable tests were made, this time with the utilization of the telemetry data: for such tests, the aim was to demonstrate the fidelity of the responses generated by the “tTool” through the off-line tests.

The tests shall comply with the following procedure: the vehicle is tested on a flat track and the driver performs the same manoeuvres in order to exploit the optimised tyres for what concern both the lateral force and the longitudinal force; then a comparison between the default tyres is made.

The manoeuvre to perform to validate the improved response of the tyres in terms of lateral forces consist in steering with a constant angle in neutral gear, starting from the maximum speed achievable by the vehicle (258km/h in 5th gear);

The manoeuvre to perform for the validation of the longitudinal improvement of the tyres consist in driving the vehicle in 5th gear at its maximum speed (258 km/h) and then breaking with the maximum force: the braking distance is then compared.

In **Figure 5.20** the result of the test is illustrated: as you can see, the lateral acceleration [g] has proved to be slightly increased for the same steering input [%]. This can be translated in higher travelling speed during the cornering phase in the track, and therefore lower lap times.

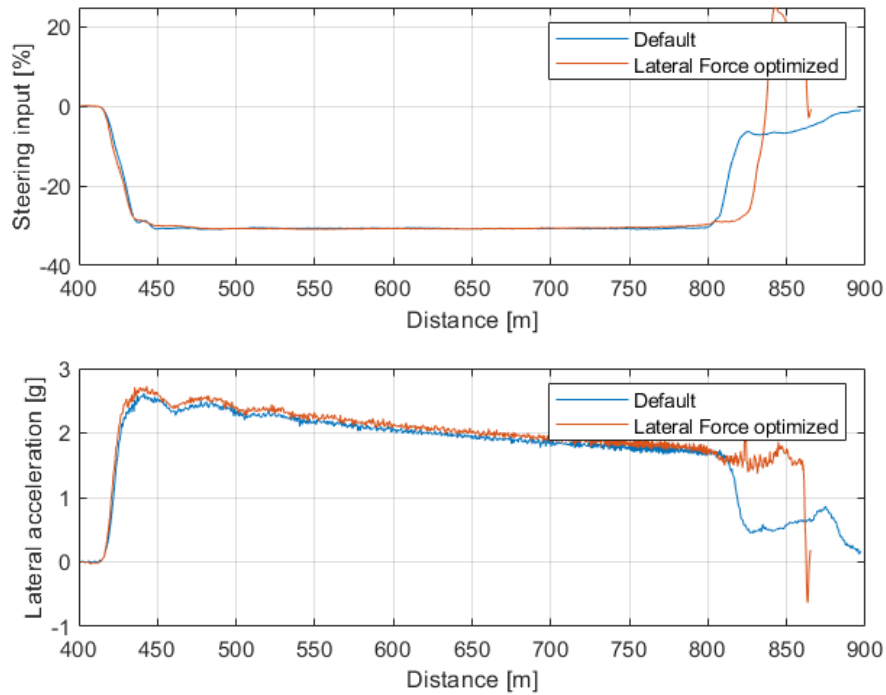


Figure 5.20 – Lateral acceleration comparison: default tyre vs the optimised one.

In **Figure 5.21** you can appreciate that the optimisation of the tyre, for what concern the longitudinal force, produces beneficial effects in the braking distance: it is lowered of about 3 meters, thanks to the improved capability of the tyres to exchange longitudinal forces with the ground.

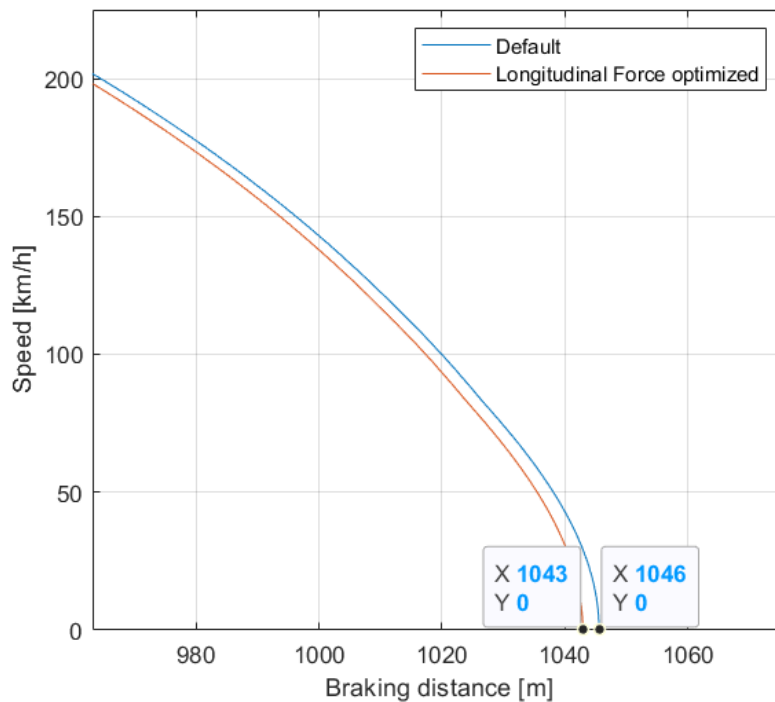


Figure 5.21 – Braking distance comparison: default tyre vs the optimised one.

5.6 Final considerations

The optimisation procedure presented in this chapter is meant for those virtual tyres (".tgm" file) that are already implemented and correlated with a ".tir" file, through which it is possible to get specific target curves that we want to reply.

The overall procedure was carried out two times, respectively for the front and for the rear tyre belonging to the same vehicle. By analysing the trend of the objective functions in relation to the parameter variation, it is possible to notice a certain similarity between the couple of tyres, despite the completely different geometrical and physical structures that have been implemented by the tyre developer. In detail, if we consider small range of variation ($\pm 5\%$) the four objective functions present an almost linear behaviour or at least a quadratic one for wider range: this confirms the initial hypothesis of independency between the parameter selected and, more important, that the parameters simply act as scaling factors of the intrinsic tyre response encoded in the Lookup Table.

The previous statement allows the final user to apply the optimisation algorithm to different tyres by using the already implemented ANN, making relatively small calculation errors but saving a lot of time. Eventually, for more reliable results, only two tests per parameter are necessary in order to reconstruct the trends of the objective functions.

Chapter 6. Thermodynamic aspect of the tyre

In the fifth chapter an optimisation method to make the virtual tyres closer to the real ones has been widely described. It consists in the appropriate tuning of the [Realtime] parameters that affect the purely “mechanical” characteristics of the tyres in terms of forces and self-aligning torque: this is possible thanks to the “.tir” file, that provides a reference to follow.

Another aspect of the virtual tyres that necessitates a deep review is the thermal behaviour. The necessity to improve this macro area of the overall tyre response comes from the fact that the “.tgm” files, provided in the vehicle suites and downloadable from the official website of rFactor2, are intended for amateur use. Therefore, it turns out to be more difficult to put in crisis the vehicles and the driving experience inevitably results distorted.

This condition is in contrast with the purpose of the “Driver R&D” training method, adopted and developed by Skydrive for the professional drivers. Nowadays, the thermodynamic aspect plays a key role for what concerns the overall vehicle performance. In fact, the racing tyres express their maximum performance in quite a narrow range: the ability of the driver to reach the right temperature of the tyres and to maintain it, without incurring in overheating, is a skill that is becoming more and more important. For this reason, it is fundamental to implement a training session for the drivers, through which they get used to perform the warm-up phase in the correct way and avoid all the possible manoeuvres that can induce overheating.

However, the situation is very different from the one analysed in the previous chapter: in this case the problems are the lack of real data to use as a reference and the inability to obtain information about the temperature of the tyres through the off-line tests. So, the only way to observe the temperature trend of the tyre’s surface is through the telemetry data. The off-line tests, widely exploited for the analysis of the mechanical characteristics, are always repeatable and this is possible by the fixed boundary conditions. Instead, it is quite impossible to replicate tests about the thermodynamic aspect with the same accuracy by means of the simulator.

Once made this dutiful premise, it is necessary to provide an accurate description of the procedure adopted to improve the thermal behaviour of the tyres. The tyres used for optimisation process are the same analysed in the previous chapter, while the reference data derive from a different vehicle with similar characteristics in terms of engine power, tyres size, weight, aerodynamics, and so on.

6.1 Formula Renault 2019 track tests

The vehicle taken into consideration is a Formula Renault 2019 made available by JD Motorsport racing team for instrumental measurements (**Figure 6.1**). In order to be able to reconstruct the whole vehicle dynamics, the vehicle was equipped with the following instruments: Datron for the slip angles measurement, infrared sensors for the tyre's surface temperature, TPMS, gyroscope, accelerometer and laser sensors for the ride height measurement. Two-days test took place at Cremona Circuit in July 2019 and the driver was Alessio Rovera, who is also the test driver of the AVEHIL simulators.



Figure 6.1 – 1st day of tests at Cremona Circuit: Formula Renault instrumentation phase [7].

During the test several runs were scheduled with different suspension settings. Each of them was carried out with the following run plan, that the driver had to follow scrupulously:

- Out lap and 1st flying lap: tyres warm up;
- 2nd lap: push;
- 3rd lap: cool down;
- 4th lap: push;
- In lap.

The measurements of the tyre's surface temperature have been used as a reference for the optimisation process. More in details, each tyre was equipped with an infrared sensor capable to measure the temperature of the tyre in four different points along the tread pattern. The run selected as reference was the one carried out in the morning with the best set up (camber angles and inflation pressure of the tyre) in terms of lap times and constancy: ambient and track temperatures have been recorded and used in the equivalent tests at the simulator. The tyre blankets have not been used, as imposed by the championship rules.

6.2 Comparison with the equivalent virtual tyre

The comparison tests for the assessment of the tyre's profile temperature was carried out again by Alessio Rovera, trying different vehicle configurations.

As a matter of interest, the Formula Renault suite downloaded by the rFactor2 website was used in the first run, in order to verify the effective discrepancy from the behaviour of the real tyres. For the comparison purpose, the lap after the cool down was taken as a reference and the measurements of the central part of the tyres were considered, in order to reduce the effects induced by the camber angle on both sides of the tyres. In **Figure 6.2** it is possible to appreciate the difference with the real trend and this is confirmed also by the driver's feedbacks.

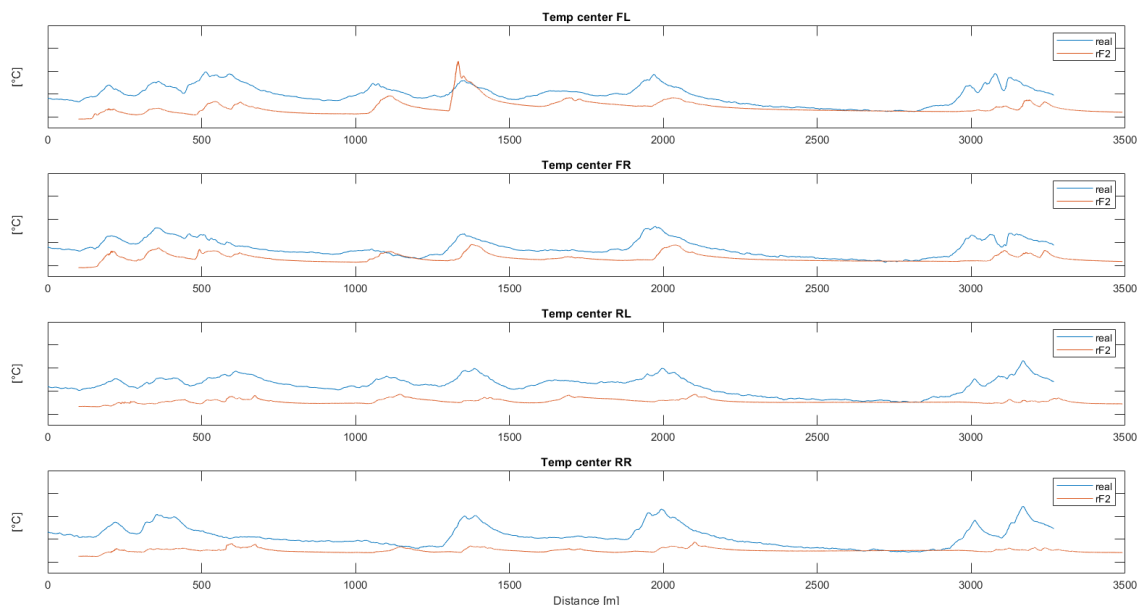


Figure 6.2 – Temperature profile comparison: real vs rF2 Formula Renault official suite.

As you can see the virtual tyres, commercialized by rFactor2 for play purposes, present a different trend of surface temperatures which are quite flat. This action is specifically induced to maintain the tyre properties constant in time and to allow the amateur user to enjoy without thinking about the tyre warm up. In fact, even if the temperature profile is definitely lower compared to the real one, leading to a worsen

performance, there is a hack parameter implemented in every “.tgm” file that allows to bypass this problem: it is called “StaticCurve”.

This parameter is structured as follows:

```
StaticCurve=(183, 0.61, 373, 1.176, 673, 0.61)
```

where the odd indices represent the temperature [K] and the even ones the corresponding grip multiplication factors at such temperatures. These three points describe the trend of the tyre performance as function of the temperature through cubic splines interpolation (**Figure 6.3**).

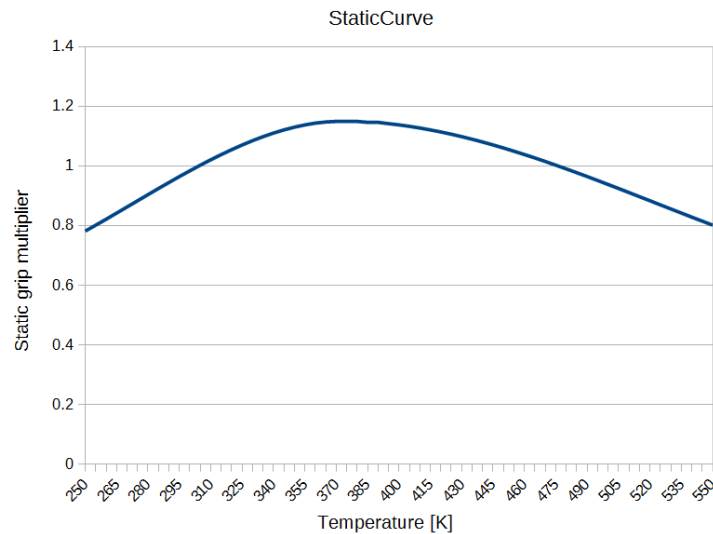


Figure 6.3 – “StaticCurve” parameter: static friction as function of temperature.

As confirmed by the theory analysed in the 2nd chapter, the rubber compound expresses its performance, in terms of friction coefficient, with an almost parabolic trend as function of the temperature: there is a certain temperature range in which the tyres work at their best condition. In order to compensate the lower temperature, rFactor2 adopts a high value of grip multiplier (1.176) at 100°C: in this way the whole curve shifts up and the tyres work at their best despite the lower temperature.

However, the Formula Renault suite is encoded, as well as the “.tgm” file, and there are no possibilities to modify the [Realtime] parameters. For this reason, the optimisation procedure, in terms of thermodynamic properties, has been carried out with the same tyre used in the previous chapter, even if it has a different size and it is equipped on a more powerful and heavier vehicle. So, the process presented in this chapter is only meant to imitate in a qualitative way the overall temperature profile of a real racing tyre.

6.3 Thermodynamic parameters tuning

Once established the effective discrepancy from the temperature trend of the real tyre, it is possible to analyse deeper the factors that affect the thermodynamic aspects of the tyres in rFactor2. As first attempt the tyres were tested with the original configuration: in **Figure 6.4** again the 4th lap of the run (after the cool down phase) is illustrated.

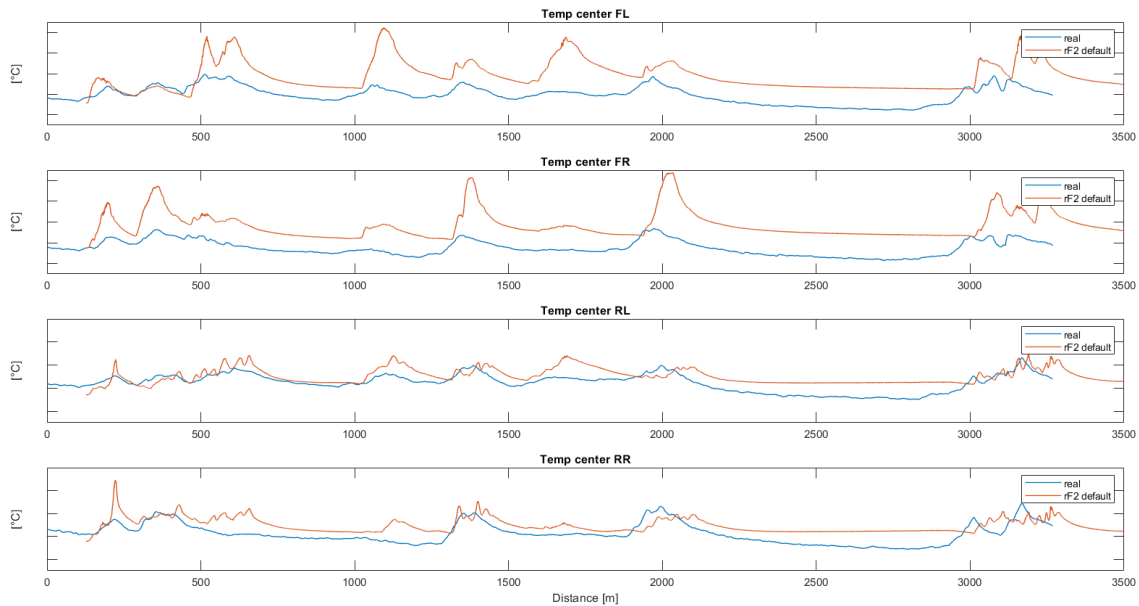


Figure 6.4 – Surface temperature comparison: real tyres vs rF2 default tyres.

As pointed out previously, the plot above illustrates the surface temperature of the tyres belonging to two different vehicles: so, the mismatch of the peaks is comprehensible. This is due to the fact that the vehicle used at the simulator is equipped with more powerful brakes that allow to bring further the braking points. In order to have a preliminary correlation with the reference, the two plots have been aligned in correspondence of the first corner, after the start finish straight.

In this case, the initial situation is opposite with respect to the Formula Renault tyres: in fact, the surface temperature of the tyre is on average increased along the whole lap, especially for what concerns the front tyres. Instead, the positive factor is that now the tyres behave as they should: the temperature rise in correspondence of the braking points is accentuated as well as the reduction of temperature on the straights due to convection with the incoming air.

Before starting the tuning process of the [Realtime] parameters, it is necessary a brief recap on the main sources of heat generation that affect the final temperature of the tyres (**Figure 6.5**), although an in-depth analysis was discussed in the 2nd chapter. Essentially the tyres generate a significant part of the heat because of the friction action which happens in the sliding zone of the contact patch, but the largest portion of heat generation acts at molecular level and comes from the energy stored in the rubber subjected to compression and tension actions (hysteretic heat generation): this last aspect assumes a very important relevance for the tyre performance, because it is the main responsible of the carcass warm up and therefore of the increase of the internal

inflation pressure and air temperature. The asphalt represents an important medium for the heat exchange in both direction by means of the conduction principle. And finally, the ambient air provides a huge contribution for the concern the tyre cooling, especially in our case with open wheels vehicles. In reality, we should consider also the heat coming from the braking system and transmitted to the tyre though the rim, but this phenomenon is not taken in consideration in the implementation of the “.tgm” file.

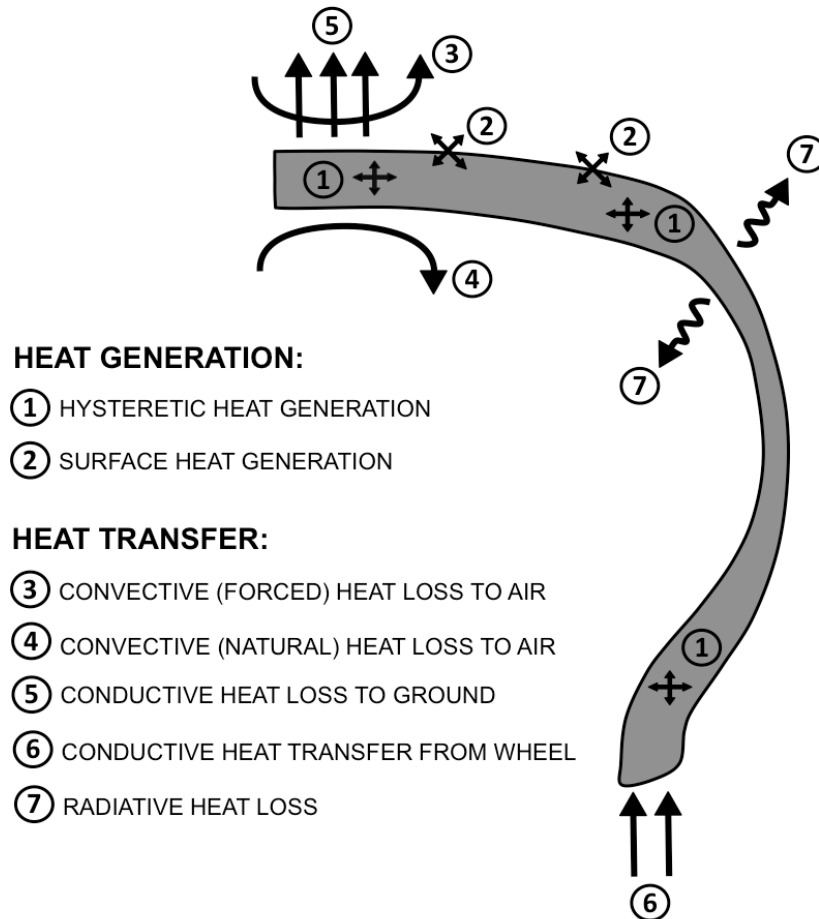


Figure 6.5 – Cross-sectional view of tire heat generation and transfer [9].

Since we have available the measurements referred only to the surface temperature of the tyres and not on the carcass temperatures, the second source of heat generation mentioned before is not taken into account (anyway this aspect is implemented in the “.tgm” file). So, the [Realtime]parameters on which the optimisation phase was focused are the following:

- `GroundConductance=(1100, 0.011, 0);`
- `ExternalGasHeatTransfer=(9, 4.5, 0.6).`

The parameter “GroundConductance” regulates the degree of heat exchange by conduction with the ground as function of the contact pressure, while the parameter “ExternalGasHeatTransfer” regulates the heat transfer by convection with the air.

Unlike the case of the previous chapter, the absence of off-line tests to get numerical results on the surface temperature forced us to try some random values, in order to get a

preliminary order of magnitude of the influence on the final behaviour of the tyre. So, the following procedure is not based on quantitative results, but on qualitative considerations based on the telemetry data and on the driver’s feedbacks.

The initial attempt was focused on the increase of the heat exchange with the asphalt through the second value of the parameter “GroundConductance”, which is a multiplication factor of the pressure distribution of the tyre along the contact patch. The values were initially increased of the 20% and then doubled at both the tyres: this method is necessary to appreciate the improvement, even if drastic. So, the parameters were set as follows:

- GroundConductance=(1100, **0.022**, 0)//(1100, 0.011, 0) @front
- GroundConductance=(1250, **0.018**, 0)//(1250, 0.009, 0) @rear

As usual, the reference lap used for the comparison is the 4th lap. In **Figure 6.5** the differences encountered are illustrated.

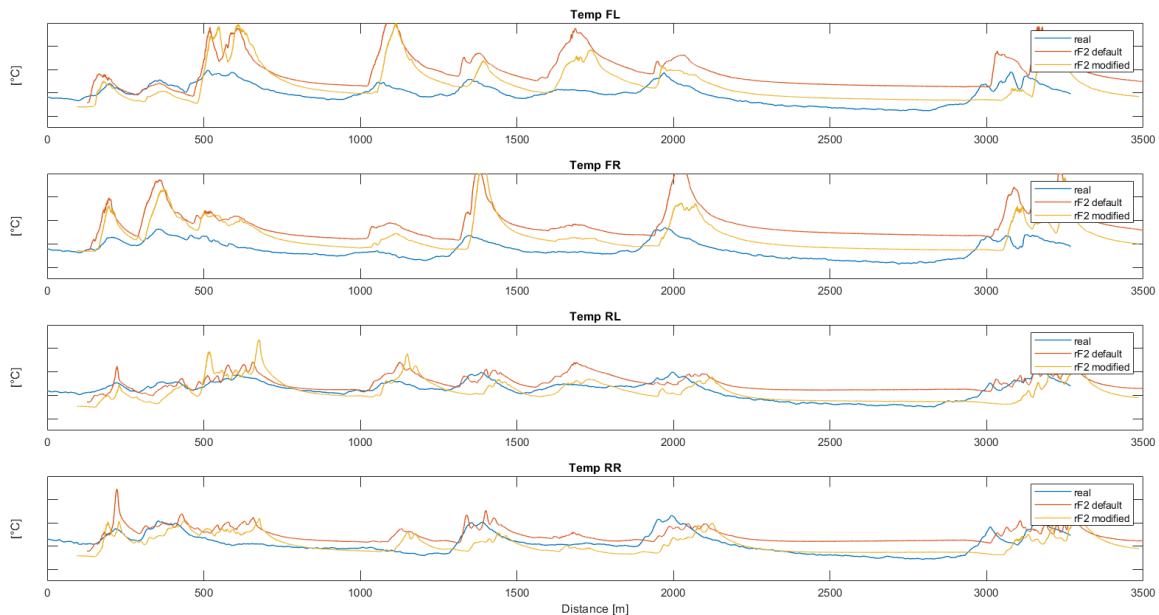


Figure 6.6 – Surface temperature comparison: real tyres vs rF2 default tyres vs rF2 modified tyres (“GroundConductance”).

Being the vertical load on the four wheels almost the same from one run to the other (since no other parameters were modified), the results shown in **Figure 6.4** were expected: the surface temperature is characterised by a pronounced decreasing on the whole lap, and this is particularly enhanced in the front tyres because of the larger modification.

An interesting aspect of the virtual tyres that differs from the real ones is the temperature descending trend in correspondence of the long straight of the Cremona Circuit: in fact, it is possible to notice an almost flat behaviour starting from the distance of 2200m up to 3000m, while the real trend is progressively decreasing. The temperature drop is generated by the incoming air which becomes incredibly high with the increasing speed. Being the vehicle used for the comparison more powerful and therefore faster, we expected an even more accentuated cooling action by convection with the ambient air.

In order to improve this aspect, the parameter “ExternalGasHeatTransfer” was modified in this way:

- ExternalGasHeatTransfer=(9, 4.5, **0.9**) //(9, 4.5, 0.6) @front
- ExternalGasHeatTransfer=(9, 4.5, **0.8**) //(9, 4.5, 0.6) @rear

The three values (a, b, c) that characterise this parameter work according to this formula:

$$\text{ExternalGasHeatTransfer} = a + (b * \text{speed}^c);$$

So, the last value affects the tyre cooling in an exponential way as a function of the vehicle speed, and therefore the difference between the default tyre is enhanced especially in the straights, where the tyres mostly suffer the discrepancy with the real ones. In **Figure 6.6** the adjustments adopted are illustrated.

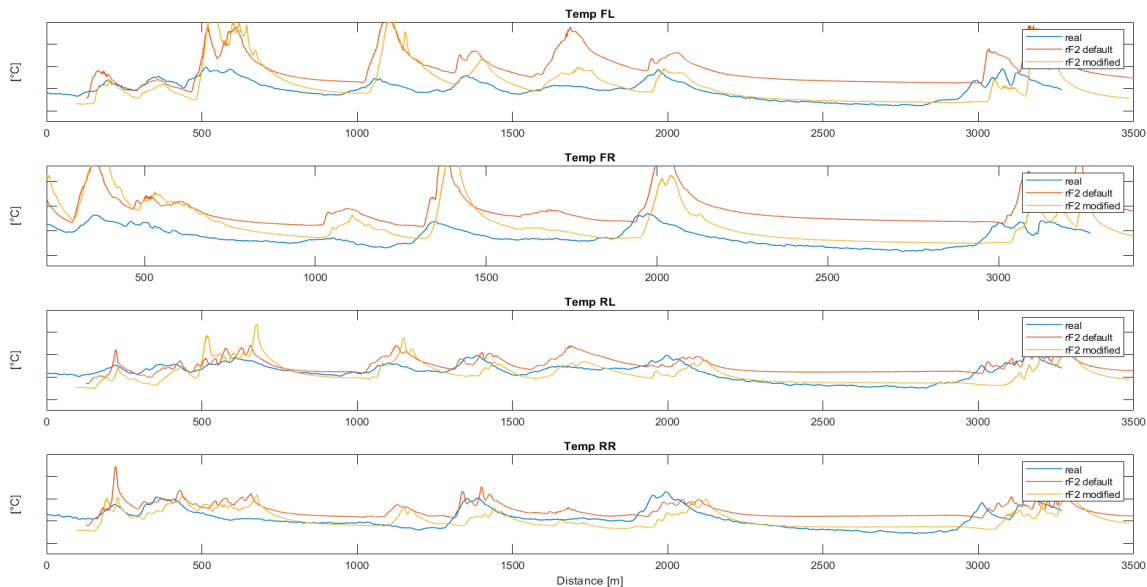


Figure 6.7 – Surface temperature comparison: real tyres vs rF2 default tyres vs rF2 modified tyres (“ExternalGasHeatTransfer”).

By analysing the above results, it is possible to notice a huge change in the surface temperature trend, especially along the straights, where the default tyres were not so affected by the cooling action of the air.

The strong alterations made in the last two examples were intended only to capture the potential influence of each parameter taken in isolation. So, a trade-off between these two values is recommended in order not to distort the overall tyre response. However, this kind of methodology must be carried on in a qualitative way, because it is very difficult to obtain two or more identical laps to compare and to derive any empirical relationship. In addition, contrarily to the approach developed in the previous chapter, this procedure has to be repeated for every different type of car because many more variables are involved (speed, engine power, aerodynamics and so on).

6.4 Tyres warm-up training

A crucial aspect to improve is the warm up phase of the tyres, with the aim to provide to the customers a training session developed in the smallest details. This type of exercise is almost always neglected in the gameplay of the driving videogame, but in our case, it can make the difference.

The warm up is the delicate procedure that must be carried on in the formation lap, before the start. Most of the times the tyre blankets are not allowed by the championship rules, so the driver needs to pay more attention on this phase because he cannot bring the core temperature of the tyres in the optimal range, as well as overheat the tyres by doing the wrong manoeuvres, causing a premature wear. During the training session developed in the “R&D Driver” program, the driver is asked to simulate the key manoeuvres that have to apply in the formation lap: the core temperatures of the tyres are checked in live time and in this way it is possible to get a rough indication of the number and on the intensity of the necessary manoeuvres.

The implementation of this exercise can be possible through the exploitation of the “StaticCurve” parameter, previously explained: it essentially regulates the grip coefficient in relation with the carcass temperature, by means of an approximated parabolic function. Even in this case the tuning of this powerful parameter was based on the driver feedbacks, according to his own experience. The initial attempt was focused on the reduction of the “StaticCurve” curve, in order to replicate the typical slippery behaviour of the tyre at low temperatures. The parameter was set as follows:

- `StaticCurve=(183, 0.3, 373, 1, 673, 0.3) //(183, 0.61, 373, 1.176, 673, 0.61) ;`

By doing so, the “StaticCurve” curve shifts downward as illustrated in **Figure 6.7**.

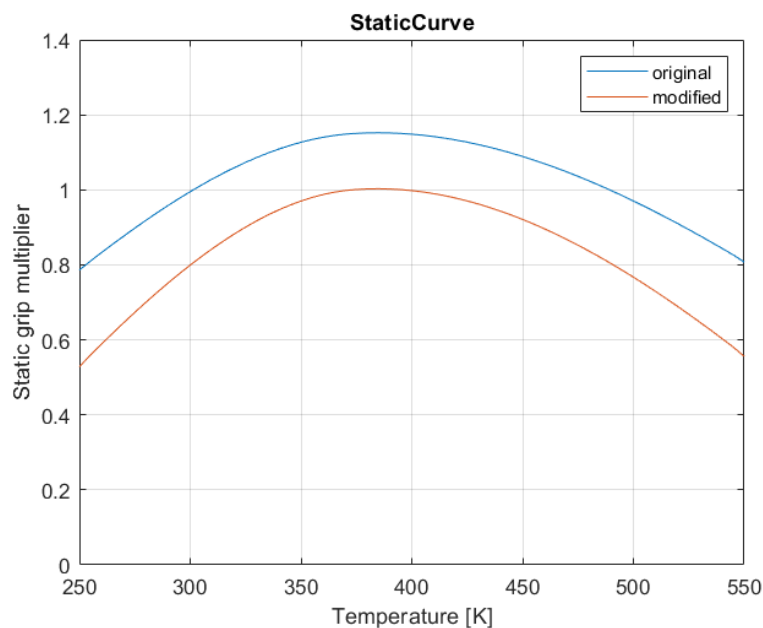


Figure 6.8 – “StaticCurve” comparison: original vs modified trend.

The change made in the grip values has partly fixed the tyre response during the formation lap: now the tyres are much more slippery in the first corners as they should be, but the induced slip causes a quick increase of the tyre temperature and therefore the grip coefficient rises to the optimal value in a while. By means of a proper tuning of the “GroundConductance” and the “ExternalGasHeatTransfer” parameters, it is possible to get around the problem induced by the extra heat provided by the tyre slip.

Chapter 7. Conclusions

The master thesis presented in these pages is the result of the work lasted six months at the Skydrive field office, located in the grandstand of the Monza Eni circuit. Skydrive produces and sells professional simulators called AVEHIL (Advance Vehicle Engineering Human In the Loop), intended for professional drivers who want to keep trained at relatively low costs and improve their driving skills.

The aim of this internship was the exhaustive comprehension of the mathematical model on which is based the software “rFactor2”, which provides the gameplay platform of the simulator. The main topic to cover was the analysis of the tyre implementation: the tyre data necessary to run the software are contained in a text file with the extension “.tgm”, which is described by tens of parameters that affect its final behaviour.

The multitude of parameters allows a complete customization of the tyre response during the gameplay: by default, all the racing tyres available are configured to be easy to manage, in order to be used by the majority of the final users. This aspect goes in contrast with the purpose of the AVEHIL simulators, in which every component is studied in the smallest details to replicate the same driving feelings on the real vehicles.

7.1 Results

The analysis work presented in this master thesis is divided in four chapter (from the 3rd to the 6th). The 3rd chapter includes an in-depth description of the theoretical aspect behind the tyre model implemented in rFactor2: this step was something dutiful in order to provide to the reader an overall view of the features that are included in the “.tgm” file. A positive aspect of rFactor2 is the possibility to build up from scratch your own tyre, in order to match the desired characteristics: the 4th chapter contains a step-by-step procedure to generate a “.tgm” file, gathering the advices provided by rFactor2 and my own experience. In the 5th chapter an optimisation process is presented: by disposing a “.tir” file and the equivalent “.tgm” file of the same tyres, I developed a MatLab code that gives as output the set of values of some parameters contained in [Realtime] section of the “.tgm” file, in order to match the three curves of lateral force, longitudinal force and self-aligning moment. Finally, the 6th chapter presents the method adopted to correct the thermodynamic behaviour of the tyres, using as reference the surface temperatures measured on a Formula Renault 2019. In this last section of the thesis, a summary of the main progress obtained through the optimisation process is presented as well as some indications for work of the future undergraduates.

The results of the optimisation algorithm presented in the 5th chapter can be summarised through the **Tables 7.1, 7.2**:

		F_lat mse	Mz mse	ΔF_long max	F_long mse
Front tyre	range of variation	[221.222 ÷ 557.626]	[45.513 ÷ 53.634]	[-183.487 ÷ 207.925]	[263.012 ÷ 401.155]
	default value	348.802	49.266	11.464	358.597
	predicted value	318.8532	49.1678	10.5433	341.0829
	real value	325.031	49.228	0.132	339.312
	weighted improvement	7.07%	0.46%	2.90%	13.96%
	weighted evaluation error	1.84%	0.74%	2.66%	1.28%

Table 7.1 – Example of optimisation process of the front tyre.

		F_lat mse	Mz mse	ΔF_long max	F_long mse
Rear tyre	range of variation	[415.714 ÷ 692.838]	[66.846 ÷ 73.701]	[-356.349 ÷ 523.519]	[1750.145 ÷ 1961.154]
	default value	523.582	70.411	86.335	1842.426
	predicted value	445.4929	73.9493	-17.3	1782.7
	real value	448.954	74.245	-35.695	1776.105
	weighted improvement	26.93%	-55.93%	13.87%	31.43%
	weighted evaluation error	1.21%	4.31%	2.09%	3.13%

Table 7.2 – Example of optimisation process of the rear tyre.

The weighted improvement [%] and the weighted evaluation error [%] are calculated with respect the range of variation of each objective function: it takes into account the best and the worst objective function value obtained in the data recording phase by changing one parameter at a time.

As you can see, the ANN was able to predict with quite high accuracy the values of the objective functions that the “tTool” off-line test would have to provide. In particular, the optimal combinations of values used in these examples were selected in order to improve globally the tyre response, without focusing only in one direction. In the front tyre it was possible to improve all fours objective functions at the same time, while in the rear tyre a compromise was adopted: the self-aligning moment mse has been overlooked in favour of a much higher correlation of the lateral force and the longitudinal force.

Better results, especially in terms of self-aligning moment mse, could be obtained with a drastic review of the structure of the plies: in fact, the relatively low discrepancy of the lateral force implicitly tells us that the pneumatic trail must be adjusted. This information is encrypted in [Lookup] section, because it depends on the contact patch properties calculated through the QSA tests and it cannot be modified with the [Realtime] parameters.

For what concerns the thermodynamic aspect of the tyre, we improved the overall tyre behaviour basing on a qualitative approach. The tyres’ surface temperatures recorded on a Formula Renault during a private test were used as a reference for the improvement of the tyre response under the thermodynamic point of view.

Being aware of the limitations of using slightly different tyres equipped on a different vehicle as a reference, the heat exchange phenomenon by conduction and by convection was improved by acting again on the [Realtime] parameters, reaching a similar trend with respect the target one (**Figure 7.1**).

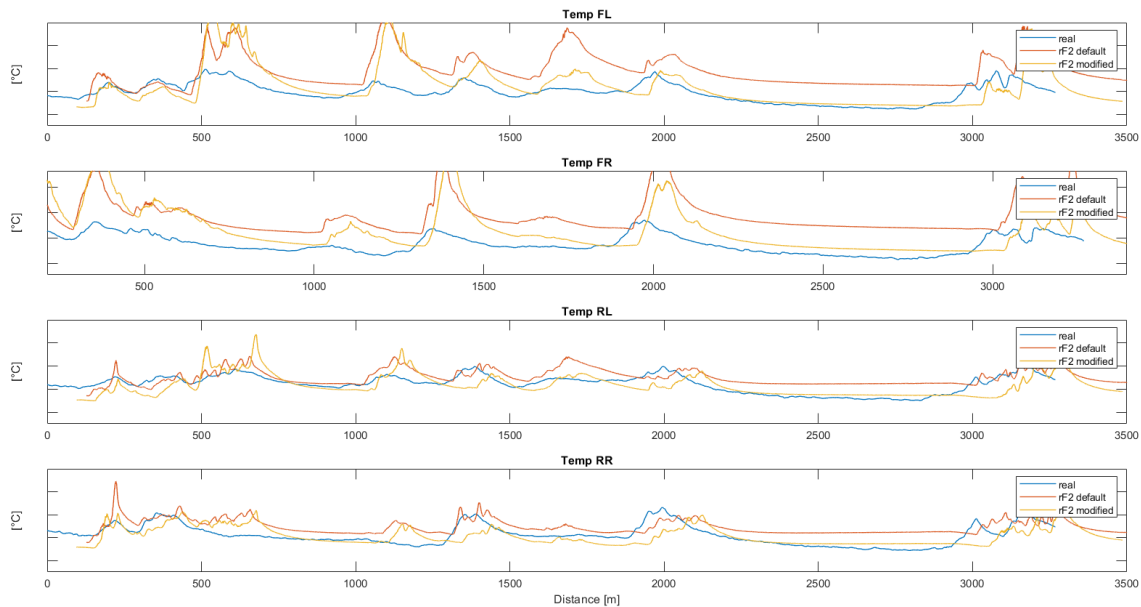


Figure 7.1 – Surface temperature comparison: real tyres vs rF2 default tyres vs rF2 modified tyres.

7.2 Future developments

The six-months work described in this master thesis can be considered as the cornerstone for the future undergraduates that will enjoy the Skydrive world. In fact, there are several ways that can be followed for the long process of the tyre comprehension: by using this thesis as tool to understand the logic behind rFactor2, the next steps could be the realisation of a complete “.tgm” file starting from scratch and the analysis and the tuning of the degradation of the tyres, both in terms of wear and heat.

The possibility to implement a totally new tyre is very important because it would provide a model completely designed for the purpose of train professional drivers, enhancing the already high level of accuracy and, most importantly, it would allow to bypass the custom limitations imposed in the rFactor2 vehicle suites. While the refinement of the degradation aspect would provide an even more realistic behaviour of the gameplay, allowing to simulate the whole race.

Bibliography

- [1] H. B. Pacejka, *Tire and Vehicle Dynamics*, Butterworth-Heinemann, 2012.
- [2] Kosgolla, J. Vishwanath, *Numerical Simulation of Sliding Friction and Wet Traction Force on a Smooth Tire Sliding on a Random Rough Pavement*, 2012.
- [3] C. Lugaro, M. Alirezaei, I. Konstantinou, A. Behera, *A Study on the Effect of Tire Temperature and Rolling Speed on the Vehicle*, 2020.
- [4] F. Farroni, M. Russo, R. Russo, F. Timpone, *Tyre-Road Interaction: Experimental Investigations About the Friction Coefficient Dependence on Contact Pressure, Road Roughness, Slide Velocity and Temperature*, 2013.
- [5] Michelin, *Tametire User Manual*, 2010.
- [6] Michelin, *The Tyre Grip*, 2001.
- [7] AVEHIL Professional Car Simulator,
<https://www.avehildrivingsimulator.com/>.
- [8] rFactor2 Track Technology Documentation,
https://www.studio-397.com/wp-content/uploads/2016/12/rF2_TGM_TyreTool_QuickStart_V3.pdf.
- [9] White Paper: Influence of Temperature on Tire Grip,
http://www.izzeracing.com/products/ewExternalFiles/Izze_Racing_White_Paper_Tire_Temperature.pdf.
- [10] Bayesian regularization backpropagation,
<https://www.mathworks.com/help/deeplearning/ref/trainbr.html;jsessionid=54328a164c819b6a0921ba6ea953>.